Aus dem Deutschen Rheuma-Forschungszentrum (DRFZ)
Institut der Leibniz-Gesellschaft

DISSERTATION

Role and potential therapeutic use of interleukin-22^{+} Innate Lymphoid Cells in colitis

zur Erlangung des akademischen Grades
Doctor medicinae (Dr. med.)

vorgelegt der Medizinischen Fakultät
Charité – Universitätsmedizin Berlin

von
Isabelle Ommert
aus Fulda

Datum der Promotion: 04.03.2022

Table of contents

List of tables

List of figures

List of abbreviations

AhR	Aryl hydrocarbon receptor
AMP	Antimicrobial peptides
aNKp44	Anti-NKp44 monoclonal antibodies
APC	Allophycocanin
CCR6	Chemokine (c-c motif) receptor 6
CD	Cluster of differentiation
CD3ζ	CD3 receptor chain zeta
CHILP	Common "helper like" ILC precursor
cNK cells	Conventional natural killer cell
CRC	Colorectal carcinoma
CT	Cycle threshold
DAP12	DNAX-activating protein 12
DSS	Dextran sulfate sodium
DC	Dendritic cell
EOMES	Eomesodermin
FACS	Fluorescence-activated cell sorting
FC	Flow cytometry
FcRγ	Fc receptor gamma chain
FSC	Forward Scatter
GM-CSF	Granulocyte-macrophage colony-stimulating factor
HA	Hemagglutinin
HN	Hemagglutinin neuraminidase
HPC	Hematopoietic progenitor cell
IBD	Inflammatory Bowel Diseases
ILZ	aminoterminal leucine-zipper
IV	Influenza virus
Id2	DNA-binding protein 2
IgA	Immunoglobulin A
IEC	Intestinal epithelial cells
IL	Interleukin
IL-7Rα	IL-7 receptor alpha

IL-12RB	IL-12 receptor beta
IL-23R	IL-23 receptor
ILC	Innate Lymphoid cells
ILF	Isolated lymphoid follicle
IFN-γ	Interferon gamma
Iono	Ionomycin
ITAM	Immunoreceptor tyrosine-based activation motif
ITIM	Immunoreceptors tyrosine-based inhibitory motif
Lin^-	Lineage negative
LN	Lymph node
LP	Lamina propria
LPMC	Lamina propria mononuclear cells
LTβR	Lymphotoxin beta receptor
LTi cells	Lymphoid Tissue inducer cells
mAb	Monoclonal antibody
MFI	Mean fluorescence intensity
MNCs	Mononuclear cells
mRNA	Messenger RNA
NCR	Natural cytotoxicity receptor
NKG2D	Natural killer group 2, member D
NOD2	Nucleotide-binding oligomerization domain 2 receptor
PAMP	Pathogen associated molecular patterns
PMA	Phorbol 12-myristate 13-acetate
PP	Peyer's Patches
PPR	Pattern recognition receptor
qPCR	Qualitative polymerase chain reaction
RAR	Retinoic acid receptor
RAG	Recombination-activating gene
RORα	Retinoic acid receptor-related orphan receptor alpha

RORγt	Retinoic acid receptor-related orphan receptor gamma t
SSC	Sideward scatter
SEM	Standard error of the mean
Th1	Type 1 T helper cells
Th2	Type 2 T helper cells
Th17	Type 17 T helper cells
TGF-β	Transforming growth factor beta
TNF	Tumor necrosis factor
Treg	Regulatory T cells
SCF	Stem cell factor
SD	Sigma diverticulitis

Abstract

Innate lymphoid cells (ILC) are a family of tissue-resident immune cells, particularly enriched at mucosal sites. Among ILCs, IL-22-producing RORγt$^+$ Innate Lymphoid cells (ILC3) preferentially reside in the intestine, where they perform important functions for epithelial barrier integrity and tissue homeostasis. These functions are mainly mediated through their signature cytokine IL-22. Despite these beneficial features, their role in the pathogenesis of intestinal inflammation has been controversially discussed. Murine and human studies have provided evidence that RORγt$^+$ ILC3 can play a pro-inflammatory role in the context of colitis. Elucidating the biologic conditions and environmental factors that potentially direct RORγt$^+$ ILC3 to either function could lead to a better understanding of their contribution to disease development and ultimately to a potential therapeutic intervention.

Previous work by our group demonstrated that triggering the activating receptor NKp44 in RORγt$^+$ ILC3 with an anti-NKp44 monoclonal antibody results in a coordinated pro-inflammatory program. The observed responses included the production of TNF, which plays a pathological role in Inflammatory Bowel Diseases (IBD). In contrast, stimulation with cytokines preferentially induces IL-22, which has important regenerative functions on the epithelium.

Building on these previous findings, we aimed

- to investigate the distribution of RORγt$^+$ ILC3 subsets (NKp44$^+$ / NKp44$^-$) in the inflamed and non-inflamed intestinal lamina propria of IBD patients by Flow Cytometry; and
- to evaluate potential ligands of NKp44 leading to activation of RORγt$^+$ ILC3.

The central finding was a significant decrease of NKp44 expression in RORγt$^+$ ILC3 exclusively in the inflamed lamina propria of IBD patients. Whether this finding is due to downregulation of NKp44 and/or a different activation status, promotion of the NKp44$^-$ ILC3 subset or plasticity between ILC subsets remains subject to further investigation.

Furthermore, several cell lines were identified to express NKp44 ligands on their cell surface, and among these some were of colon epithelial origin. By analyzing physiologic engagement of the NKp44 receptor, NKp44 ligand-expressing cell lines led to the production of TNF in human RORγt$^+$ ILC3.

These findings taken together with previous results of our work group, suggest a dual nature of RORγt$^+$ ILC3 depending on the environmental context. NKp44 might represent a therapeutic target to modulate pro-inflammatory versus protective features of RORγt$^+$ ILC3 in IBD.

Zusammenfassung

Innate Lymphoid Cells (ILC) sind eine Gruppe von ortsständigen Immunzellen des angeborenen Abwehrsystems, welche insbesondere in der Mukosa verschiedener Organe zu finden sind. Unter den ILCs sind IL-22-produzierende RORγt$^+$ ILC3 vornehmlich im Darm ansässig, wo sie wichtige Funktionen für die Integrität der epithelialen Barriere sowie der Gewebshomöostase erfüllen. Diese werden hauptsächlich durch ihr Signatur-Zytokin IL-22 vermittelt. Trotz dieser protektiven Eigenschaften wird ihre Rolle in der Pathogenese intestinaler Entzündung kontrovers diskutiert. Murine wie auch humane Studien haben Hinweise ergeben, dass RORγt$^+$ ILC3 eine proinflammatorische Rolle im Kontext von entzündlichen Darmerkrankungen einnehmen können. Ein besseres Verständnis der biologischen Mechanismen sowie der Umgebungsfaktoren, die RORγt$^+$ ILC3 möglicherweise zu der einen oder der anderen Funktion leiten, scheint wesentlich, um ihre Rolle in der Krankheitsentstehung aufzuklären. Dies könnte schließlich zu einer therapeutischen Intervention führen.

Vorangehende Forschungsergebnisse meiner Arbeitsgruppe haben gezeigt, dass die Stimulation des aktivierenden Rezeptors NKp44 in RORγt$^+$ ILC3 zu einem koordinierten pro-inflammatorischen Programm führt. Hierbei wurde unter anderem die Produktion von TNF beobachtet, welches eine pathologische Rolle bei chronisch entzündlichen Darmerkrankungen (CED) spielt. Im Gegensatz dazu induziert die Stimulation mit Zytokinen bevorzugt das Zytokin IL-22, welches wichtige regenerative Funktionen für das Epithel vermittelt.

Aufbauend auf diese bisherigen Erkenntnisse war das Ziel dieser Arbeit

- die Verteilung von RORγt$^+$ ILC3 Subgruppen (NKp44$^+$/NKp44$^-$) in der entzündeten und nicht-endzündeten intestinalen Lamina propria von CED-Patienten mittels Durchflusszytometrie zu untersuchen
- sowie potentielle Liganden des Rezeptors NKp44, welche zur Aktivierung von RORγt$^+$ ILC3 führen, zu evaluieren.

Die wesentliche Erkenntnis hierbei war eine signifikant niedrigere NKp44-Expression in RORγt$^+$ ILC3, die aus der entzündeten Lamina propria von CED-Patienten stammten. Ob dieser Befund auf eine Herabregulierung von NKp44 und/oder einen anderen Aktivierungsstatus der

Zellen, auf die Förderung der NKp44$^-$ ILC3-Subpopulation oder auf Plastizität zwischen ILC-Subpopulationen zurückzuführen ist, bleibt Gegenstand weiterer Untersuchungen.

Zudem wurden mehrere Zelllinien identifiziert, darunter einige kolon-epithelialem Ursprungs, welche NKp44 Liganden auf ihrer Zelloberfläche exprimieren. In der Analyse einer physiologischen Rezeptoraktivierung von NKp44 führten NKp44 Liganden exprimierende Zelllinien zur Produktion von TNF in humanen RORγt$^+$ ILC3.

Diese Befunde, zusammen mit den früheren Ergebnissen meiner Arbeitsgruppe, deuten auf eine mögliche zweischneidige Rolle von RORγt$^+$ ILC3 hin, die von umgebenden Faktoren abhängt. NKp44 könnte ein therapeutisches Ziel darstellen, um proinflammatorische bzw. protektive Eigenschaften von RORγt$^+$ ILC3 in CED zu modulieren.

1. Introduction

This introduction will outline the current knowledge of intestinal homeostasis and the epithelial barrier function, its disruption in chronic inflammatory bowel diseases (IBD), and the putative role of innate lymphoid cells (ILC) herein.

1.1 Intestinal epithelial barrier function and the intestinal immune system

Inner and outer surfaces demarcate the human body from the exterior world and ensure the body's integrity towards physical and chemical stressors. The skin, as the main outer surface, is covered by a multilayered keratinized squamous epithelium. In contrast, inner surfaces such as the respiratory tract, the gastrointestinal tract and the urogenital tract are lined with mucosal tissue. The mucosa is characterized by a thinner and more permeable epithelium that enables the absorption of nutrients (gastrointestinal tract), gas exchange (respiratory tract) and reproduction (urogenital tract). In return, this higher permeability renders the mucosa more vulnerable for infections and tissue injuries (Kenneth M. Murphy, 2014).

The mucosa of the intestine represents, with an area of over 100 m^2, the largest interface of the human body with the exterior (Artis, 2008). At that site, a constant confrontation with nutritional components, potentially toxic substances, and microbes takes place. An abundant commensal flora resides in the form of a symbiotic relationship on top of the epithelial layer. Besides resembling a barrier towards the components of the intestinal lumen, the epithelium is responsible for digesting and resorbing vitally necessary nutritional substances. In order to meet both of these tasks, the epithelium consists of highly specialized cells and is substantially supported by the associated mucosal immune system. Together, they contribute to a delicate equilibrium. On the one hand, commensal and pathogenic microbes as well as toxic products are prevented from crossing the epithelial border and thus from harming the host. On the other hand, an immunologic tolerance is maintained towards the commensal flora and nutritional antigens. Thereby, an overshooting immunologic activity is prevented (Artis, 2008), which could result in inflammatory disorders such as inflammatory bowel diseases or food allergies, respectively (Mowat, 2003). This equilibrium is crucial for epithelial homeostasis and tissue integrity. The contributing compartments and their complex interplay will be subject of the following sections.

1.1.1 Anatomical and histological characteristics of the intestinal mucosa

The mucosa of the intestine is a highly specialized tissue. Its functions include the digestion and resorption of nutrients and fluids, the defense against pathogens and toxins, and the maintenance of a symbiotic relationship with the commensal flora. In addition, it provides the space and environment for immunologic processes, such as the education and activation of immune cells as well as the induction of immunologic tolerance (Kenneth M. Murphy, 2014).

The intestinal mucosa is composed of three layers (Figures 1 and 2). The epithelium consists of a monolayer of epithelial cells and is separated from the underlying lamina propria (LP) by a basal membrane. The LP is a connective tissue characterized by a rich network of blood and lymph vessels and accommodates abundant immune cells. Finally, the muscular layer of the mucosa forms the transition to the submucosa.

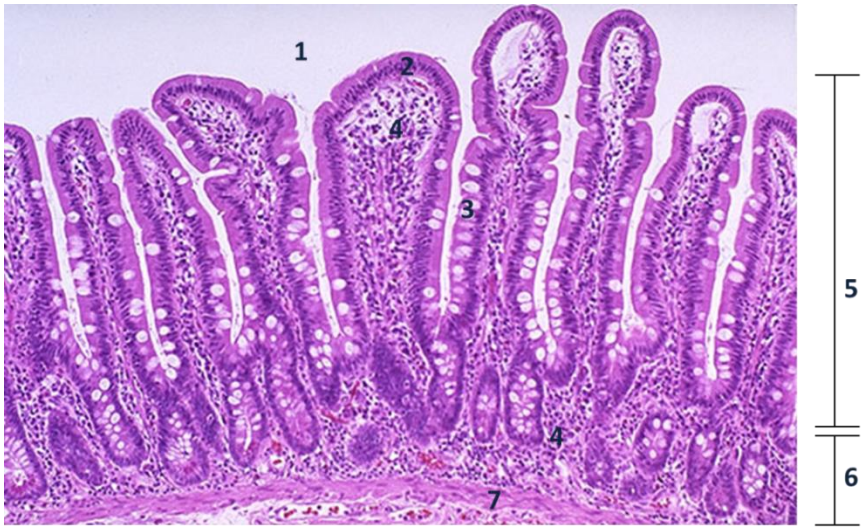

Figure 1 The mucosa of the small intestine

This is a histological slide with a hematoxylin and eosin staining. 1) Intestinal lumen 2) Monolayer of epithelial cells with an underlying basal membrane 3) Mucus-producing goblet cells within the epithelium 4) Lamina propria with vessels and scattered immune cells 5) Villi 6) Crypts 7) Thin muscular layer of the mucosa. (Klatt, 2015).

Accounting for its major functions, the area of the mucosa is increased largely by forming folds, namely: large circular folds of the small intestine, called plicae circulares; smaller folds, called villi; and microvilli on the epithelial cell surface. In addition to the villi that protrude into the lumen, there are crypts that extend to the mucosal muscular layer. From the small intestine (Figure 1) downward to the colon (Figure 2), the number of villi gradually decreases as the number of crypts increases.

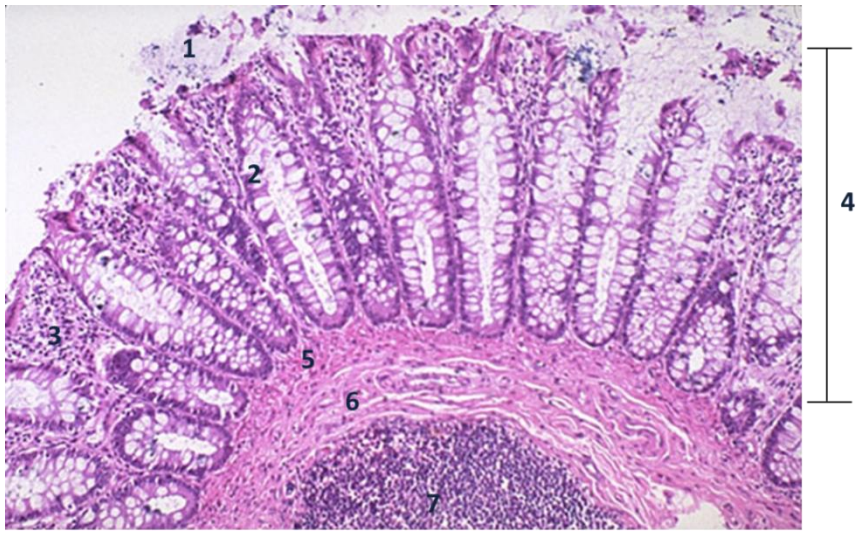

Figure 2 The mucosa of the colon

This is a histologic slide with a hematoxylin and eosin staining. 1) Intestinal lumen with mucus 2) Monolayer of epithelial cells and abundant goblet cells with an underlying basal membrane 3) Lamina propria 4) Colonic crypts 5) Thin muscular layer of the mucosa 6) Submucosa 7) Lymphatic nodule. (Klatt, 2015).

1.1.2 The intestinal epithelial barrier

The monolayer of intestinal epithelial cells (IEC) consists of different types of cells, among them enterocytes, mucus-producing goblet cells, Paneth cells, endocrine cells and stem cells. These cells are strongly connected by intercellular tight junctions in order to prevent paracellular trafficking (Artis, 2008). The surface is coated with a thick mucus layer that represents a physical barrier and additionally serves as matrix for antimicrobial substances. Examples for these antimicrobial substances include plasma cell-derived immunoglobulin A (IgA) and an array of IEC-derived antimicrobial peptides (AMP) such as lysozymes, defensins, cathelicidins, lipocalins and RegIIIγ (Maloy and Powrie, 2011). IECs are equipped with receptors that enable direct sensing of commensal and pathogenic microbes. These receptors are referred to as pattern recognition receptors (PRR) as they recognize unique, conserved structures present on the surface of microorganisms (Artis, 2008). Upon recognition of microbial components, IECs react with an increased secretion of AMPs, as well as with the activation and regulation of innate and adaptive immune cells (Artis, 2008).

1.1.3 The commensal microflora

As mentioned earlier, the intestine is colonized by a diverse community of microorganisms that live in a symbiotic relationship with the human host (Artis, 2008). With approximately 98 %, bacteria are the largest fraction. The remaining part consists of viruses, fungi and archaea

(Kostic et al., 2014). It is estimated that 10^{14} bacteria colonize the intestinal tract and that these bacteria belong to approximately 1,000 different species. The majority of the bacteria belong to the species *Bacteroides* and *Firmicutes*, and a smaller fraction to *Proteobacteria* and *Actinobacteria*. The composition of the commensal bacteria differs considerably between individuals and is influenced by many factors, such as diet, age, drug administration, birth route, breastfeeding, and genetic host factors. The commensal bacteria fulfill various useful functions for the host. They enable the digestion of substrates inaccessible for host enzymes, degrade toxins and provide vitamin K. In addition, beneficial bacteria repress the outgrowth of pathogenic microbes by occupying environmental niches, secreting antimicrobial peptides and competing for nutrients (Artis, 2008). The contribution of the commensal microbiota to the education of the host's immune system is of major importance. Studies with gnotobiotic (germ-free) mice have shown a significant underdevelopment of all peripheral lymphoid organs, as well as reduced levels of immunoglobulins (Kenneth M. Murphy, 2014). Furthermore, there is increasing evidence that the presence of commensal microbiota facilitates the development and function of innate and adaptive lymphocyte populations that are significantly involved in epithelial homeostasis and tissue repair (Sanos et al., 2009, Sawa et al., 2011, Ivanov et al., 2008, Ivanov et al., 2009).

1.1.4 The intestinal immune system

The intestinal immune system can be divided into organized lymphoid tissues and effector sites. Organized lymphoid tissues include secondary lymphoid organs, namely the Peyer's patches (PP) of the small intestine and mesenteric lymph nodes. These tissues form prenatally according to a developmental program. In addition, there are inducible organized lymphoid tissues in the form of isolated lymphoid follicles (ILF) that develop postnatally after bacterial colonization. Collectively, these structures are referred to as gut-associated lymphoid tissue (GALT) (Mowat, 2003). Organized lymphoid tissues are regarded as the major inductive sites for intestinal antigen-specific immune responses as well as the regulation of peripheral tolerance. The effector sites of the intestinal immune system are scattered immune cells in the LP and the epithelium. The epithelial layer mainly contains $CD8^+$ T cells (Mowat, 2003). The LP hosts an especially large number of immune cells that belong to diverse lineages of the innate as well as adaptive immune systems, and among them are T cells, IgA-producing plasma cells, DCs and macrophages (Mowat, 2003). The populations of the Innate Lymphoid cell (ILC) family are particularly enriched at these sites, which are increasingly considered to contribute significantly to the maintenance of epithelial barrier integrity. (Spits and Cupedo, 2012).

1.2 Chronic inflammatory bowel diseases

A disruption of the above-mentioned sophisticated interplay between the intestinal epithelium, microbiota and mucosal immune system, that contributes to a stable intestinal barrier function, is found in the pathophysiology of chronic inflammatory bowel diseases.

1.2.1 Definition and etiology

Chronic inflammatory bowel diseases (IBD) are defined as chronic relapsing or progressive inflammatory conditions that lead to a dysfunction of the gastrointestinal epithelium and underlying tissues (Kaser et al., 2010). IBD are comprised of two clinical forms - Crohn's disease (CD) and Ulcerative colitis (UC). The two diseases share the inflammation and degradation of the intestinal wall. Furthermore, they overlap in numerous genetic risk factors and have similar treatment approaches. However, their different clinical presentation, and characteristic anatomical and histologic features make them two independent entities. CD affects all layers of the gut wall and can affect all parts of the gastrointestinal tract. The main symptoms are abdominal pain, fever, diarrhea and weight loss. Its course is frequently complicated by stricturing and fistulation. In UC, the inflammation is limited to the mucosa and submucosa of the colon. It typically manifests with hematochezia, diarrhea with mucus or pus and abdominal cramping. It can lead to severe anemia, a toxic megacolon or colonic perforation. Both diseases can be associated with extra intestinal manifestation and an increased risk for developing other autoimmune disorders, such as psoriasis, primary sclerosing cholangitis, or ankylosing spondylitis (Baumgart and Sandborn, 2007, Wallace et al., 2014)

Etiologically, IBDs have so far been classified as idiopathic. With regard to the pathophysiology, both clinical forms are based on a multifactorial genesis, including genetic, immunologic and environmental factors (Kaser et al., 2010). Central to the pathogenesis is a sustained activated immune reaction that takes place in the affected mucosa itself and from there exhibits systemic effects. There is increasing evidence that an inadequate immune reaction is directed towards the commensal microflora, and based on this, antibodies can be detected that react or cross react with bacterial antigens (Kaser et al., 2010). It has long been known that aberrant adaptive immune mechanisms are implicated in IBD pathogenesis. However, in recent years, multiple studies have indicated that the innate compartment of the intestinal immune system also plays an important part in the disease development and possibly shapes the adaptive mechanisms (Jostins et al., 2012).

1.2.2 Cytokines in the disease pathophysiology and targeted therapy

Cytokines play a major role in the pathogenesis and perpetuation of IBD. They are a heterogeneous group of small proteins that mediate cell signaling and that are crucial in the dialogue between immune cells, epithelial cells and stromal cells of the intestinal mucosa. In the context of intestinal inflammation, it has been observed that there is an imbalance between pro- and anti-inflammatory cytokines, which impedes the resolution of inflammation. As a consequence, a chronic inflammatory condition develops which locally results in tissue destruction and systemically in disease-associated clinical symptoms (Neurath, 2014). In the inflamed mucosa of IBD patients and of colitis mouse models, elevated levels of pro-inflammatory cytokines, among them interleukin 1β (IL-1β), IL-6, Il-17A/F, TNF, IFN-γ, IL-23 and IL-12 (in particular in Crohn's disease) and IL-5 and IL-13 (in particular in ulcerative colitis) as well as reduced levels of anti-inflammatory cytokines such as IL-10 have been measured (Neurath, 2014). Also, several of the IBD-associated genetic risk loci are linked to cytokines and cytokine signaling, namely *IL-10R*, *IL-6*, *IFN-γ*, *TNF*, *IL-23R* and *IL-2* (Jostins et al., 2012). Consistent with these findings, targeted blocking of pro-inflammatory cytokines by monoclonal antibodies has proven to be an efficient therapy in both Crohn`s disease and Ulcerative colitis. In the standard therapy, the inhibition of TNF has been established for many years. TNF is a membrane-bound protein that can be released to the extracellular space by proteolytic cleavage through a metalloproteinase TNF-converting enzyme (ADAM 17). Known sources of TNF in IBD are effector T cells, $CD14^+$ macrophages, fibroblasts and adipocytes. TNF exhibits pleiotropic pro-inflammatory effects that collectively contribute to a persistent inflammation and tissue destruction - namely, the activation of macrophages and effector T cells, the induction of Paneth cell death and damage of IECs, the production of tissue-degrading metalloproteinases by myofibroblasts and the angiogenesis by endothelial cells. Furthermore, TNF facilitates the survival of effector T cells by mediating apoptosis resistance (Neurath, 2014). The administration of TNF-inhibitors has proven to be a potent treatment option especially in severe disease courses, e.g. steroid-refractory and steroid-dependent conditions, fistulas and extra-intestinal manifestations. To date, they are recommended in moderate-to-severe disease activity in IBD patients who do not respond to the conventional therapy and/or have not tolerated it (Torres et al., 2020). However, in the course of the anti-TNF treatment, adverse effects and loss of efficiency can be two limiting factors. The major adverse effects are allergic reactions, reactivation of chronic infections such as tuberculosis or herpes simplex virus infection, and opportunistic infections. In addition, long-term TNF therapy may be associated with a higher risk for malignancy such as the hepatosplenic T cell lymphoma, though the

corresponding long term studies are still pending (Dignass et al., 2010). Thus, there are subgroups of patients who primarily do not respond to anti-TNF therapy, lose response over time and/or show adverse effects. Therefore, the development of further targeted therapeutic agents has been a focus of intense investigation (Table 1).

	Crohn's disease	Ulcerative colitis	Remarks
Cytokines			
TNF inhibitors			
Infliximab	✓	✓	
Adalimumab	✓	✓	
Certolizumab	✓	Phase II trial ongoing	
Golimumab	(✓)*	✓	* Retrospective studies in Crohn's disease
Etanercept	Not effective	No data	
IL-23/Th17			
Ustekinumab	✓	Phase III trial ongoing	
Risankizumab	✓ (phase II)	Phase III trial ongoing	
Brazikumab	✓ (phase II)	Phase II trial ongoing	
Mirikizumab	Phase II trial ongoing	✓ (phase II)	
IL-17			
Secukinumab	Not effective*	No data	* Even higher Crohn's disease activity with secukinumab
IL-6			
Tocilizumab	Not effective*		* Only clinical response
PF-04236921	✓ (phase II)*		* Higher rates of perforation
PDE4 inhibitor			
Apremilast	No data	✓ (phase II)	
JAK inhibitors			
Tofacitinib	Not effective (phase II)	✓	
Filgotinib	✓*	Phase III trial ongoing	* Mucosal healing comparable to that with placebo
Upadacitinib	✓ (phase II)	Phase III trial ongoing	
Peficitinib	No data	Not effective*	* Trends for increased remission and response
Anti-trafficking therapies			
Anti-cell adhesion			
Natalizumab	✓	No data (only one open-label trial)	Increased risk of PML
Vedolizumab	✓	✓	
Etrolizumab	Phase III trial ongoing	✓ (phase II)	
Abrilumab	Not effective (phase II)	✓ (phase II)	
Anti-MAdCAM-1			
PF-00547659	Not effective*	✓ (phase II)	* High placebo clinical response and remission rates
Small-molecule integrin antagonists			
AJM300	Not effective	✓	
PTG-100	No data	Phase II trial stopped	Study discontinued due to futility-based outcome
S1P receptor modulators			
Ozanimod	Phase III trial ongoing	✓ (phase II)	
Etrasimod	No data	✓ (phase II)	

Table 1 Targeted therapy in IBD

Table taken with kind permission from Schreiner et al., 2019

The administration of two other monoclonal antibodies has been approved and incorporated into the treatment guidelines in moderate-to-severe CD. Ustekinumab binds to the p40 subunit shared by the pro-inflammatory cytokines IL-12 and IL-23. Vedolizumab blocks the α4β7 integrin and results in a gut-selective anti-inflammatory activity. It is thus considered an anti-trafficking therapy (Torres et al., 2020). However, other monoclonal antibodies that likewise block pro-inflammatory cytokines that are known to be involved in the disease pathophysiology have not been efficient. The anti-IL-17A antibody Secukinumab has even led to an aggravation of the disease activity (Schreiner et al., 2019). These findings reflect that the underlying

immunopathologic mechanisms and cytokine networks of the disease are highly complex and that deepening their understanding promises a refinement and extension of targeted therapy.

1.3 Innate Lymphoid cells

ILC are a heterogeneous group of innate immune cells that all share a lymphoid morphology and developmental requirements such as the transcription factor inhibitor of DNA binding (Id2) and the cytokine receptor γ-chain. Being part of the innate immune system, they do not undergo recombination-activating gene dependent receptor rearrangement - a mechanism by which adaptive immune cells acquire antigen specificity (Spits and Cupedo, 2012). Instead, their differentiation and activation state mainly depend on cytokines and the direct recognition of cellular ligands and pathogen-associated molecular patterns (PAMP) (Killig et al., 2014). Besides the above-mentioned shared features of ILC, the ILC subsets differ substantially with regard to tissue distribution, differentiation requirements, and physiologic functions. Their differentiation is a result of different cytokine signaling and master transcription factors. For example, whereas IL-15 induces the development of ILC progenitor cells into Eomesodermin expressing NK cells, IL-7 induces the development into retinoic acid receptor (RAR)-related orphan receptor gamma t^+ ($ROR\gamma t^+$) ILC and $GATA3^+$ ILC. To address these differences, a classification for ILC subsets was suggested that is based on developmental, phenotypic and functional characteristics (Figure 3) (Vivier et al., 2018).

Natural killer cells express the T-box transcription factors T-bet and Eomesodermin (EOMES) and developmentally depend on IL-15. They display cytotoxic activity and their main function lies in anti-tumor activity and defense against intracellular viruses and other intracellular pathogens (Vivier et al., 2008). ILC1 express high levels of T-bet, but in contrast to NK cells, they mostly do not express EOMES (Spits et al., 2013). For their differentiation, they depend on the cytokine IL-7 and the transcription factor GATA3. They are non- or weakly cytotoxic and produce IFN-γ and GM-CSF at much higher levels than cNK cells. It has been shown that ILC1 are protective against viruses, certain bacteria, and protozoa such as the intracellular Toxoplasmosis gondii. However, their physiologic function has not been fully resolved yet (Klose et al., 2014).

ILC2 require the transcription factor GATA3 and the RAR-related orphan receptor alpha (RORα) (Price et al., 2010, Moro et al., 2010) for their differentiation and function. They produce the effector cytokines IL-4, IL-5, IL-13 in response to IL-25 and IL-33 (Monticelli et

al., 2011, Mjosberg et al., 2011, Neill et al., 2010). These cytokines correspond to the cytokine profile of T helper type 2 (Th2) cells and in line with this, ILC2, like Th2 cells, have been shown to be involved in the defense against helminth infections (Neill et al., 2010). Moreover, ILC2

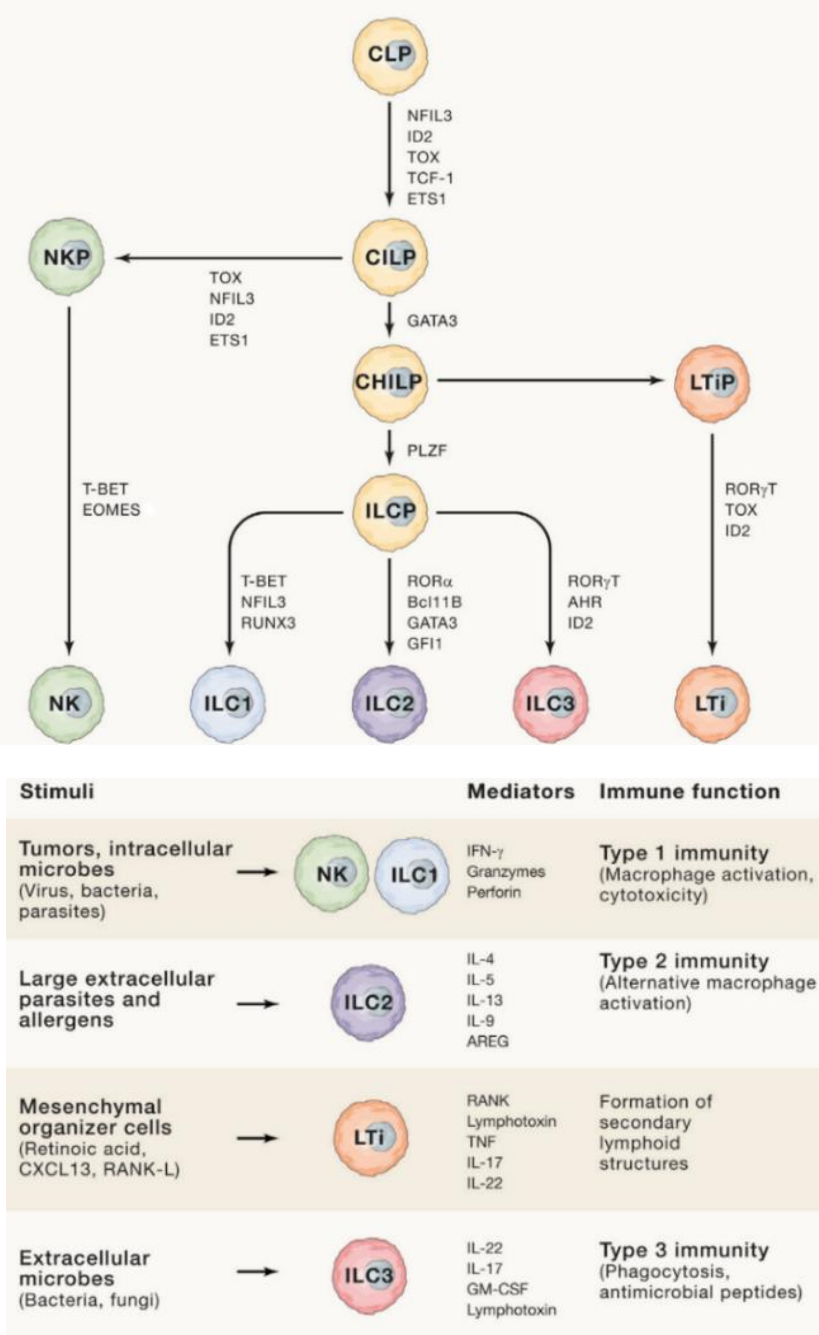

Figure 3 Developmental relationship, classification and function of Innate Lymphoid cells

Above: ILC development is schematizied as it is known mainly from mouse ILC developmental paths. CLP - common lymphoid progenitors, CILP - common innate lympoid progenitors, NKP - NK cell precursors, CHILP - common helper innate lymphoid progenitor, ILCP - innate lymphoid cell precursors, LTiP - Lymphoid tissue inducer progenitors. *Below*: Summary of the most known immunologic function of the five ILC subsets. Figures taken with kind permission from Vivier et. al., 2018 (License number 5006980111623)

.

express the epidermal growth factor family member amphiregulin and have been implied in airway epithelium recovery after influenza virus infection (Monticelli et al., 2011).

Lymphoid tissue inducer (LTi) cells have been discovered in the context of prenatal lymphoid organogenesis. They are one of the first cells clustering at the site of future lymph nodes (LN), the lymph node anlagen (Mebius, 2003). It has been shown that they are indispensable in the development of LNs and PPs. Mice deficient in *Id2* and *Rorc* lack LTi cells and neither form LNs nor PPs. Furthermore, these mice fail to form cryptopatches and ILFs postnatally (Eberl, 2005). In humans, LTi are defined as $CD3^-$ $CD4^-$ IL-7Rα^+ ($CD127^+$) RORγt^+ cells (Cupedo et al., 2009). They express lymphotoxin $\alpha_1\beta_2$, which is important for the interaction with mesenchymal lymphoid tissue organizers. Ligation of the lymphotoxin β-receptor on the latter results in the secretion of chemokines and adhesion molecules, subsequently leading to the attraction and retention of more LTi, B and T cells and DCs that build up the lymphoid tissue (Mebius, 2003).

1.4 ILC3 and their role in intestinal homeostasis and in inflammatory bowel diseases

Postnatal RORγt^+ ILC3 are highly enriched at mucosal sites and secondary lymphoid organs. In particular, they are found in humans in tonsils (Cupedo et al., 2009, Cella et al., 2009, Crellin et al., 2010, Hoorweg et al., 2012), in the intestinal LP (Cella et al., 2009, Takayama et al., 2010, Geremia et al., 2011), and PPs (Cella et al., 2009). Additionally, ILC3 are present in the human skin, but very few are found in the peripheral blood (Teunissen et al., 2014). Similarly as in humans, in mice RORγt^+ ILC3 are mainly present in the intestinal LP (Satoh-Takayama et al., 2009, Luci et al., 2009, Cupedo et al., 2009), either scattered or clustered in cryptopatches and ILFs. Furthermore, a small population of splenic RORγt^+ ILC3 has been found both in humans and mice (Magri et al., 2014, Takatori et al., 2009).

1.4.1 Phenotype and developmental requirements of RORγt^+ ILC3

RORγt^+ ILC3 are characterized by the expression of the cytokines IL-22 and/or IL-17, and by their developmental dependency on the transcription factor RORγt encoded by the *RORC* gene in humans or *Rorc* in mice. They require IL-7 signaling and express the IL-7 receptor α (IL-7Rα) uniformly (Spits et al., 2013). Moreover, they express the receptor tyrosine kinase c-kit (CD117), the IL-23 receptor (IL-23R) and, similarly to fetal LTi cells, lymphotoxin α and β, albeit at lower levels. With NK cells they partially share the expression of natural cytotoxicity

receptors (NCR) and CD56. Contrarily to NK cells, they do not express perforin and only slightly express granzyme B (Cella et al., 2009, Cupedo et al., 2009).

RORγt$^+$ ILC3 can be divided into two subsets according to the expression of the NCR NKp44 (in humans) and NKp46 (in mice). In tonsils, PPs, and intestinal LP, NKp44$^+$ and NKp44$^-$ RORγt$^+$ ILC3 are discriminated and the former subset exhibits a preferential expression of IL-22, but no IL-17 (Cella et al., 2009, Hoorweg et al., 2012). IL-17 expressing NKp44$^-$ RORγt$^+$ ILC3 are found in fetal mesenteric LNs (Hoorweg et al., 2012). CD56 is another surface molecule that RORγt$^+$ ILC3 share with NK cells. In human tonsils, approximately 50% of RORγt$^+$ ILC3 express CD56 (Hoorweg et al., 2012). In mice, NKp44 is not conserved and instead, two main subsets have been distinguished according to the expression of the chemokine receptor type 6 (CCR6) and the NCR NKp46. A study has shown that CCR6$^+$ RORγt$^+$ ILC3 neither express T-bet nor NKp46, and produce IL-22 and IL-17. CCR6$^-$ RORγt$^+$ ILC3 express T-bet and NKp46 and produce IL-22, IFN-γ and TNF-α (Klose et al., 2013). In human RORγt$^+$ ILC3, this co-expression of RORγt and T-bet has not been observed so far, whereas CCR6 is uniformly expressed.

The current concept of the development considers peripheral tissue-resident ILC to be non-self-regenerating and a fate mapping study has shown that LP RORγt$^+$ ILC have a half-life of between 22-26 days (Sawa et al., 2010). Constant regeneration starts with a CD34$^+$ hematopoietic progenitor cell (HPC) that has been identified in the bone marrow, tonsil, and the peripheral blood (Montaldo et al., 2014). From thereon, differential expression of transcription factors as well as signals derived from cytokines or from the environment determine the lineage commitment into different lymphocyte populations. For ILC3 lineage commitment, acquisition of the transcription factor RORγt$^+$ is the key element. The developmental steps preceding RORγt$^+$ acquisition have only vaguely been described in humans. However, in mice it has been shown that these steps firstly include an Id2-expressing precursor cell for all ILC cells, the common innate lymphoid progenitors (CILP). Secondly, a common helper innate lymphoid progenitor (CHILP) gives rise to the Lymphoid Tissue inducer progenitors (LTiP) as well as to Innate Lymphoid cell precursors (ILCP), which differentiate further into ILC1, ILC2 and ILC3. (Klose et al., 2014, Vivier et al., 2018). The developmental pathway and the required transcription factors are displayed in detail in Figure 3. In humans, a CD34$^+$ RORγt$^+$ cell has been identified that preferentially differentiates into mature, IL-22-producing RORγt$^+$ ILC. Notably, CD34$^+$RORγt$^+$ cells were exclusively found in the tonsil and the intestinal LP, but not in the bone marrow, thymus, or peripheral blood (Montaldo et al.,

2014). Thus, the final differentiation and the acquisition of effector functions seems to take place at peripheral effector sites, in close proximity to the lumen of the gastrointestinal tract, with its commensal microflora and environmental antigens. The differentiation and maintenance of RORγt$^+$ ILC3 depends, among other factors, on the activity of the aryl hydrocarbon receptor (AhR) which can be ligated by exogenous ligands derived from bacteria or plants. Additionally, there is evidence that the commensal microflora influences the differentiation of RORγt$^+$ ILC3, and in particular of the NCR$^+$ RORγt$^+$ ILC3 subset. Studies have shown that gnotobiotic mice exhibit largely reduced numbers of IL-22-producing NKp46$^+$ ILC3 (Satoh-Takayama et al., 2009, Sanos et al., 2009).

1.4.2 Regulation of the RORγt$^+$ ILC3 activation status

Similarly to the development of RORγt$^+$ILC3, their activation status seems to be regulated by the cytokine milieu on the one hand and environmental signals on the other. Basic requirements for the production of IL-22 are Id2 and RORγt, which are also indispensable for the development of RORγt$^+$ ILC3. Furthermore, The AhR plays an important role in IL-22 expression. RORγt interacts with AhR and facilitates its binding to the IL-22 gene locus (Qiu et al., 2012). One of the main stimuli for IL-22 expression has been shown to be IL-23, both *in vitro* (Cella et al., 2009) as well as *in vivo* upon infection with Citrobacter rodentium or Helicobacter hepaticus (Zheng et al., 2008, Sawa et al., 2011, Buonocore et al., 2010). IL-23 can be derived from activated DCs or macrophages (Sanos et al., 2009, Cella et al., 2009, Takayama et al., 2010, Longman et al., 2014). However, in the steady state *in vivo*, IL-22 production seems to be little influenced by IL-23. Nearly no difference has been observed between wild-type mice and IL-23-deficient mice or wild-type mice treated with neutralizing anti-IL23R antibodies (Sawa et al., 2011). Instead, it has been observed that IL-1β is important for both the basal as well as the IL-23-induced production of IL-22 (Reynders et al., 2011). Another important signaling pathway for IL-22 production includes lymphotoxin. RORγt$^+$ ILC3 express lymphotoxin α and lymphotoxin β. The lymphotoxin beta receptor (LTβR), expressed among others by DCs, is critical for IL-22 production upon infection in Citrobacter rodentium. It is possible that this dependence exists through a positive feedback loop between DCs and RORγt$^+$ ILC3 (Tumanov et al., 2011). There is evidence that IL-22 expression is additionally regulated by epithelial cells and the commensal microflora. A study has shown that epithelial cells upregulate IL-25 in the presence of the commensal microflora, which indirectly represses IL-22 expression. In line with this concept, RORγt$^+$ ILC3 of IL-25-deficient mice exhibit a significantly higher IL-22 production, and this can be repressed by oral administration

of recombinant IL-25. However, upon infection or tissue injury, this repression is abrogated and RORγt$^+$ ILC3 take up full IL-22 expression (Sawa et al., 2011).

Besides IL-22, RORγt$^+$ ILC3 are capable of expressing the pro-inflammatory cytokines TNF, IL-17 and IFN-γ. To date, the stimulus requirements for their expression has been poorly understood. TNF expression has been observed *ex vivo* in human tonsil RORγt$^+$ ILC3 (Cupedo et al., 2009), as well as in human LP RORγt$^+$ ILC3 in inflammation (Takayama et al., 2010). Similarly, IL-17 production has been mainly observed in inflammation. IL-17 transcription has been found in *ex vivo* isolated LP RORγt$^+$ ILC3 from human inflamed mucosa (Geremia et al., 2011), as well as upon stimulation with IL-23 (Buonocore et al., 2010, Powell et al., 2012). Also, IL-17 expression independent from IL-23 has been observed in the defense against Candida albicans (Gladiator et al., 2013). Finally, IFN-γ has mainly been observed in mice after downregulation of RORγt and upregulation of T-bet under the influence of IL-12 and IL-18 (Vonarbourg et al., 2010, Klose et al., 2013).

1.4.3 Natural cytotoxicity receptors

RORγt$^+$ ILC3 can be divided into two functionally different subsets according to their NCR expression, these being NKp44 in humans and NKp46 in mice. The NKp44$^+$ subset preferentially produces IL-22 (Cella et al., 2009, Hoorweg et al., 2012). However, whether NKp44 or NKp46 are functional in RORγt$^+$ ILC3 and are ligated *in vivo* remains elusive so far.

NCRs have primarily been discovered and investigated in NK cells. In that context, signaling via NCRs leads to HLA class I-independent NK cell activation, including cytotoxic activity and cytokine production (Moretta et al., 2001). NCRs comprise three receptors: NKp46 (NCR1) (Sivori et al., 1997), NKp44 (NCR2) (Vitale et al., 1998), and NKp30 (NCR3) (Pende et al., 1999). All of them are expressed by RORγt$^+$ ILC3, although at lower levels than by NK cells (Cupedo et al., 2009).

The three NCRs are all type I transmembrane proteins. They are composed of an extracellular portion, a transmembrane portion with one single α helix, and a cytoplasmic tail. Within the extracellular portion, all of the NCRs have one or two immunoglobulin-like domains and are therefore assigned to the immunoglobulin superfamily (Cantoni et al., 1999). NKp46 has two C-type Ig-like domains, NKp44 has one single V-type Ig-like domain and NKp30 a V-like Ig domain or a C-type like domain, depending on the splicing variant (Kruse et al., 2014). NCRs have long been considered to be exclusively activating receptors. However more recently,

inhibitory effects on NK cell activity have also been described (Kruse et al., 2014). The corresponding activating and inhibitory signaling cascades include the pathways listed below. Upon ligand binding, receptor molecules are cross-linked, forming homodimers, and associate with a transmembrane adaptor molecule that contains an immunoreceptor tyrosine-based activation motif (ITAM). As a consequence, the so-called “first line” protein tyrosine kinases of the Src family phosphorylate the ITAM. Subsequently, “second line” protein tyrosine kinases of the Syk family are recruited and activated. Next, a series of transmembrane and cytosolic adaptor molecules are activated, which finally results in calcium influx into the cell, and thus cytotoxic activity and cytokine secretion (Vivier et al., 2004). The adaptor molecule of NKp44 is DNAX-activating protein (DAP12), whereas NKp46 utilizes CD3 zeta chain (CD3ζ) and Fc receptor gamma chain (FcRγ), and NKp30 only uses FcRγ (Vivier et al., 2004). Despite associating with different adaptor molecules, the NCRs exhibit synergism in NK cell activation, and cross-phosphorylation is thought to be the underlying mechanism (Moretta et al., 2001, Augugliaro et al., 2003).

1.4.4 Natural cytotoxicity receptor ligands

Multiple studies have shown that NCRs play an essential role in recognizing danger signals, such as pathogens or pathologic changes of a host cell, subsequently leading to their lysis. However, the identity of these ligands has so far been poorly characterized. Several methods have been developed that detect NCR ligand expression, albeit without knowing the ligand’s molecular identity. NCR-fc fusion proteins were constructed by cloning, in which the extracellular portions of the NCRs were fused to the fc portion of human IgG (Mandelboim et al., 2001). Another group fused an aminoterminal leucine-zipper (ILZ) to the extracellular portions of the NCRs. The NCR could then be detected after staining with an anti-ILZ antibody (Byrd et al., 2007). With these methods at hand, a broad spectrum of primary cells, tumor cell lines, bacteria as well as viral components have been investigated for NCR ligand expression.

The first NCR ligands identified were the viral proteins hemagglutinin (HA) of the influenza virus (IV) and hemagglutinin neuraminidase (HN) of the Sendai virus. It was reported that both NKp46 (Mandelboim et al., 2001) and NKp44, but not NKp30 (Arnon et al., 2001), bind IV HA and HN. Additionally, HAs of other viruses, for example of the Newcastle disease virus (Jarahian et al., 2009), have been shown to be ligands of NKp44 and NKp46. The corresponding experiments were performed *in vitro*, by using either virally infected cells or cells that were transfected with an expression plasmid of HA or HN. However, addressing the significance of

NCR engagement during viral infection in a mouse model is limited, since NKp44 and NKp30 are not expressed by rodents (Moretta et al., 2001). But indeed, NKp46-deficient mice are more often subjected to severe influenza infection than control mice, suggesting a critical role of NCR in combating influenza virus *in vivo* (Gazit et al., 2006). Besides HAs, several other viral components ligate NCRs. For example, the envelope glycoproteins of Dengue and West Nile virus activate NK cell cytotoxicity via NKp44 (Hershkovitz et al., 2009). The main tegmentum protein of human cytomegalovirus inhibits NK cell cytotoxicity via NKp30 (Arnon et al., 2005). In addition to viral components, bacterial ones have been identified as pathogen-derived NCR ligands. It was shown that Mycobacterium bovis Bacille Calmette-Guérin, Mycobacterium tuberculosis, mycobacteria-related species of Nocardia farcinica, and Pseudomonas aeruginosa express ligands of the NKp44 receptor (Esin et al., 2008). Besides these exogenous ligands, there is clear evidence for endogenous ligands, since it has been shown that NCR are involved in NK cell lysis of tumor cells (Moretta et al., 2001). A broad variety of tumor cell lines have been shown to express NCR ligands (Arnon et al., 2001, Byrd et al., 2007). The density of NCR expression correlates with the strength of NK cell cytolytic activity against non-MCH class I-bearing tumor cells (Moretta et al., 2001). Despite this evidence, the molecular identity of endogenous ligands is only beginning to be understood.

1.4.5 Physiologic functions of IL-22-producing lamina propria RORγt$^+$ ILC3

RORγt$^+$ ILC3 are mainly found at mucosal sites and are the predominant ILC subset in the intestinal lamina propria. According to the current knowledge, the main function of RORγt$^+$ ILC3 lies in the maintenance of the intestinal homeostasis and the innate immune response against extracellular bacteria. Their hallmark cytokine is IL-22. Besides this, they are also capable of producing TNF, IL-17A, GMCSF, IL-2, IL-13 and IFN-γ, depending on the tissue and the context of activation (Klose and Artis, 2016, Vivier et al., 2018, Artis and Spits, 2015).

The cytokine IL-22 plays a key role in the tissue homeostatic functions of RORγt$^+$ ILC3. The IL-22 receptor is exclusively expressed by non-hematopoietic cells and in the intestine especially by epithelial cells. It is known that IL-22 exerts several beneficial effects on epithelial cells that contribute to the maintenance of epithelial integrity, innate immunity against pathogens, and tissue regeneration after injury or inflammation (Sonnenberg et al., 2011a). IL-22 is also produced by different T cell subsets and in particular by the Th17 subset. But it has been shown that the main IL-22 producers of the intestinal LP are RORγt$^+$ ILC3 (Sanos et al., 2009, Sawa et al., 2011). Furthermore, mucosal IL-22 is not significantly reduced in *RAG*-

deficient mice, as they lack all mature T cells (Satoh-Takayama et al., 2009, Cella et al., 2009). In the following, the most important functions of IL-22 and IL-22-producing LP RORγt$^+$ ILC3 are summarized.

Maintenance of the epithelial integrity: The intestinal epithelium is in charge of keeping the commensal bacteria and pathogens from crossing the epithelial barrier. IL-22 substantially supports this function by inducing the production of AMPs, such as β-defensins (Brand et al., 2006), RegIIIβ and γ (Zheng et al., 2008). Furthermore, it induces mucus production by goblet cells that builds up a physical barrier on top of the epithelial layer (Sugimoto et al., 2008). Apart from IL-22-induced innate defense mechanisms, RORγt$^+$ ILC3 are involved in T cell-dependent and T cell-independent IgA production via lymphotoxin signaling, namely the production of soluble lymphotoxin α_3 and the surface expression of lymphotoxin $\alpha_1\beta_2$ (Kruglov et al., 2013).

Innate defense against pathogens: IL-22-producing RORγt$^+$ ILC3 have been shown to play a critical role in the early defense against extracellular bacteria, such as the gram-negative bacterium Citrobacter rodentium. They contribute to this defense by mediating acute inflammation in response to infection, inclusively of the upregulation of chemokines and AMPs (Zheng et al., 2008, Satoh-Takayama et al., 2009, Cella et al., 2009, Sonnenberg et al., 2011b). Also, they have been shown to keep intestinal commensal bacteria from systemic dissemination (Sonnenberg et al., 2012). Furthermore, IL-22 can promote colonization by beneficial commensal bacteria, which in return are able to protect the intestinal epithelium from pathogenic microorganisms (Pickard et al., 2014, Pham et al., 2014). In addition to anti-bacterial functions, RORγt$^+$ ILC3 have been shown to be involved in the defense mechanisms against Candida albicans in the oral cavity. This defense mechanism was mediated via IL-17 instead of IL-22 production (Gladiator et al., 2013).

Tissue regeneration: IL-22 signaling facilitates both the proliferation of intestinal epithelial stem cells as well as the migration of epithelial cells. These two functions contribute to epithelial regeneration after tissue injury (Brand et al., 2006, Pickert et al., 2009, Hanash et al., 2012). In line with this function, RORγt$^+$ ILC3-derived IL-22 mediated tissue repair after graft-versus-host-reaction induced destruction of the intestinal mucosa (Hanash et al., 2012).

Anti-inflammatory effects: Upon IL-22 binding, intestinal epithelial cells secrete the anti-inflammatory cytokine IL-10, which in turn was shown to favor the induction of regulatory T cell (Treg) and T helper 2-cell responses over T helper 1-cell responses (Cella et al., 2009, Maloy and Powrie, 2011). Another mechanism by which RORγt$^+$ ILC3 might contribute to

prevent an exuberant activation of pro-inflammatory T cells is by controlling the outgrowth of certain types of commensal bacteria, such as segmented filamentous bacteria that are known to promote pro-inflammatory Th17 cells (Qiu et al., 2013).

1.4.6 Role of RORγt$^+$ ILC3 in IBD

As described in the previous section, IL-22-producing RORγt$^+$ ILC3 perform important, beneficial functions for maintaining intestinal tissue homeostasis and for epithelial barrier integrity. However, there has been increasing evidence that RORγt$^+$ ILC3 can also play a pro-inflammatory role in the pathogenesis of intestinal inflammation.

In order to investigate the role of RORγt$^+$ ILC3 in intestinal inflammation, different types of mouse colitis models have been used that aim to resemble IBD, among them the chemical-induced dextran sulfate sodium (DSS) colitis (Sawa et al., 2011), the agonistic CD40 antibody-induced colitis (Uhlig et al., 2006, Buonocore et al., 2010, Vonarbourg et al., 2010, Fuchs et al., 2013) and the bacteria-induced Helicobacter hepaticus colitis (Buonocore et al., 2010). TRUC mice, that are T-bet- and *RAG*-deficient mice, develop a condition that resembles ulcerative colitis (Garrett et al., 2007).

It has been shown in a murine colitis model that IL-22 ameliorates inflammation by enhancing goblet cell restauration and mucus production (Sugimoto et al., 2008). In a DSS colitis model, IL-23-induced-IL-22 expression by RORγt$^+$ ILC3 is enhanced and confers protection. In comparison to *RAG*-deficient mice, *Rorc*-deficient *RAG*-deficient mice showed a clearly heightened weight loss (Sawa et al., 2011). Furthermore, IL-22-deficient mice show delayed recovery (Sugimoto et al., 2008).

In 2010, the first studies appeared that delivered evidence for a pro-inflammatory role of RORγt$^+$ ILC3 in intestinal inflammation. In an innate colitis model with Helicobacter hepaticus, a Thy1^{high} SCA-1, RORγt$^+$ ILC population mediates inflammation by producing the pro-inflammatory cytokines IL-17 and IFN-γ in response to IL-23. Furthermore, mice deficient of the RORγt$^+$ ILC population (*Rag*$^{-/-}$, *Rorc*$^{-/-}$ mice) develop only mild intestinal inflammation in comparison to *Rag*$^{-/-}$ mice (Buonocore et al., 2010). In innate colitis induced by the agonistic C40 antibody, the Thy1^{high} SCA-1, RORγt$^+$ ILC population produced IFN-γ but not IL-17, and also mediated inflammation (Buonocore et al., 2010). Another murine study observed that NKp46$^+$ RORγt$^+$ ILC progressively lost RORγt expression under the influence of the pro-inflammatory cytokine milieu of IL-12 and IL-15. Whereas NKp46$^+$ RORγt$^+$ ILC produce IL-

22, the NKp46^{+} RORγt^{-} ILC subset produces IFN-y and induces colitis (Vonarbourg et al., 2010). From a TRUC mouse model, it was reported that the colitogenic population consists of IL-17- and (to a smaller extent) IL-22-producing RORγt^{+} ILC. Depletion of them or blockade of IL-17 both attenuate colitis (Powell et al., 2012).

Looking at human studies, ILC subsets have been investigated in the inflamed mucosa of IBD patients. A study by Takayama et al. showed that an IFN-γ-producing CD3^{-} CD56^{+} NKp44^{-} NKp46^{+} RORC^{DULL} CD122^{+} CD127^{-} population is enriched in the inflamed LP of IBD patients, whereas an IL-22-producing CD3^{-} CD56^{+} NKp44^{+} NKp46^{-} RORC^{high} CD122^{-} CD127^{+} ILC population (likely to be RORγt^{+} ILC3) diminished (Takayama et al., 2010). Another study showed an increased frequency of IFN-γ producing CD127^{+} c-kit^{-} NKp44^{-} ILC which express T-bet (assigned to ILC1), at the expense of IL-22-producing NKp44^{+} RORγt^{+} ILC3. The IFN-γ-producing ILC subset can develop *ex vivo* from RORγt^{+} ILC3 under the influence of IL-12, while downregulating RORγt and NKp44 (Bernink et al., 2013). Geremia et al. showed that IL-17 and IL-22 are overexpressed in inflamed mucosa of IBD patients. The significant difference of this cytokine expression is found among innate (CD3^{-}) cells. In particular, CD56^{-} CD127^{+} ILC that show high levels of IL-17 are increased in the intestinal mucosa of IBD patients (Geremia et al., 2011).

Considering these findings from mouse and human studies, it is evident that RORγt^{+} ILC3 are substantially involved in maintaining intestinal tissue homeostasis as well as in the pathogenesis of intestinal inflammation. However, the question of when - and under which conditions - RORγt^{+} ILC3 play either a tissue protective or a pro-inflammatory role needs further investigation. Mechanisms that could underly a possibly variable function of RORγt^{+} ILC3 could be plasticity between ILC subsets, different effector programs, environmental factors, or all of them in combination. Interestingly, the role of RORγt^{+} ILC3 in TNF production during IBD has hardly been investigated yet, despite the fact that TNF is one of the key cytokines involved in the disease development and that targeted therapy with TNF inhibitors is currently the most efficacious treatment (Kaser et al., 2010).

2. Aims of the thesis

The role of IL-22-producing RORγt$^+$ ILC3 in the pathogenesis of intestinal inflammation such as IBD has so far been controversially discussed. On the one hand, this ILC population performs important functions for the epithelial barrier integrity and maintenance of intestinal tissue homeostasis. These functions are mainly mediated through the production of their signature cytokine IL-22. On the other hand, increasing evidence from murine and human studies suggests a tissue-damaging, pro-inflammatory role in the context of intestinal inflammation. Elucidating the biologic conditions and environmental factors that potentially direct RORγt$^+$ ILC3 to either function could lead to a better understanding of their contribution to disease development and ultimately to a potential therapeutic intervention.

Besides IL-22, RORγt$^+$ ILC3 are able to produce further cytokines such as granulocyte-macrophage colony-stimulating factor (GM-CSF), tumor necrosis factor (TNF), IL-2, IL-17 and interferon-γ (IFN-γ). It is well established that their cytokine-secretion profile is regulated by other cytokines, primarily IL-23 and IL-1β, and by environmental signals that stimulate the aryl hydrocarbon receptor and other pattern recognition receptors. The contribution of receptor-ligand interactions in regulating pro- versus anti-inflammatory fate decisions is less well understood.

Our work group has previously shown that the natural cytotoxicity receptor NKp44 is expressed and functional in human RORγt$^+$ ILC3. In particular, crosslinking of the NKp44 receptor in tonsil-derived RORγt$^+$ ILC3 by a monoclonal antibody results in increased production of the pro-inflammatory cytokine TNF and in a pro-inflammatory transcriptome signature. In contrast, stimulation with specific cytokines (IL-1, IL-7, IL-23) preferentially induces IL-22 production, which has important regenerative functions on the epithelium (data published in Glatzer et al., 2013). The physiologic relevance of NKp44 engagement in RORγt$^+$ ILC3 as well as the nature and distribution of NKp44 ligands remain to be investigated.

The research question of this thesis has been developed on the basis of the preceding results of our work group as well as the controversially discussed role of RORγt$^+$ ILC3 in the development of IBD. We hypothesized that the NKp44 receptor is engaged *in vivo* during intestinal inflammation, possibly directing RORγt$^+$ ILC3 from a tissue-protective role towards a pro-inflammatory activation status. In this thesis, we aimed to investigate the distribution of RORγt$^+$

ILC3 subsets ($NKp44^+/NKp44^-$) in the context of IBD and evaluate a possible physiologic NKp44 engagement.

Specifically, we defined the following sub-aims:

- to investigate the distribution of $ROR\gamma t^+$ ILC3 subsets ($NKp44^+/NKp44^-$) in the inflamed and non-inflamed intestinal lamina propria of IBD patients by Flow Cytometry
- to evaluate potential ligands of NKp44 leading to activation of $ROR\gamma t^+$ ILC3

3. Material and methods

3.1 Materials

Glass and plastic ware, buffers, chemicals and culture media as well as devices and software used for this thesis are summarized in the following tables (Tables 2-4). The remaining reagents are marked in the text.

3.1.1 Glass and plastic ware

Glass and plastic ware	Manufacturer
Cell culture flasks (25 cm^2 and 75 cm^2)	Greiner bio-one
Cell strainer (100 µm)	BD Biosciences
Conical centrifuge tubes (Falcon 15 ml and 50 ml)	BD Biosciences
Round bottom tubes (Falcon 5 ml)	BD Biosciences
Glass pipettes (5, 10, 20 ml)	Eppendorf
Pipette tips (10, 20, 100, 200 µl)	Sarstedt
Petri dish (10 mm diameter)	Greiner Bio-One
Plastic pipettes sterile (5, 10, 20 ml)	Greiner Bio-One
Safe-lock-tubes (0.5, 1.5, 2 ml)	Eppendorf
Steel sieve	Carl Roth
Syringe (5 ml)	BD Biosciences
96-well microtiter plate (round bottom)	Greiner Bio-One

Table 2 Glass and plastic ware

3.1.2 Buffers, chemicals and culture media

Reagent	Description / Substances	Manufacturer
Brefeldin A	Inhibitor of protein secretion by interfering with the transport from the endoplasmic reticulum to the Golgi apparatus	Sigma Aldrich
BSA	Bovine serum albumin	Boehringer Mannheim GmbH
DMEM	Dulbecco's modified eagle medium, supplemented with: - 2-mercaptoethanol - penicillin 100 U/ml - streptomycin 0.1 mg/ml - 10% fetal calf serum	Gibco, Life Technologies Sigma Aldrich Gibco, Life Technologies Gibco, Life Technologies Sigma Aldrich

EDTA	Ethylenedinitrilotetraacetic acid disodium salt dihydrate, used as chelator in PBS pH = 7.2	Merck
Enzyme-free dissociation buffer	Detaches adherent cells from the cell culture flask wall without enzymatic activity	Gibco, Life Technologies
Gentamycin	Antibiotic used at 50 µg/ml	GE Healthcare Life Sciences
Influenza virus infection buffer	PBS supplemented with: - 0.1% BSA - 0.1 mg/ml $MgCl_2$ - 0.1 mg/ml $CaCl_2$	DRFZ Boehringer Mannheim GmbH Sigma Aldrich Sigma Aldrich
Influenza virus infection medium	DMEM supplemented with: - 2-mercaptoethanol - penicillin 100 U/ml - streptomycin 0.1 mg/ml - 0.1% BSA	 Sigma Aldrich Gibco, Life Technologies Gibco, Life Technologies Boehringer Mannheim GmbH
Paraformaldehyde 16%	Fixation reagent, diluted with PBS down to a concentration of 2%	Electron Microscopy Sciences
PBS	Phosphate buffered saline Water based salt solution containing: - 1.5 mM KH_2PO_4 - 2.7 mM KCl - 8.1 mM Na_2HPO_4 - 137 mM NaCl	DRFZ Merck Roth Roth Th. Greyer
PBS/BSA	5 g/l (5%) in PBS-buffer	DRFZ
PBS/BSA/EDTA	2 mM EDTA in PBS/BSA-buffer	DRFZ
Penicillin	Antibiotic used at 100 U/ml	Gibco, Life Technologies
RNAse Away® Reagent	Removes RNase and DNA contamination	Ambion, Life Technologies
RPMI 1640	Roswell Park Memorial Institute medium 1640 supplemented with: - 2-mercaptoethanol - penicillin 100 U/ml - streptomycin 0.1 mg/ml - 10% human AB serum or 10% fetal calf serum	Gibco, Life Technologies Sigma Aldrich Gibco, Life Technologies Gibco, Life Technologies Lonza/Sigma Aldrich
Saponin	Cell wall permeabilizing reagent Used at 0.5% dissolved in PBS	Sigma Aldrich
Streptomycin	Antibiotic used at 0.1 µg/ml	Gibco, Life Technologies
Trypsin-EDTA	0.05%	Gibco, Life Technologies

Table 3 Buffer, chemicals and culture media

3.1.3 Devices and software

Device / Software	Manufacturer
Cell counter Casy®	Schärfe Systems
FACSDiva™ 6.0 software	BD Biosciences
FACSCanto™ II	BD Biosciences
FACSAria™ II	BD Biosciences
Freezer -20°C	Liebherr
Fridge 4°C	Liebherr
GraphPad Prism version 6	GraphPad Software
Herasafe™ (Laminar flow box)	Thermo Scientific
Incubator 37°C, 5% CO_2	Thermo Scientific
NanoDrop	Peglab
PCR cycler (Thermocycler)	Biometra
Pipettes (2, 5, 10, 20, 200, 1000 µl)	Eppendorf
Pipetting aid accu-jet®pro	Brand
QuadroMACS™ Separator	Miltenyi Biotec
Single cell analysis software FlowJo	Tree Star
StepOnePlus™ real-time PCR system	Applied Biosystems, Life Technologies
Microcentrifuge Heraeus™ Fresco™ 17	Thermo Scientific
Ultracentrifuges:	
- Heraeus™ Multifuge 3SR	Thermo Scientific
- Heraeus™ Megafuge 1.0	Thermo Scientific
Vacuum pump	Vacuubrand
Vortex-Genie	Scientific Industries
Water bath 37°C	Memmert

Table 4 Devices and software

3.2 Cell line culture

The following cell lines were purchased from American Type Culture Collection (ATCC): Caco2 (human colorectal carcinoma cell line), HEK293T (human embryonic kidney cell line), HT29 (human colon adenocarcinoma cell line), MDCK (Madin-Darby canine kidney cell line) and SW620 (human colon adenocarcinoma cell line). In addition, hemagglutinin 5 transfected HEK293T (H5-HEK293T) as well as the NKp44-reporter cell line BW-NKp44 and the control cell line BW (murine thymoma cells) were kindly provided by O. Mandelboim (Hebrew University Hadassah Medical School, Jerusalem, Israel). Cell lines were either cultured in DMEM (Caco2, HEK293T, H5-HEK293T, MDCK, SW620) or RPMI 1640 (HT29, BW, BW-NKp44) in 25cm^2 or 75cm^2 cell culture flasks. For maintenance, cell cultures were continuously

incubated at 37° and 5% CO2, and were split every 3 days. Detachment of adherent cells from the cell culture flask wall was performed as follows. Firstly, old cell culture medium was removed entirely and the cell layer was washed two times thoroughly with PBS. Then, either 5 ml of enzyme-free dissociation buffer, or 2 ml of 0.25% Trypsin-EDTA was added and distributed evenly on the cell layer. Excessive detachment solution was removed after approximately 30 seconds. After incubation for 10 minutes at 37°C, new cell culture medium was added, cells were suspended by gentle pipette action, and were then finally transferred to new cell culture flasks. All work with the cell culture was performed with sterile equipment and in the sterile environment of the laminar flow box.

3.3 Cell isolation of human tissue samples

3.3.1 Acquisition of human tissue samples

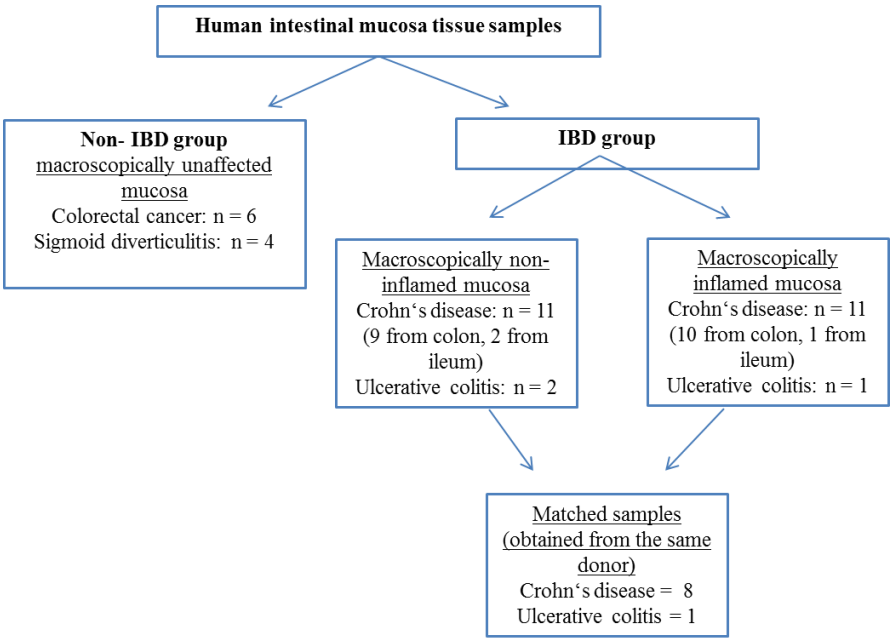

Figure 4 Origin of human intestinal mucosa tissue samples

Human intestinal mucosa samples were obtained from surgical resections of patients undergoing either partial or total colectomy because of colorectal carcinoma (CRC), sigmoid diverticulitis, ulcerative colitis (UC) or Crohn's disease (CD), or partial small bowel resection because of Crohn's disease (Figure 4). From CD and UC resections, mostly two mucosa samples were sampled, one from macroscopically non-inflamed- and one from macroscopically inflamed mucosa. From CRC and sigmoid diverticulitis resections, tissue was sampled from macroscopically unaffected mucosa. Tissue samples were obtained directly after resection and

were subsequently rinsed with water, put into PBS, 0.1 mg/ml Streptomycin and 50 µg/ml Gentamycin and transported at 4°C to the laboratory.

Human tonsil tissue was obtained from patients undergoing partial or total tonsillectomy.

Written informed consent was obtained from all patients prior to sample acquisition and the experiments were approved by the Ethics Committee of the Charité Medical University, Berlin (EA4/106/11 and EA1/107/10).

3.3.2 Isolation of lamina propria mononuclear cells

Human intestinal mucosa tissue was rinsed with PBS/BSA and cut into approximately 1 cm^2 pieces in a 10 mm diameter petri dish, while visible fat was removed. Tissue pieces were then predigested twice in 50 ml RPMI 1640 (containing 10% human AB serum), 1 mM 1.4-dithio-DL-threitol (AppliChem), 10 mM EDTA, 50 µg/ml Gentamycin, 100 U/mL Penicillin and 0.1 mg/ml Streptomycin for 15 minutes at 37°C while shaking. The predigestion step led to the detachment of the epithelial layer from the lamina propria (LP). Epithelial cells were dissolved in the supernatant medium, whereas the LP was still unaffected. The further isolation of epithelial cells is described in section 3.4.2. LP tissue pieces were rinsed in PBS/BSA/EDTA and cut into smaller pieces of approximately 0.3 - 0.5 cm^2, followed by incubation in 50 ml RPMI 1640 Medium (containing 10% human AB serum), 50µg/ml Gentamycin, 1 mg/ml collagenase (type IV, Sigma Aldrich) and 0.5 mg/ml DNase (type 1, Sigma Aldrich) for 1 h at 37°C while shaking. The resulting cell suspension was filtered through a 100 µm cell strainer. Next, mononuclear cells (MNCs) were isolated from the cell suspension by density gradient centrifugation (Figure 5). For that, each 35 ml of the cell suspension was layered on top of 15 ml lymphocyte separation medium in a 50 ml conical centrifuge tube and centrifuged at 800 x g for 20 minutes at room temperature without brake. The lymphocyte separation medium used was Ficoll-Paque™ (GE Healthcare Life Sciences), which has a density of 1.078 g/ml at 20°C. According to the densities of the different cell types relative to the density of the Ficoll-Paque, different layers form after centrifugation. The bottom layer contains erythrocytes, which aggregate and sediment completely. Above that, granulocytes are found that migrate through the Ficoll-Paque due to a high enough density attained under the osmotic pressure of the Ficoll-Paque medium. Immediately above the Ficoll-Paque layer, the MNCs form a layer that can be visibly distinguished from the overlying medium. Thus, after lymphocyte density centrifugation, the medium was carefully removed and the MNC layer was aspirated and transferred to a new centrifuge tube. The MNCs were washed two times by redissolving in

PBS/BSA/EDTA and centrifuging at 300 x g for 10 minutes at 4°C. The resulting MNCs were used for further flow cytometric analysis and cell sorting, as described in the sections below.

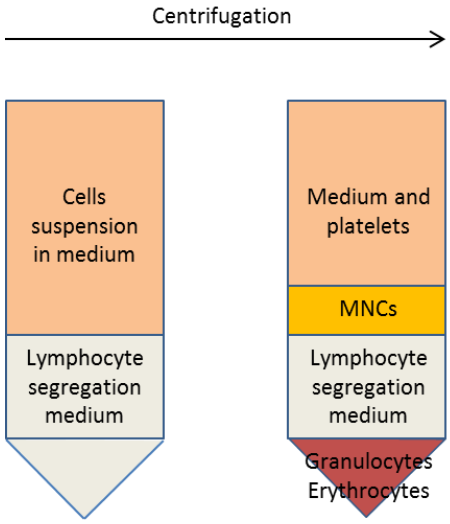

Figure 5 Lymphocyte density centrifugation

The cell suspension (LP cells in medium) was layered on top of a lymphocyte segregation medium in a 50 ml conical centrifuge tube (left). After centrifugation, the mononuclear cells (MNCs) formed a layer between the medium and the lymphocyte segregation medium.

3.3.3 Isolation of intestinal epithelial cells

Intestinal epithelial cells (IECs) were isolated from the same intestinal mucosa samples as the LP MNCs (see sections 3.3.1 and 3.3.2). After the described two-step predigestion (section 3.3.2), epithelial cells were dissolved in the supernatant medium. They were centrifuged at 300 x g for 10 minutes at room temperature and resuspended in RPMI 1640 medium (containing 10% human AB serum) up to a volume of 3 ml. Subsequently, the 3 ml of medium containing IECs was carefully layered on top of a four-layer Percoll density gradient in a 15 ml conical centrifugation tube, as displayed in Figure 6. Percoll (GE Healthcare Life Sciences) consists of colloidal silica particles coated with polyvinylpyrrolidone and has a density of 1,130 g/ml. The different Percoll dilutions (30%, 40%, 60% and 100%) were prepared by diluting with RPMI 1640 medium. The Percoll density centrifugation was performed at 535 x g for 30 minutes at room temperature without brake.

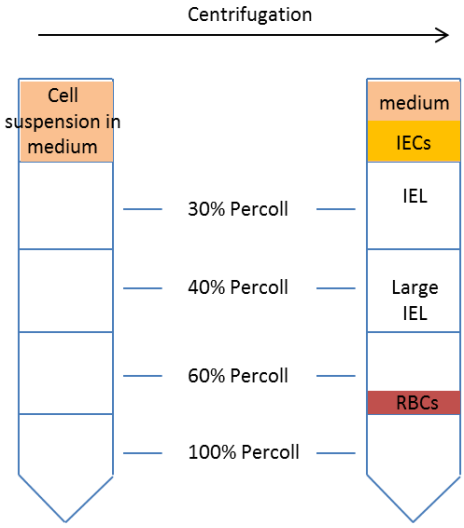

Figure 6 Percoll density centrifugation

Intestinal epithelial cells (IECs) were separated from intraepithelial lymphocytes (IEL) and red blood cells (RBCs) by a four-layer Percoll density centrifugation. After centrifugation, the IECs formed a layer between the medium and the 30% Percoll layer.

Subsequently, IECs were aspirated from the interphase between the medium and the 30% Percoll layer, transferred to a new 15 ml centrifuge tube and washed twice with PBS/BSA, and then centrifuged at 300 x g for 10 minutes at room temperature. IECs were then used for flow cytometric analysis as described below.

3.3.4 Isolation of tonsil mononuclear cells

Tonsil tissue was washed in PBS/BSA/EDTA. It was then cut into approximately 0.5 cm^2 pieces in a 10 mm diameter petri dish and RPMI 1640 (containing 10% human AB serum). Subsequently, it was passed through a sieve by applying gentle pressure with a syringe plunger. The cell suspension obtained thereby was filtered through a 100 µm cell strainer and the MNCs were isolated by density gradient centrifugation as described in section 3.4.1. Before flow cytometric analysis or cell sorting, tonsil-derived MNCs were enriched for $CD56^+$ cells by using magnetic cell separation. Up to 5 x 10^7 MNCs per ml dissolved in PBS/BSA/EDTA were incubated with CD56 microbeads (Miltenyi Biotec) at a ratio of 1:5. LS columns (Miltenyi Biotec) were equilibrated with 1 ml PBS/BSA/EDTA and placed into the magnetic field of a QuadroMACS™ separator (Miltenyi Biotec). The columns were loaded with the CD56 microbead-incubated MNCs. Under rinsing with 1 ml PBS/BSA/EDTA, CD56-labeled cells remained within the column due to the magnetic field, whereas $CD56^-$ cells were washed out and were discarded. After rinsing twice, the columns were removed from the magnetic field and

the positively selected cells were eluted with 2 ml PBS/BSA/EDTA and the application of additional pressure on the column with a syringe plunger. The MNCs positively selected for CD56 were washed with PBS/BSA/EDTA and centrifuged at 300 x g for 10 minutes at 4°C, and were subsequently used for further flow cytometric analysis and cell sorting as described below.

3.4 Flow cytometric analysis and cell sorting

Flow cytometric (FC) analysis was used to analyze the expression of cell surface molecules as well as the expression of intracellular cytokines. Cell sorting enabled the isolation of RORγt^{+} ILC3 for further stimulation experiments (section 3.6) and polymerase chain reaction (PCR) analysis (section 3.7).

The FC analysis used is based on the quantitative detection of fluorescence signals emitted by single cells which are stained with monoclonal antibodies coupled to fluorescent dyes, a method that is also referred to as fluorescence-activated cell sorting. In general, fluorescence-activated cell sorting devices are composed of the following major components: a fluidic system, laser excitation optics, collection optics with photomultipliers, and a connected computer. First, the fluorescently labeled cells are driven through a flow cell under pressure. There, they are lined up into a single-file stream due to hydrodynamic focusing by a sheath flow liquid (Figure 7).

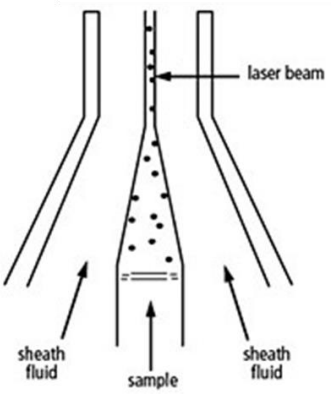

Figure 7 Hydrodynamic focusing in FC analysis

The sample (fluorescently labeled cells) is driven through a flow cell under pressure and cells are lined up into a single-file stream by a sheath flow liquid, an effect referred to as hydrodynamic focusing. Figure taken from BD FACSCanto™ Brochure (Biosciences, 2015).

The single-file cell stream passes by laser beams of different wavelengths that excite the fluorescently labeled cells. The resulting emission light in response to the excitation is detected by the collection optics. Different fluorescent dyes have characteristic peak excitation and

emission wavelengths. In order to detect the different emission wavelengths separately, the emission light of each fluorochrome is directed through spectral filters toward the target detectors by serial light reflection. In the course of this, long pass filters reflect all wavelengths shorter than the actual one. Subsequently, band pass filters allow the transmission of a defined spectrum. Having arrived at the target detector, the photons of the emission light strike a photomultiplier tube, and the signal becomes enhanced and converted into electrical current pulses. Besides the emission signals of the fluorescent dyes, two additional signals are detected for each cell. When the laser beams strike the cell, the light is scattered and diffracted. The detected forward scatter (FSC) light provides information on the relative size of the cells, whereas the side scatter (SSC) light correlates to their granularity (Radbruch, 2000).

The FC device used was FACSCanto™ II (BD Biosciences) and the corresponding software was FACSDiva™ 6.0 (BD Biosciences). The excitation source of FACSCanto II is comprised of three lasers, i.e., a blue (488 nm), red (633 nm) and violet (405 nm) laser. Its collection optics consist of an octagon (with 5 photomultiplier tubes) for the blue laser and a trigon (with 2 photomultiplier tubes) each for the red and the violet laser (Biosciences, 2015). An overview of the FACSCanto II lasers and the fluorochromes used is given in Table 5. Even though each fluorochrome has its own peak emission wavelength, their emission spectra overlap. Taking this into account, single and combined control staining for the fluorochromes were performed on peripheral blood MNCs (staining for CD3, CD14, CD19, CD45, CD56, CD127, NKp44, NKp46), HT29 (staining for CD326 = EpCAM), and HEK293T (staining for NKp44-fc and anti-IgG1), and spectral overlap was compensated manually by comparing the single color median fluorescence intensity of positive and negative cell populations. Data files were exported from the FACSDiva 6.0 software (BD Biosciences) in FCS 3.0 format and analyzed with the FlowJo Software Version 9 (Tree Star).

Laser	Excitation laser wavelength (nm)	Fluorochromes used	Fluorochrome's emission peaks (nm)
Blue	488	FITC	519
		PE	578
		PerCP-Cy5.5	695
		PE-Cy7	785
Red	633	APC	660
		APC-Cy7 / APC-H7	785
Violet	405	Brilliant Violet™ 570	570
		Pacific Blue™ / eFluor®450	455 / 450

Table 5 FACSCanto II lasers with the fluorochromes used

3.4.1 List of monoclonal antibodies

For cell surface and intracellular staining of LP and tonsil-derived MNCs, as well as IECs and epithelial cell lines, monoclonal antibodies conjugated to fluorescent dyes were used. An overview of the monoclonal antibodies used is given in Table 6.

Antibody	Clone	Conjugated fluorochrome	Manufacturer
anti-CD3	UCHT-1	FITC	DRFZ
	SK7	PerCP-Cy5.5	eBioscience
anti-CD14	MφP9	APC-H7	BD Biosciences
anti-CD19	SJ25C1	APC-H7	BD Biosciences
	LC1	PerCP-Cy5.5	eBioscience
anti-CD45	HI 30	Pacific Blue	Biolegend
	2D1	eFluor450	eBioscience
anti-CD56	NCAM16.2	PE-Cy7	BD Biosciences
anti-CD127	A019D5	Brilliant Violet 570	Biolegend
	eBioRDR5	FITC	eBioscience
anti-CD326	HEA-125	PE	Miltenyi Biotec
anti-mouse IgG2	Poly4060	FITC	BioLegend
anti-human IgG1	IS11-12E4.23.20	APC	Miltenyi Biotec
anti-IL-22	14298	PE	R&D
	22URTI	PerCP-5.5	eBioscience
anti-NKp44	2.29	APC	Miltenyi Biotec
	2.29	PE	Miltenyi Biotec
anti-NKp46	9E2	PE	Miltenyi Biotec
anti-TNF	MAb11	APC	BD Biosciences
	MAb11	Pacific Blue	eBioscience

Table 6 List of monoclonal antibodies used for cell surface and intracellular staining

3.4.2 Cell surface staining

Cell surface antigens, classified according to the cluster of differentiation (CD) system, were stained with the above listed monoclonal antibodies conjugated to fluorescent dyes. Up to $1x10^7$ cells/100µl were stained at the indicated titres in the dark at 4° C for 20 minutes, washed afterwards with PBS/BSA, and centrifuged at 300 x g for 10 minutes at 4° C. For the exclusion of non-viable cells in the FC analysis, a LIVE/DEAD® fixable dead cell stain kit (Invitrogen, Life Technologies) was used. The LIVE/DEAD dyes exclusively stain non-viable cells due to a loss of cell membrane integrity and access to amines.

3.4.3 Intracellular staining

After stimulation of LP and tonsil-derived RORγt$^+$ ILC3 as described in section 3.5, intracellular cytokines were stained for FC analysis. For this, the cells were firstly fixated with 2% paraformaldehyde for 10 minutes in the dark at room temperature. Next, the wall of the

fixated cells was permeated by washing in 0.5% saponin (diluted with PBS). Finally, the intracellular cytokines IL-22 and TNF were stained with the corresponding monoclonal antibodies (Table 6) at the indicated titers for 30 minutes at room temperature in the dark, washed afterwards with PBS/BSA, and then centrifuged at 300 x g for 10 minutes at 4° C.

3.4.4 Flow cytometric cell sorting

For stimulation experiments (section 3.6) as well as PCR analysis (section 3.7), human LP ILC3 and human tonsil ILC3 were sorted out from the MNC suspension by fluorescence-activated cell sorting (FACS). FACS sorting was performed with FACSAria^{TM} II (BD Biosciences) by Toralf Kaiser and Jenny Kirsch of the DRFZ flow cytometry core facility. Cell surface molecules were stained as described in section 3.4.2. Human LP MNCs were sorted as viable (LIVE/DEAD negative) CD3$^-$ CD14$^-$ CD19$^-$ CD127$^+$ cells (RORγt$^+$ ILC3). Human tonsil CD56-enriched MNCs were sorted as viable CD3$^-$ CD19$^-$ CD127$^+$ CD56$^+$ cells (RORγt$^+$ ILC3) or as CD3$^-$ CD19$^-$ CD127$^+$ CD56$^+$ NKp44$^{+/-}$ cells (NKp44$^+$ or NKp44$^-$ RORγt$^+$ ILC3).

3.5 NKp44 ligand detection

3.5.1 NKp44-fc staining

NKp44 ligands were stained on Caco2 cells, HEK-293T cells, H5-HEK293T cells, HT-29 cells, MDCK cells, and SW620 cells as well as human IECs, and then analysed by flow cytometry. Adherent cell lines were detached from the cell culture flasks with either Trypsin-EDTA or enzyme-free dissociation buffer (see section 3.2), transferred to a conical centrifugation tube and washed in PBS/BSA, and then centrifuged at 300 x g for 10 minutes at 4° C. Cells were counted with the cell counter Casy and diluted with PBS/BSA to a final concentration of 5 x 10^5/100 µl. Human IECs were isolated (as described in section 3.3.3), counted with the cell counter Casy and diluted with PBS/BSA to a final concentration of 5 x 10^5/100 µl. NKp44 ligands were stained indirectly, meaning that the primary reagent was not directly coupled to a fluorescent dye, but was bound in a second step by a fluorescent secondary antibody. The primary reagent used was a recombinant protein consisting of the extracellular domain of the NKp44 receptor fused to the fc-chain of human IgG1, referred to as NKp44-fc (kindly provided by A. Porgador, Ben Gurion University of the Negev, Beer Sheva, Israel, or purchased from R&D systems). As control, an uncoupled human IgG1-fc (kindly provided by A. Porgador) or CD99-fc (R&D systems) were used. 5 x 10^5 cells/100 µl were stained with 10, 20 or 40 µg/ml of primary reagent for 90 minutes on ice in the dark, washed afterwards with PBS/BSA, and

then centrifuged at 300 x g for 10 minutes at 4 °C. The secondary antibody used was anti-human IgG1 (Miltenyi Biotec), stained for 30 minutes on ice in the dark, followed by another washing step. When the primary reagent (NKp44-fc, human IgG1-fc or CD99-fc) was used at a concentration of 10 µg/ml, the staining was followed by two steps of APC enhancement using the APC Faser Kit (Miltenyi Biotec) according to the manufacturer's instructions, as illustrated in Figure 8.

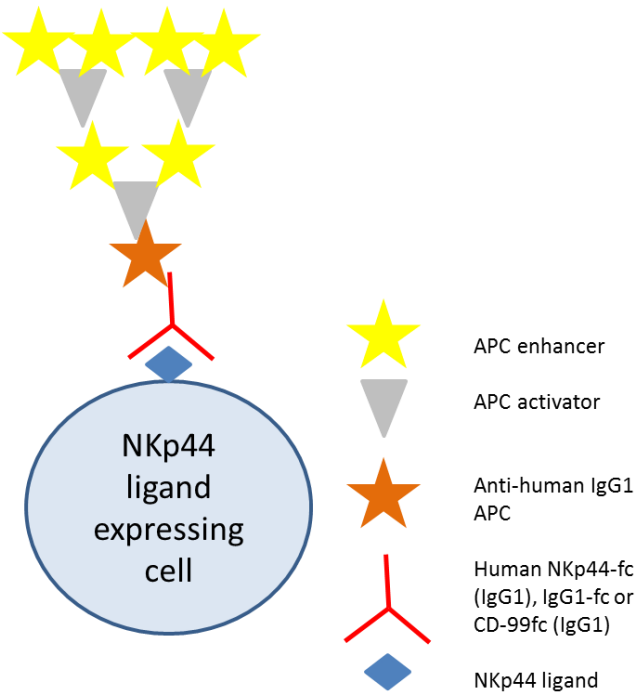

Figure 8 NKp44-fc staining and enhancement of the APC fluorescence intensity

Cells were primarily stained with human NKp44-fc (red symbol), or control IgG1-fc/CD99-fc and secondarily with an anti-human IgG1 monoclonal antibody coupled to the fluorescent dye APC (orange star). Using the APC Faser Kit (Miltenyi Biotec), the APC signal was enhanced twice with an APC activator (grey triangle) followed by an APC enhancer (yellow star).

3.5.2 NKp44 ligand detection by BW-NKp44 reporter cells

Murine BW cells (murine thymoma cells) were transfected with the extracellular portion of NKp44 fused to the CD3ζ chain. Both non-transfected and NKp44-transfected BW cells (BW-NKp44 cells) were kindly provided by O. Mandelboim (Hebrew University Hadassah Medical School, Jerusalem, Israel). 50,000 BW or BW-NKp44 cells were co-cultured with either 10,000 irradiated (3000Gy) SW620 or MDCK cells for 24 h. Cell supernatants were collected and murine IL-2 was measured by ELISA (eBioscience) according to the manufacturer's instructions.

3.6 In vitro stimulation of human RORγt$^+$ ILC3

Human LP and tonsil RORγt$^+$ ILC3 were isolated and sorted as described in sections 3.3 and 3.4. They were then stimulated with either anti-NKp44 monoclonal antibodies for NKp44 crosslinking, phorbol 12-myristate 13-acetate (PMA)/Ionomycin, the cytokines IL-1, IL-7 and IL-23, H1N1 influenza virus, or H5-HEK293T, or different transformed or tumor cell lines. In general, approximately 20,000 sorted RORγt$^+$ ILC3s were used per condition and stimulation was performed in RPMI 1640 (containing 10% human AB serum), 100 U/mL Penicillin and 0.1 mg/ml Streptomycin at 37° C in 5 ml round bottom tubes. After the first hour of stimulation, 10 µg/ml Brefeldin A was added in order to block the cytokine secretion, so that cytokine production could afterwards be measured by intracellular cytokine staining and FC analysis as described in section 3.4.3. In the following, the different stimulation conditions are described in detail.

3.6.1 NKp44 crosslinking and cytokine stimulation

Monoclonal antibody-mediated (mAb-mediated) NKp44 crosslinking was performed with biotinylated anti-NKp44 conjugated to anti-biotin MACSiBead particles (Miltenyi Biotec) according to the manufacturer's instructions. They were used to stimulate LP and tonsil-derived RORγt$^+$ ILC3 at a bead:cell ratio of 5:1, which was determined by a titration series. PMA (Sigma Aldrich) was employed at a concentration of 20 ng/ml, and Ionomycin (Sigma Aldrich) at 1 µg/ml. IL-1, IL-7 (both Miltenyi Biotec) and IL-23 (R&D systems) were each used at a concentration of 50 ng/ml.

3.6.2 Co-culture with H5-HEK293T and influenza virus

Per condition, 20,000 sorted tonsil-derived RORγt$^+$ ILC3 were co-cultured with 40,000 H5-HEK293T or non-transfected HEK293T in the presence or absence of IL-1, IL-7 and IL-23 for 15 hours. H5 expression of H5-HEK293T was measured by FC analysis, after an indirect cell surface staining with an anti-influenza A H5 monoclonal antibody (clone 15A6, isotype IgG2, AbD Serotec) at a titer of 1:100 as the primary antibody, and anti-mouse IgG2 FITC as the secondary antibody. Direct stimulation with the influenza virus (IV) was performed with the strain A/WSN/33 (H1N1). It was grown in the allantoic cavities of 11-day-old embryonated chicken eggs. The virus and the required facilities were kindly provided by A. Karlas (Max Planck Institute for Infection Biology, Berlin, Germany). 20,000 sorted tonsil-derived RORγt$^+$ ILC3 were stimulated with H1N1 IV at a multiplicity of infection (MOI) of 0.5, 5 and 50 for

12 hours in serum-free infection medium or RPMI 1640 (containing 10% FCS). Indirect stimulation with IV was performed after infecting MDCK cells, which subsequently presented viral particles on their cell surface. 15,000 MDCK cells were seeded and cultured overnight in a 96-well microtiter plate to a confluency of over 80%. Then, the MDCK cells were infected with H1N1 IV at a MOI of 0.5 in infection buffer for 1 hour at room temperature. Afterwards, a washing step with PBS removed excessive virus, and infected MDCK cells were cultured in infection medium for 8 hours at 37°C. Then, 25,000 sorted RORγt$^+$ ILC3 suspended in RPMI 1640 (containing 10% FCS) were added and co-cultured for 12 hours at 37°C.

3.6.3 Co-culture with the epithelial cell lines MDCK and SW620

Per condition, 20,000 sorted tonsil-derived RORγt$^+$ ILC3 were co-cultured with 40,000 MDCK cells or SW620 cells in the presence or absence of IL-1, IL-7 and IL-23 for 12-14 hours at 37°C. NKp44 ligand expression of the MDCK or SW620 cells used was confirmed for each stimulation experiment by NKp44-fc staining, as described in section 3.5.1.

3.6.4 NKp44 blockade

For blockade of the NKp44 engagement by either anti-NKp44 mAb, influenza virus or the different NKp44 ligand-expressing cell lines, sorted tonsil-derived RORγt$^+$ ILC3 were incubated, prior to stimulation, with a blocking anti-NKp44 mAb (IgM, KS38) or with an anti-CD56 mAb (IgM, A6-220) at a concentration of 10 g/ml for 1 hour at 4 °C, kindly provided by S. Parolini (University of Brescia, Brescia, Italy) and A. Moretta (University of Genova, Genova, Italy), respectively.

3.7 Quantitative real-time polymerase chain reaction

mRNA transcripts were measured in sorted LP-derived RORγt$^+$ ILC3 (for isolation and sorting see sections 3.3.2 and 3.4.4) after stimulation with mAb-mediated NKp44 crosslinking and/or cytokines (see section 3.6.1). For this, mRNA was isolated by using NucleoSpin RNAII (Macherey Nagel) according to the manufacturer's instructions. The resulting mRNA concentration was determined with NanoDrop (PeqLab). Next, cDNA was synthesized from the mRNA transcript by adding the following TaqMan® Reverse Transcription Reagents (Applied Biosystems) (volume is given per 6.95 µl of RNA): 2 µl 10 x PCR buffer, 4.4 µl magnesium chloride, 4 µl deoxynucleotide triphosphates, 0.5 µl random hexamer, 0,5 µl oligo dT primers, 0.4 µl RNAse inhibitor, and 1.25 µl reverse transcriptase. cDNA was synthesized

with a PCR cycler (Thermocycler, Biometra). Qualitative real-time polymerase chain reaction (PCR) was performed in duplicates using the StepOne Plus real-time PCR system (Applied Biosystems), after having added TaqMan Gene expression assays (Applied Biosystems) to the cDNA. The TaqMan Gene expression assays used were Hs01076112_m1 *RORC,* Hs00169233_m1 *AHR* and 4333764F *GAPDH.* The content of mRNA was quantified by the cycle threshold (CT). CT values for the genes of interest were normalized to the CT values of the housekeeping gene *glyceraldehyde 3-phosphate dehydrogenase (GAPDH)*. The mean relative gene expression was determined with the ΔΔ CT method.

3.8 Graphics and statistical analysis

With the software GraphPad Prism version 5 (GraphPad Software), data generated by FC analysis and evaluated by FlowJo was statistically analyzed and visualized graphically. The distribution of different lymphocyte populations of non-inflamed and inflamed LP of IBD patients and unaffected LP of control patients was tested with the Mann Whitney test. NKp44, NKp46 and CD56 expression by LP RORγt$^+$ ILC3 was analyzed with the Mann-Whitney test (comparing the pool of control, non-inflamed IBD and inflamed IBD samples) and with the Wilcoxon matched-pairs signed rank test (comparing matched non-inflamed and inflamed IBD samples). Datasets of the stimulation experiments with tonsil-derived RORγt$^+$ ILC3 were analyzed with the Wilcoxon signed rank two-tailed test and included, if not indicated separately, at least 6 independent experiments (*$p < 0.05$, **$p < 0.01$).

4. Results

4.1 Intestinal lamina propria RORγt$^+$ ILC3 express NKp44

Previous work (Cella et al., 2009, Takayama et al., 2010) has shown that human tonsil and lamina propria RORγt$^+$ ILC3 can be divided into two subsets according to their natural cytotoxicity receptor (NCR) NKp44 expression. These subsets are functionally distinct, since production of IL-22 is confined to the NKp44$^+$ population. Furthermore, our group has shown that crosslinking of the NKp44 receptor in tonsil-derived RORγt$^+$ ILC3 by a monoclonal antibody results in the production of the pro-inflammatory cytokine TNF and in a pro-inflammatory transcriptome signature.

The first sub-aim of the thesis was to investigate the distribution of RORγt$^+$ ILC3 in human intestinal LP and assess their NKp44 expression. Furthermore, we aimed to test whether there are alterations of this distribution in the context of IBD.

In a first step, an isolation procedure as well as a gating strategy were established. Tissue samples were obtained from unaffected mucosa of colonic/colorectal resections of patients undergoing surgery for either colorectal carcinoma or sigmoid diverticulitis. The resections were taken from macroscopically healthy colon segments. LP mononuclear cells (MNC) were isolated by enzymatic digestion and lymphocyte density centrifugation and analyzed by flow cytometry with the indicated gating strategy (Figure 9). Specifically, the lymphocytic gate was defined in the FSC/SSC plot reflecting the size and granularity of analyzed cells, respectively. Within this lymphocytic population, the hematopoietic surface marker CD45 was used to exclude non-hematopoietic cells. Additionally, cells of the T cell lineage (CD3$^+$), the B cell lineage (CD19$^+$) and the monocyte lineage (CD14$^+$) were excluded, and the remaining cells are referred to in the following as lineage negative cells (Lin$^-$ cells). The Lin$^-$ cell compartment contained a CD127^{high} population, which was heterogeneous in the expression of CD56 and which we defined as ILC. Conventional NK (cNK) cells were defined within the Lin$^-$ cell compartment as CD127$^-$ CD56^{high} NKp46$^+$ cells. These results are in agreement with previous findings (Cupedo et al., 2009, Crellin et al., 2010, Geremia et al., 2011).

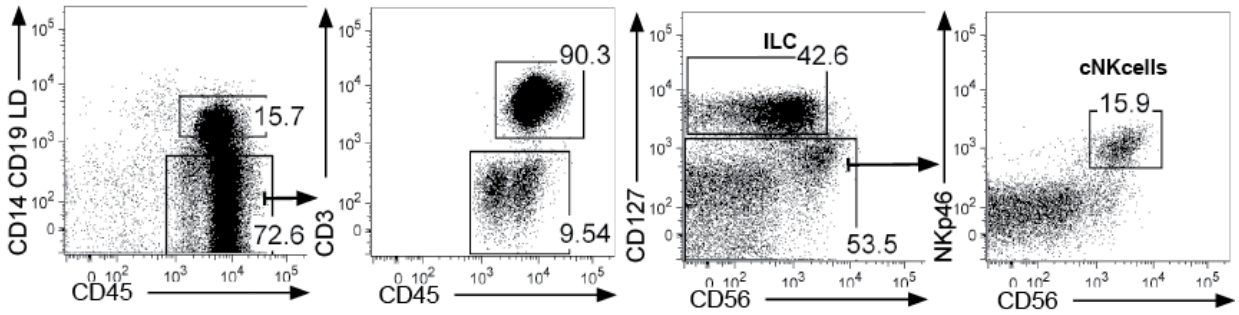

Figure 9 Gating strategy to identify ILC and cNK cells among human intestinal LP MNC

Flow cytometry experiments were performed on colon-derived LP MNC obtained from colorectal carcinoma or sigmoid diverticulitis patients. Displayed above is a representative gating strategy to define ILC and cNK cells among all LP MNC. ILC were defined as $CD45^+$ $CD14^-$ $CD19^-$ $CD3^-CD127^{high}$ $CD56^{+/-}$. cNK cells were defined as $CD45^+$ $CD14^-$ $CD19^-$ $CD3^-$ $CD127^-$ $CD56^{high}$ $NKp46^+$. Dead cells were excluded by a LIVE/DEAD (LD) staining.

Quantitative PCR was used to assess *RORC* transcript expression among the Lin^- $CD45^+$ $CD127^{high}$ $CD56^{+/-}$ in comparison to the cNK population. *RORC* encodes the protein RORγt. There was an approximately 10-fold higher *RORC* mRNA expression in Lin^- $CD45^+$ $CD127^{high}$ $CD56^{+/-}$ cells compared to cNK cells. Besides *RORC*, *AHR* transcripts were clearly more highly expressed in Lin^- $CD45^+$ $CD127^{high}$ $CD56^{+/-}$ compared to cNK cells (Figure 10). Although we cannot exclude a minor contamination of other ILC subsets, these findings corroborate a strong enrichment of $ROR\gamma t^+$ ILC3 in the Lin^- $CD45^+$ $CD127^{high}$ $CD56^{+/-}$ population.

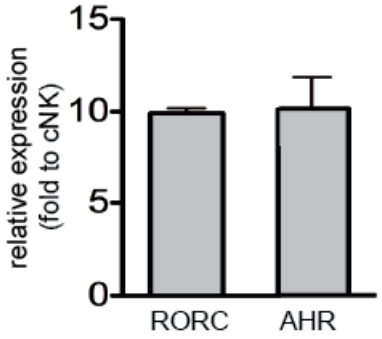

Figure 10 mRNA transcripts of *RORC* and *AHR* in LP Lin^- $CD45^+$ $CD127^{high}$ $CD56^{+/-}$ cells

Shown above is the expression of *RORC* and *AHR* mRNA transcripts in FACS-sorted colonic LP Lin^- $CD45^+$ $CD127^{high}$ $CD56^{+/-}$ cells ($ROR\gamma t^+$ ILC3) compared to FACS-sorted LP Lin^- $CD45^+$ $CD127^-$ $CD56^{high}$ $NKp46^+$ cells (cNK cells) (n = 3). This data was generated by Timor Glatzer.

Next, the expression of NKp44 and NKp46 receptor within the Lin^- $CD45^+$ $CD127^{high}$ $CD56^{+/-}$ population ($ROR\gamma t^+$ ILC3) was evaluated by FC and compared to the expression by cNK cells. cNK cells were used as a reference, since these cells are known to express low levels of NKp44 and high levels of NKp46 (Moretta et al., 2001). These experiments showed a relatively high

expression of NKp44 and low expression of NKp46 in RORγt$^+$ ILC3 cells compared to cNK cells (Figure 11).

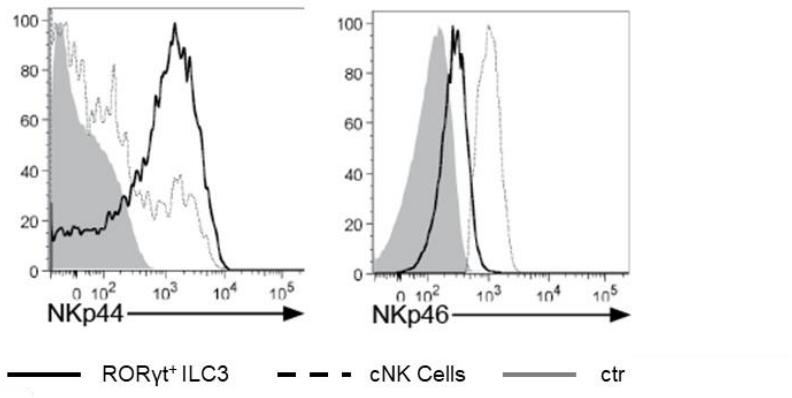

Figure 11 NKp44 and NKp46 expression by LP RORγt$^+$ ILC3

Displayed above are FC histograms of NKp44 and NKp46 expression among LP RORγt$^+$ ILC3 cells (black solid line) in comparison to LP cNK cells (grey dotted line). Samples were obtained from colonic/colorectal resections and populations defined according to the gating strategy shown in Figure 9. One representative is shown (n = 10).

Altogether, this data indicates that the human LP contains a population of RORγt$^+$ ILC3 that can be defined by flow cytometric analysis as CD45$^+$ CD3$^-$ CD19$^-$ CD14$^-$ CD127^{high} CD56$^{+/-}$ cells that are enriched in *RORC* and *AHR* transcripts. A substantial fraction of RORγt$^+$ ILC3 express NKp44, whereas NKp44 expression is low compared to cNK cells.

4.2 Functionality of NKp44 of human lamina propria RORγt$^+$ ILC3

After having confirmed the presence of RORγt$^+$ ILC3 in the human LP and the expression of the NKp44 receptor by a substantial fraction of this population, the functionality of the receptor was tested. To this end, the same stimulation conditions that had been previously established by our group in human tonsil RORγt$^+$ ILC3 were used in the intestinal samples. From these previous experiments, it was known that crosslinking of the NKp44 receptor via an anti-NKp44 monoclonal antibody results in the production of TNF, while the cytokine combination IL-1 + IL-7 + IL-23 preferentially induces the production of IL-22. NKp44 crosslinking acts synergistically with IL-1 + IL-7 + IL-23 stimulation and together results in an enhanced production of both TNF and IL-22.

In order to test for a similar responsiveness in RORγt$^+$ ILC3 derived from the intestinal LP, FACS-sorted Lin$^-$ CD45$^+$ CD127^{high} cells were stimulated with either Phorbol 12-myristate 13-acetate (PMA) / Ionomycin (Iono) and IL-23 (PMA + Iono + IL-23), the cytokine combination IL-1 + IL-7 + IL-23, anti-NKp44 monoclonal antibody (aNKp44), or aNKp44 in combination

with IL-1, IL-7 and IL-23 (aNKp44 + IL-1 + IL-7 + IL-23). After a stimulation period of 20 hours, intracellular cytokine expression was assessed by flow cytometry (Figure 12).

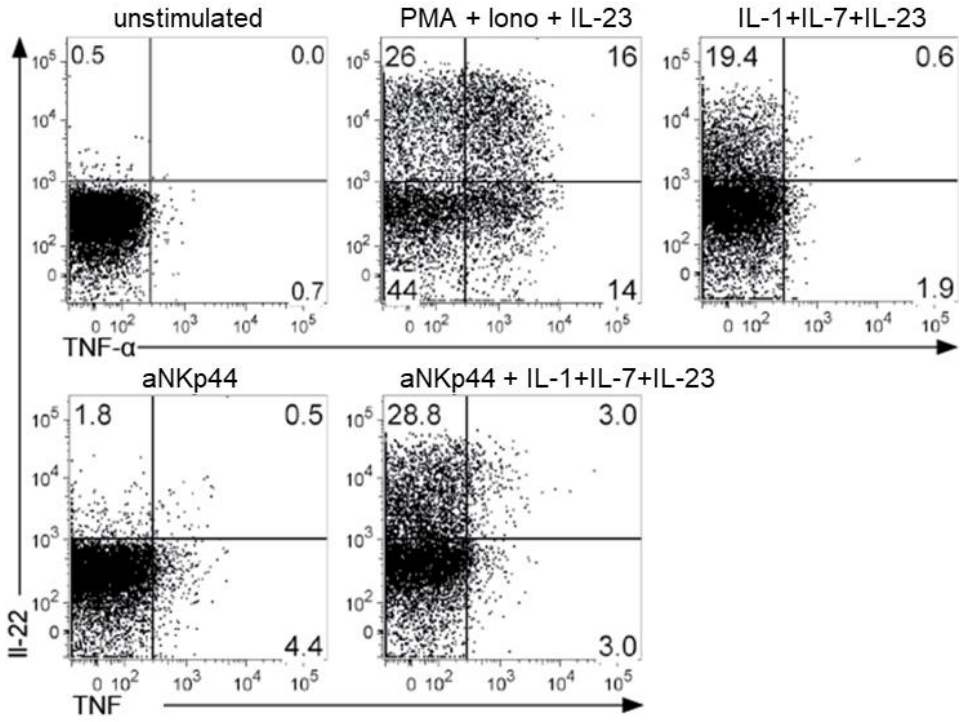

Figure 12 Responsiveness of human LP RORγt$^+$ ILC3 to stimulation via NKp44 and cytokines

FACS-sorted Lin$^-$ CD45$^+$ CD127^{high} CD56$^{+/-}$ cells (RORγt$^+$ ILC3) were stimulated with the different stimuli indicated. Intracellular cytokine expression (IL-22 and TNF) was detected afterwards by FC. Results from one representative sample (n = 3) are shown. The stimulation was performed in cooperation with Timor Glatzer.

Similarly to their tonsil counterparts, human LP RORγt$^+$ ILC3 produced TNF and IL-22 upon polyclonal stimulation with PMA + Iono + IL-23. The cytokine stimulation (IL-1 + IL-7 + IL-23) preferentially induced IL-22, whereas the mAb-mediated NKp44 crosslinking (aNKp44) mainly resulted in TNF production, albeit only at a low level. NKp44 crosslinking in combination with the cytokine stimulation (aNKp44 + IL-1 + IL-7 + IL-23) resulted in a synergistic effect for IL-22, however there was no clear synergy seen for TNF production.

Taken together, these results indicate the functionality of the NKp44 receptor in human LP RORγt$^+$ ILC3, albeit TNF production upon receptor crosslinking was low compared to their tonsil counterparts. Nevertheless, there was a clear synergistic effect of NKp44 triggering together with cytokine stimulation with regard to IL-22 production.

4.3 NKp44 expression is decreased in the inflamed lamina propria of inflammatory bowel disease patients

The next question was whether there are alterations in the distribution of RORγt$^+$ ILC3 and/or their NKp44 expression in the context of IBD. To approach this question, human LP MNC were isolated from macroscopically non-inflamed and inflamed mucosa of IBD patients (Crohn's disease and Ulcerative colitis), as well as from non-affected mucosa of colorectal carcinoma patients (controls) and analyzed by flow cytometry. Besides ILCs, we aimed to also get an overview of intestinal T cell and B cell distribution and thus accordingly modified the gating strategy that is shown in Figure 13.

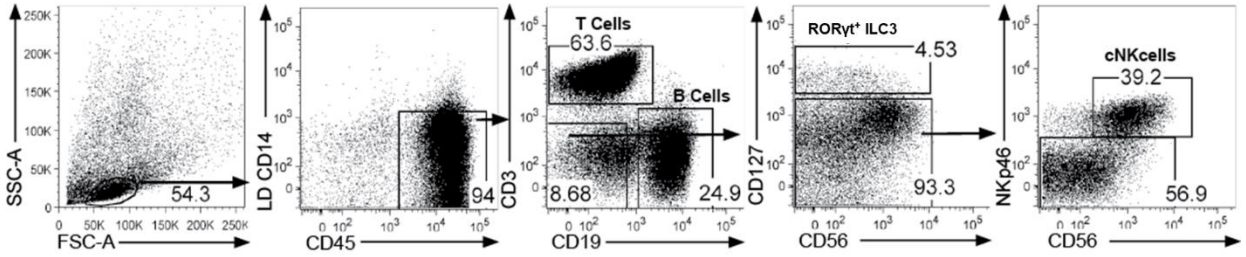

Figure 13 Gating strategy to analyze LP MNC of IBD and control patients

Displayed above is the FC gating strategy to analyze the distribution of T cells, B cells, RORγt$^+$ ILC3 and cNK cells among LP MNC derived from non-inflamed or inflamed LP of IBD patients or the unaffected LP of control patients. Dead cells were excluded by a LIVE/DEAD (LD) staining. The represented sample was obtained from the inflamed LP of a Crohn's disease patient.

There were no clear differences seen in the relative distribution of T cells, B cells, RORγt$^+$ ILC3 and cNK cells between the non-inflamed and inflamed LP of IBD patients, or in comparison to the LP of control patients (Figure 14).

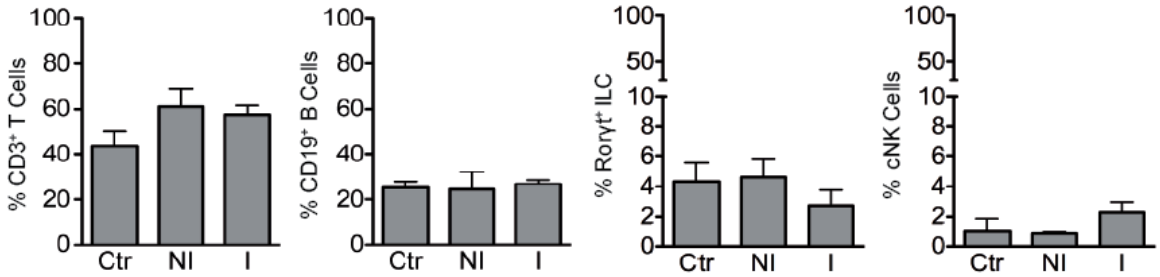

Figure 14 Relative distribution of T cells, B cells, RORγt$^+$ ILC3 and cNK cells in inflamed and non-inflamed LP

Displayed above are the mean percentages ± SEM of T cells, B cells, RORγt$^+$ ILC3 and cNK cells of all CD45$^+$CD14$^-$ LP MNC as determined by FC according to the gating strategy shown in Figure 13. Ctr = LP of control patients, NI = non-inflamed LP of IBD patients, I = inflamed LP of IBD patients. (Ctr: n = 6, NI and I: n = 5).

Next, the expression of NKp44 by RORγt$^+$ ILC3 was analyzed. A comparison was made between the non-inflamed (NI) and inflamed (I) LP of IBD patients and the non-affected LP of control patients (Ctr) (Figure 15).

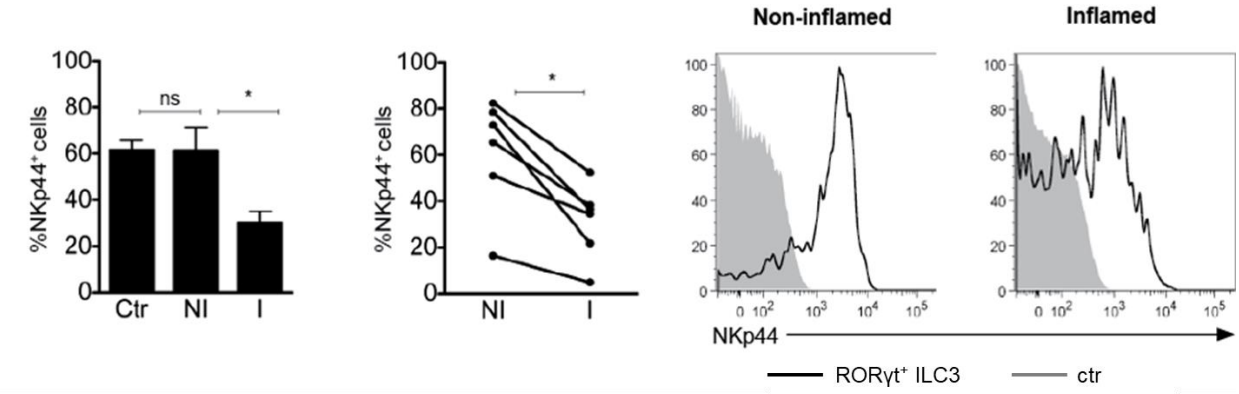

Figure 15 Expression of NKp44 by RORγt$^+$ ILC3 in inflamed and non-inflamed LP

RORγt$^+$ ILC3 derived from non-inflamed (NI) and inflamed (I) LP of IBD patients, as well as from control patients' LP (Ctr) were analyzed by FC, using the gating strategy shown in Figure 13. Left: Expression of NKp44 is displayed as mean percentage ± SEM of all LP RORγt$^+$ ILC3 (Ctr: n= 10, NI: n = 6, I: n= 8). Middle: Matched NI and I LP samples of IBD donors. Right: Representative FC histograms showing the expression of NKp44 by LP RORγt$^+$ ILC3 in NI and I LP from one IBD patient.

The NKp44 expression among RORγt$^+$ ILC3 was significantly lower in the inflamed compared to the non-inflamed LP of IBD patients, whereas comparable levels were observed between non-inflamed LP of IBD patients and non-affected LP of control patients. Looking at individual IBD donors, the decrease in the NKp44 expression was consistent in all donors analyzed, although the baseline of NKp44 expression levels varied inter-individually.

Collectively this data shows that the percentage of RORγt$^+$ ILC3 is not altered in the inflamed LP of IBD patients. However, the expression of NKp44 by RORγt$^+$ ILC3 is significantly decreased in the inflamed LP of IBD patients compared to the non-inflamed mucosa of IBD or non-IBD patients.

4.4 Establishment of NKp44-fc staining

The reason for the decreased expression of NKp44 in RORγt$^+$ ILC3 in the inflamed LP of IBD patients remains to be elucidated. One could hypothesize that NKp44 might be engaged *in vivo* in the inflammatory state of IBD and subsequently gets downregulated. However, the identity and distribution NKp44 ligands are poorly characterized and have not been analyzed in the context of intestinal inflammation. In order to identify NKp44 ligands that are able to

physiologically engage NKp44 of RORγt$^+$ ILC3 cells, we firstly established a staining method for NKp44 ligands by flow cytometry.

To this end, we adapted a previously published technique (Arnon et al., 2001) using an NKp44 fusion protein. This reagent consists of the extracellular domain of the NKp44 receptor fused to the Fc portion of human IgG1 and is referred to as recombinant NKp44-fc fusion protein (Arnon et al., 2001). The NKp44-fc is not directly coupled to a fluorescent dye but can be made detectable by flow cytometry using anti-human IgG1 APC as secondary antibody.

The human embryonic kidney cell line 293T (HEK 293T) has been reported to express NKp44 ligands (Byrd et al., 2007, Arnon et al., 2001). Therefore, HEK 293T were used to establish an NKp44-fc staining protocol. The flow cytometric gating strategy to identify viable HEK 293T is shown in Figure 16. The NKp44-fc was first used at a concentration of 10 µg/ml, which resulted in weak staining and thus poor discrimination between NKp44-fc-stained and non-stained cells (Figure 17). In order to improve the fluorescent signal of the NKp44-fc staining, the concentration of NKp44-fc was raised to 20 µg/ml and 40 µg/ml. Both concentrations resulted in a better discrimination of NKp44-fc-stained and non-stained cells (Figure 17).

As an alternative, the APC signal of the secondary antibody itself was enhanced. After staining with NKp44-fc at the lower concentration of 10 µg/ml, the commercially purchased APC FASER kit (Miltenyi Biotec) was applied. Two enhancement steps delivered the best discrimination between NKp44-fc-stained and non-stained cells, which was even superior to the staining with NKp44-fc at 40 µg/ml (Figure 17; see also Material and methods, Figure 8).

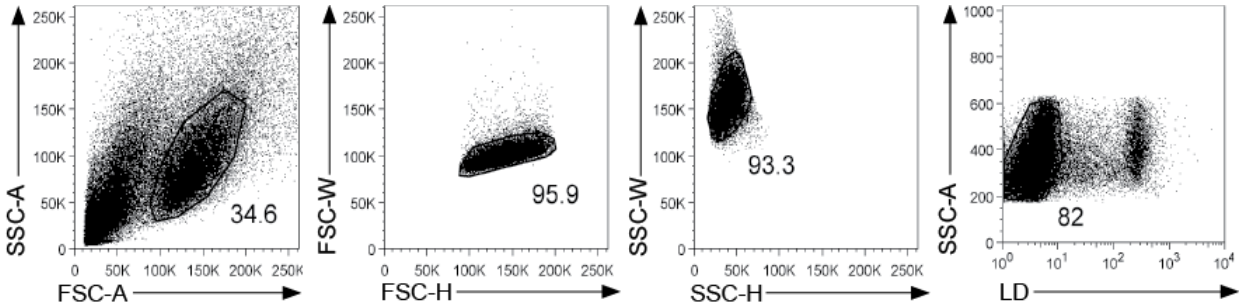

Figure 16 Gating strategy to identify viable, single HEK 293T cells in FC

Displayed above is the gating strategy to identify single, viable HEK 293T cells in FC. Firstly, the cell line gate was defined in the SSC/FSC plot, then doublets were excluded (FSC-W/FSC-H and SSC-W/SSC-H). Dead cells were excluded by a LIVE/DEAD (LD) staining.

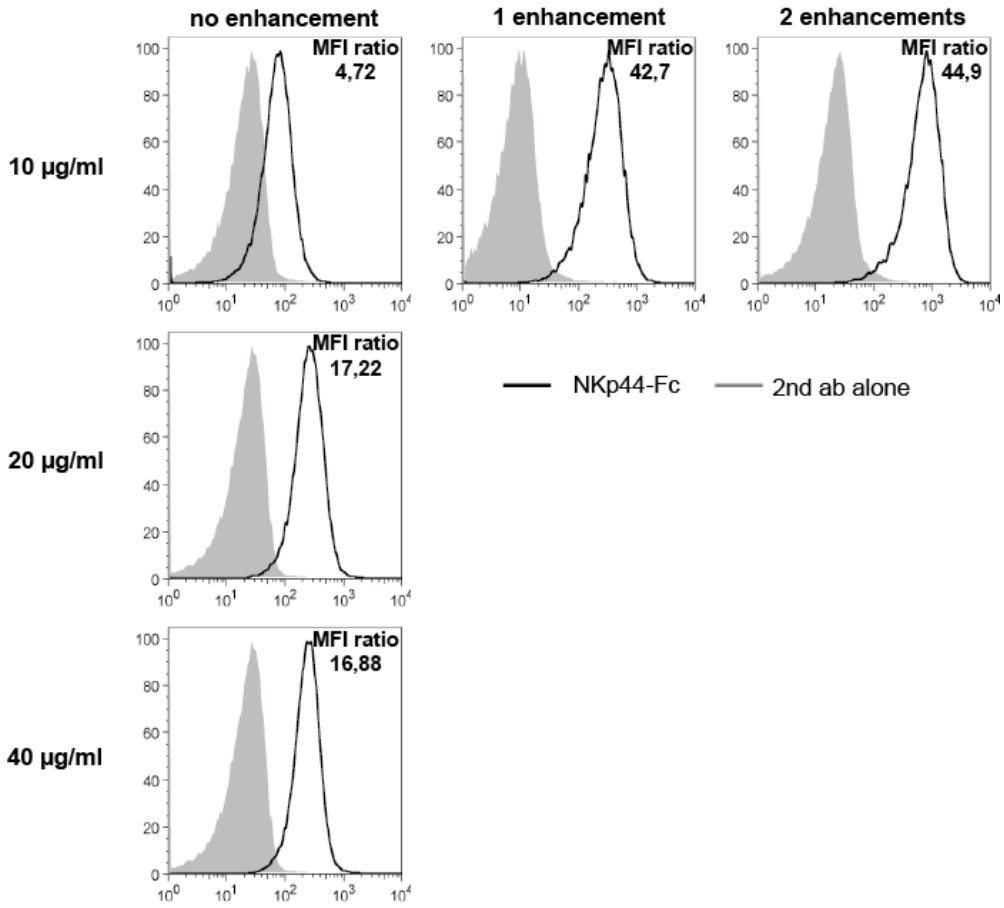

Figure 17 NKp44-fc staining at different concentrations and with or without APC enhancement

Displayed above are the FC histograms of the NKp44-fc staining on HEK 239T at different concentrations of the primary monoclonal antibody NKp44-fc (vertical row) and different numbers of APC signal enhancement steps (horizontal row). The black line corresponds to the staining with NKp44-fc + secondary antibody (2^{nd} ab), while the solid histogram corresponds to the staining with the 2^{nd} ab alone. Mean fluorescence intensity (MFI) ratio = MFI of NKp44-fc + 2^{nd} Ab / 2^{nd} ab alone.

In order to test for the potential existence of unspecific binding between the fc-portion of the NKp44-fc protein and HEK 293T cells, fc-control antibodies were introduced. Both an uncoupled human IgG1-fc as well as a CD99-fc fusion protein stained with secondary anti-human IgG1 did not bind HEK 293T cells (Figure 18).

Taken together, this data shows that the staining with NKp44-fc fusion protein as primary reagent and anti-human IgG1 as secondary antibody is able to detect NKp44 ligand expression on target cells. The discrimination between NKp44-fc-stained and non- or control-fc-stained cells can be improved by either enhancing the secondary antibody's fluorescence signal or elevating the concentration of the NKp44-fc.

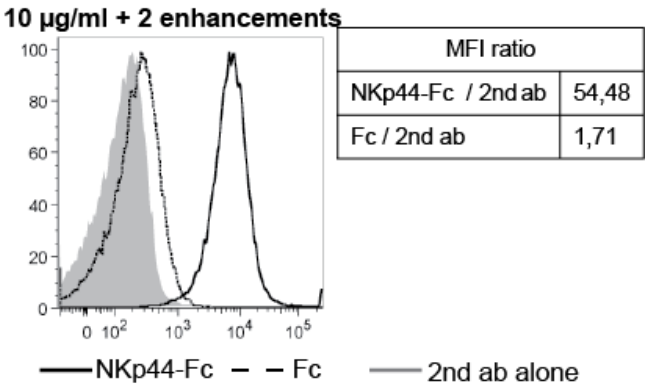

Figure 18 Introduction of a control-fc for the NKp44-fc staining

The represented FC histogram shows the fluorescence intensities of HEK 293T after staining with NK44-fc + 2nd ab (black line), control-fc + 2nd ab (black dotted line) and 2nd ab alone (grey solid histogram). NKp44-fc and control-fc were used at a concentration of 10 µg/ml and APC was enhanced two times in all three conditions. The corresponding MFI ratios are displayed on the right.

4.5 Influenza hemagglutinin is not a high-affinity ligand of NKp44 in RORγt$^+$ ILC3

One of the first ligands of NKp44 described in literature is hemagglutinin (HA) of influenza virus (IV). HA expression on the surface of IV-infected cells promotes their lysis by NK cells through interaction with the NKp44 receptor (Arnon et al., 2001). We wanted to test whether NKp44 of RORγt$^+$ ILC3 is also able to recognize IV HA and whether this interaction results in a similar cytokine response as mAb-mediated NKp44 crosslinking.

We used three different methods to stimulate RORγt$^+$ ILC3 with IV HA. First, co-culture was performed with HEK 293T cells that had been transfected with an expression plasmid encoding IV hemagglutinin 5, and that are referred to in the following as H5-HEK 293T (Ho et al., 2008). H5 surface expression was confirmed by flow cytometry on approximately one third of H5-HEK 293T, whereas non-transfected HEK 293T did not express H5 at all (Figure 19).

Our previous results showed that non-transfected HEK 293T also express NKp44 ligands. Although H5-HEK 293T cells exhibited only slightly higher binding to NKp44-fc (Figure 20), HEK 293T and H5-HEK 293T were tested for their ability to stimulate RORγt$^+$ ILC3.

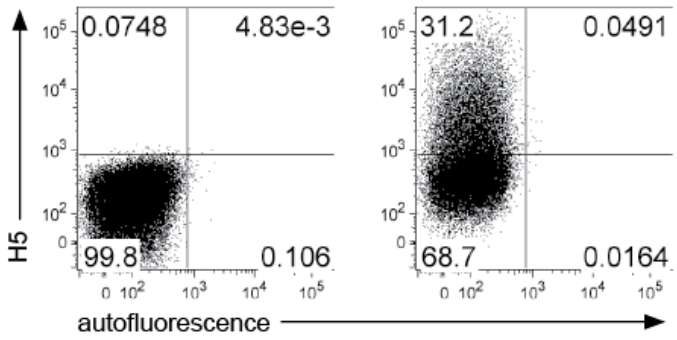

Figure 19 H5 surface expression by H5-HEK 293T

Displayed above are FC dot plots showing the expression of H5 on the cell surface of non-transfected HEK 293T (left) and H5 transfected H 293T (right).

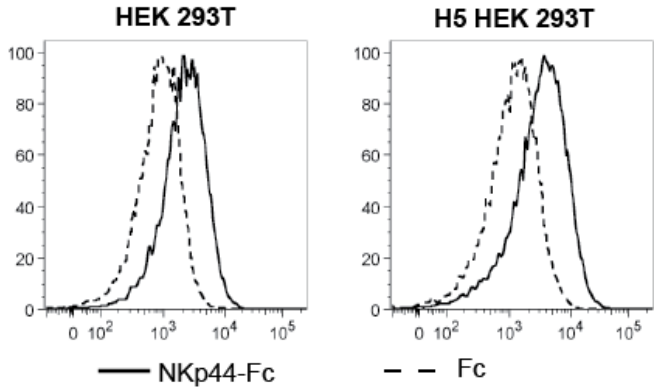

Figure 20 NKp44-fc binding of HEK 293T and H5 HEK 293T

Displayed above are the FC histograms indicating the binding of NKp44-fc (black solid line) or control-fc (black dotted line) to HEK 293T (left) and H5-HEK 293T (right).

The resulting intracellular cytokine production was analyzed by flow cytometry (Figure 21). Neither HEK 293T nor H5-HEK 293T induced considerable amounts of IL-22 or TNF when co-cultured without cytokines. However, both HEK 293T and H5-HEK 293T acted synergistically with cytokines inducing the production of IL-22 and to a small extent that of TNF. In comparison, mAb-mediated NKp44 crosslinking in synergy with cytokines induced the production of both IL-22 and TNF at similar levels. As there was no detectable difference between HEK 293T and H5-HEK 293T in their ability to stimulate RORγt$^+$ ILC3, these data suggest that RORγt$^+$ ILC3 might be stimulated by natural NKp44 ligands or other molecules expressed on HEK293 T rather than by H5. Thus H5-HEK 293T do not represent an ideal experimental setting to analyze NKp44 engagement of RORγt$^+$ ILC3.

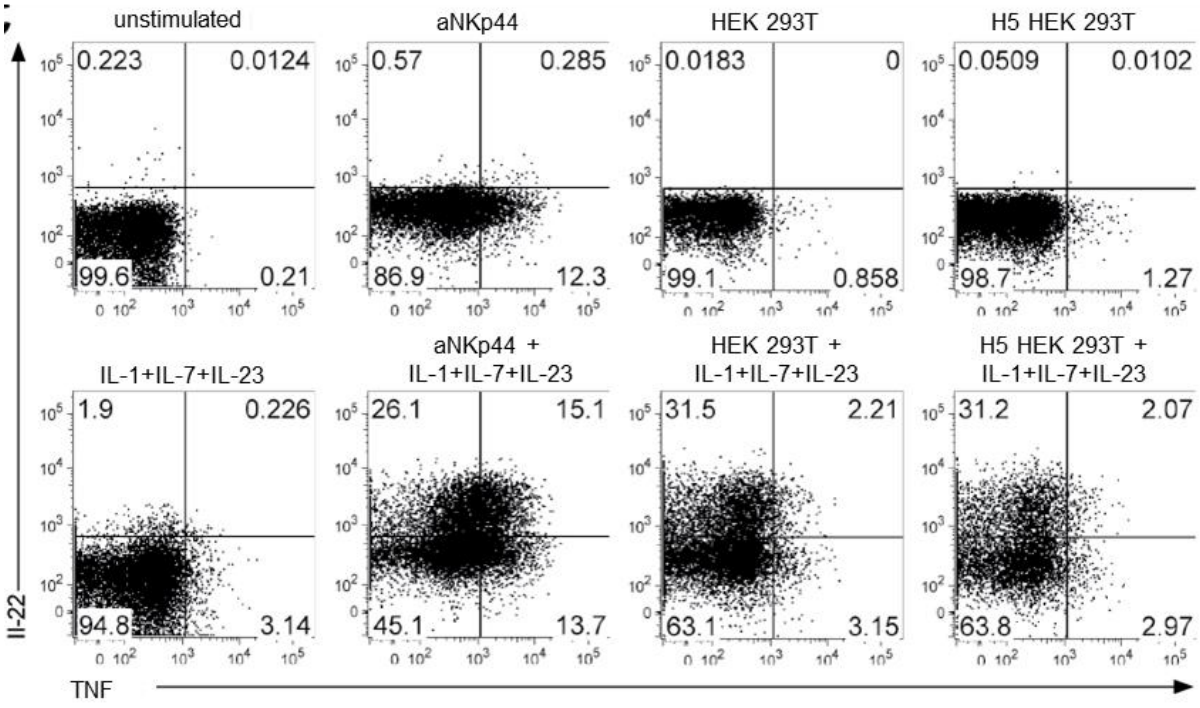

Figure 21 Co-culture of human RORγt$^+$ ILC3 with HEK 293T and H5-HEK 293T

FACS-sorted human tonsil CD3$^-$ CD19$^-$ CD127^{high} CD56$^+$ cells (RORγt$^+$ ILC3) were stimulated under the indicated conditions and the expression of TNF and IL-22 was analyzed afterwards by an intracellular staining and FC. One representative is shown (conditions without cytokines: n = 3, conditions with cytokines: n = 2).

A second experimental setup was therefore tested. RORγt$^+$ ILC3 were stimulated directly with IV of the strain A/WSN/33 (H1N1) with or without cytokines (IL-1 + IL-7 + IL-23) (Figures 22 and 23). IV was employed at a multiplicity of infection (MOI) of 50. IV stimulation alone did not elicit either an IL-22 or a TNF response in RORγt$^+$ ILC3. However, in the presence of the cytokines IL-1 + IL-7 + IL-23, IV synergistically enhanced the induction of IL-22, but had nearly no effect on the production of TNF. mAb-mediated NKp44 crosslinking acted, as previously shown, synergistically with cytokines, enhancing both IL-22 and TNF induction.

Thus, the synergistic effect of IV with cytokines (IL-1 + IL-7 + IL-23) compared to mAb-mediated NKp44 crosslinking with cytokines was disparate and it was questionable whether the effect of IV was NKp44-dependent or not. In order to test this, IV + cytokine stimulation was performed in the presence or absence of an IgM anti-NKp44 blocking monoclonal antibody or a control blocking monoclonal antibody (Figure 24). Neither anti-NKp44 blocking nor control blocking resulted in a clear inhibition of IV-mediated effects on RORγt$^+$ ILC3. Thus, the IV-mediated effects seem to be NKp44-independent.

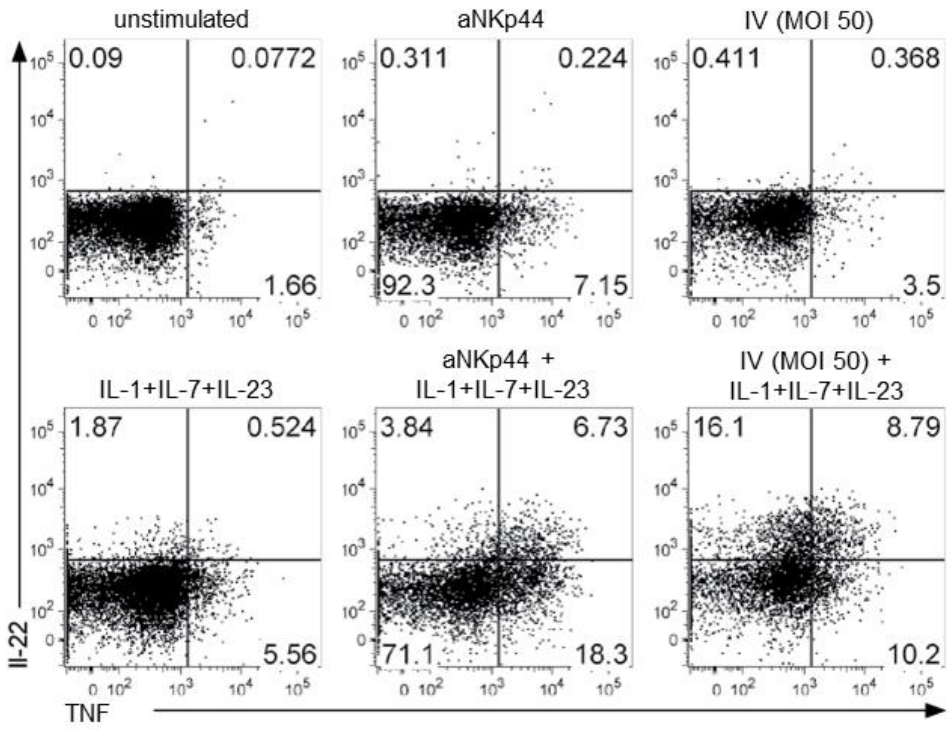

Figure 22 Direct stimulation of human RORγt$^+$ ILC3 with influenza virus

FACS-sorted human tonsil CD3$^-$ CD19$^-$ CD127^{high} (RORγt$^+$ ILC3) were incubated with influenza virus (IV) at a multiplicity of infection (MOI) of 50 with or without the presence of IL-1 + IL-7 + IL-23. As control conditions, mAb-mediated NKp44 crosslinking (aNKp44), IL-1 + IL-7 + IL-23, and aNKp44 + IL-1 + IL-7 + IL-23 were used. The expression of TNF and IL-22 after stimulation was analyzed by an intracellular staining and FC. One representative is shown (n ≥ 6). Experiments were performed in cooperation with Monica Killig.

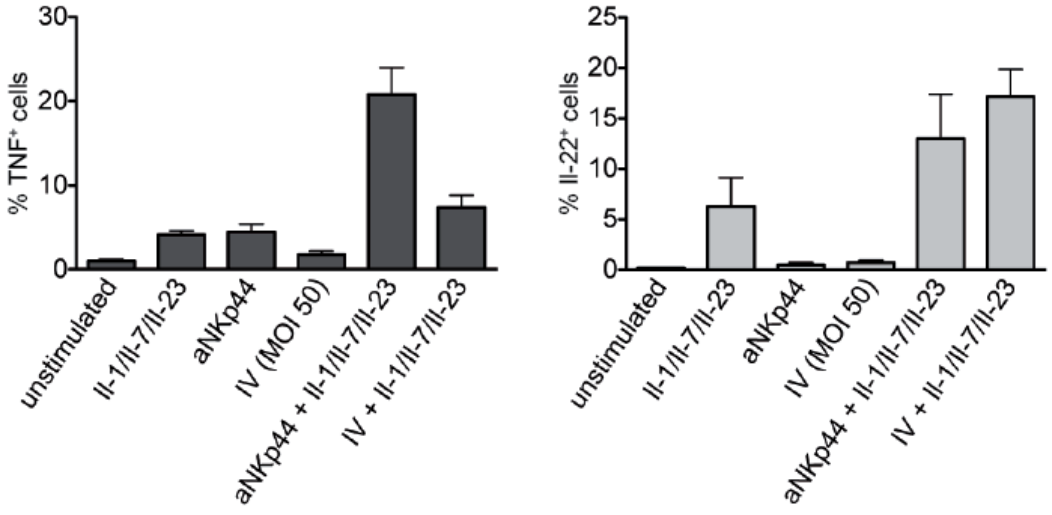

Figure 23 Summary of direct stimulation experiments of human RORγt$^+$ ILC3 with influenza virus

Stimulation under the indicated conditions was performed as described in Figure 22. Shown above are the mean percentages ± SEM of TNF$^+$ (left) and IL-22$^+$ (right) cells after stimulation, detected by FC (n ≥ 6). Experiments were performed in cooperation with Monica Killig.

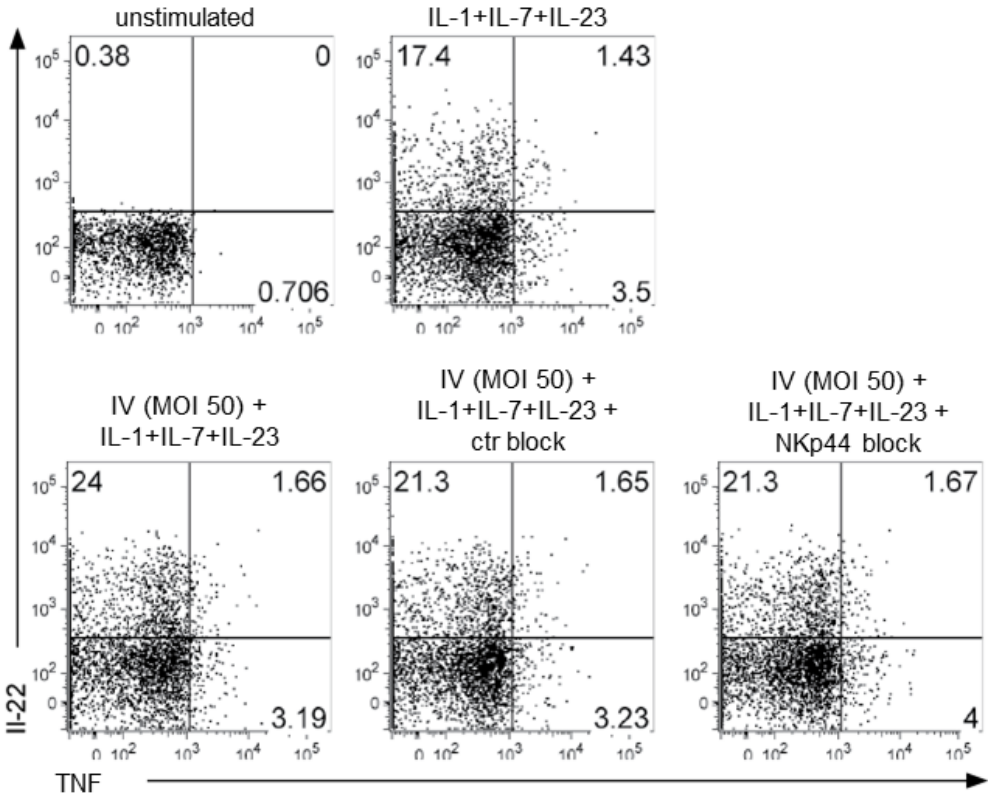

Figure 24 Influenza virus-mediated cytokine enhancement in human RORγt$^+$ ILC3 is NKp44-independent

FACS-sorted human tonsil CD3$^-$ CD19$^-$ CD127^{high} cells (RORγt$^+$ ILC3) were incubated with influenza virus (IV) at a MOI of 50 with cytokines (IL-1 + IL-7 + IL-23) in the presence or absence of anti-NKp44 blocking monoclonal antibody (NKp44 block) or a control blocking monoclonal antibody (ctr block). The expression of TNF and IL-22 after stimulation was analyzed by an intracellular staining and FC. One representative is shown (n = 6). Experiments were performed in cooperation with Monica Killig.

Finally, since neither H5-HEK 293T nor H1N1 IV elicited a clear NKp44-dependent response in RORγt$^+$ ILC3, we tested whether IV-infected cells could represent an effective NKp44 stimulus. To this end, Madin-Darby canine kidney (MDCK) cells, which are known to be highly susceptible to IV infection (Gaush et al., 1966), were infected with H1N1 IV and co-cultured with human RORγt$^+$ ILC3. IV-infected as well as non-infected MDCK cells elicited a comparable cytokine expression in RORγt$^+$ ILC3, which was also similar to the one induced by mAb-mediated NKp44 crosslinking (Figure 25).

In summary, IV hemagglutinins in the form of either H5 expressed on the surface of H5-HEK 293T or the form of H1N1 IV do not induce an IL-22 or TNF production in human RORγt$^+$ ILC3. In a synergistic manner with the cytokines IL-1 + IL-7 + IL-23, IV hemagglutinins enhance the induction of IL-22. However, this effect is not clearly NKp44-dependent as it cannot be inhibited by NKp44 blocking. Instead, we observed that MDCK cells, independent of whether they were previously infected with IV or not, elicit a cytokine expression that is

comparable to the one seen after mAb-mediated NKp44 crosslinking. This finding prompted us to further analyze NKp44 ligand expression on MDCK cells as well as to perform further stimulation experiments with these cells.

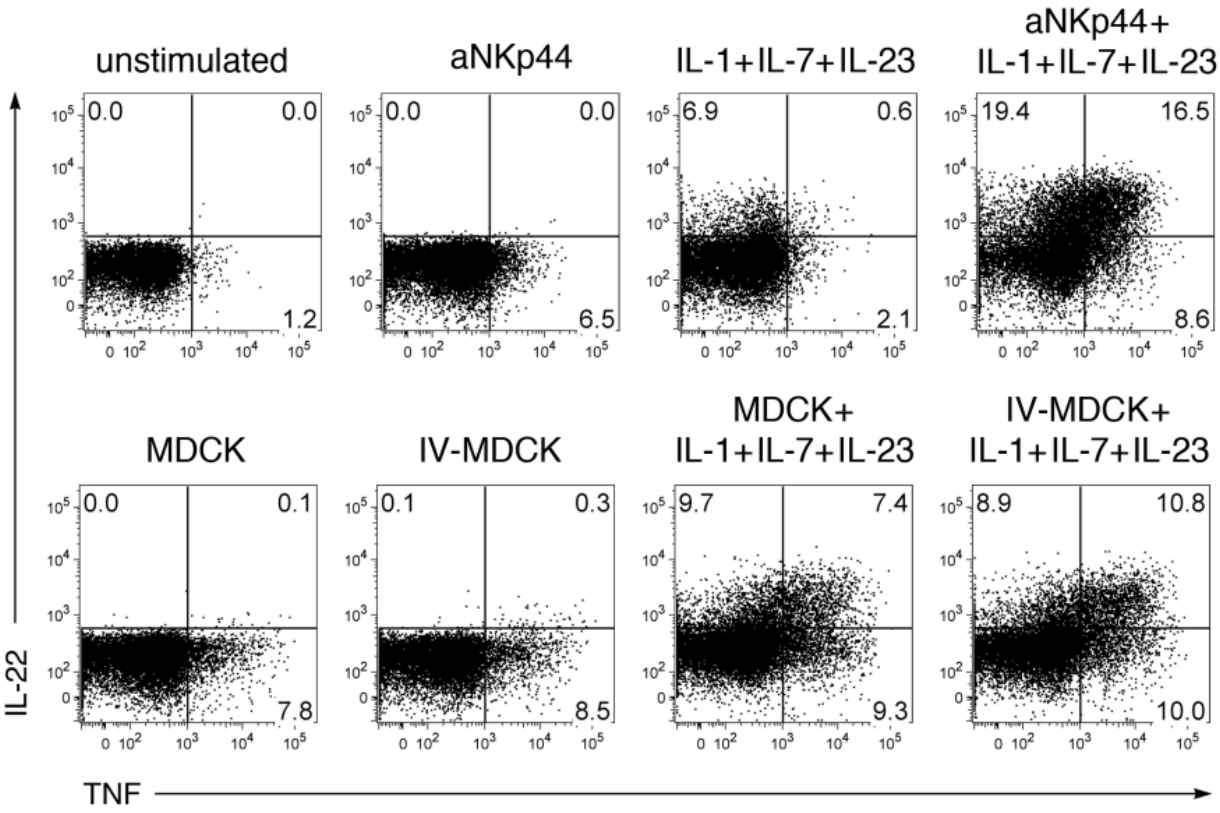

Figure 25 Co-culture of RORγt$^+$ ILC3 with influenza virus-infected MDCK cells

FACS-sorted human tonsil CD3$^-$ CD19$^-$ CD127^{high} (RORγt$^+$ ILC3) were co-cultured with either non-infected or IV-infected MDCK cells with or without the presence of IL-1 + IL-7 + IL-23. As control conditions, mAb-mediated NKp44 crosslinking (aNKp44), IL-1 + IL-7 + IL-23 and aNKp44 + IL-1 + IL-7 + IL-23 were used. The expression of TNF and IL-22 after stimulation was analyzed by an intracellular staining and FC. One representative is shown (n = 2). Experiments were performed in cooperation with Monica Killig.

4.6 Detection of NKp44 ligands on transformed or tumor epithelial cell lines

It has been reported before that there are, besides pathogen associated NKp44 ligands, endogenous NKp44 ligands that are upregulated on transformed cells (Byrd et al., 2007). However, their molecular identity is so far undefined. In line with this, the expression of NKp44 ligands by the transformed cell line HEK 293T was confirmed during the establishment of NKp44-fc staining, as described in section 4.4. Following the observation of the cytokine response in RORγt$^+$ ILC3 after co-culture with MDCK cells, we wanted to test whether non-

IV-infected MDCK cells correspondingly express NKp44 ligands on their cell surface. To this end, the NKp44-fc staining on MDCK cells was performed.

One difficulty encountered in the NKp44-fc staining of MDCK cells was their strongly adherent cell surface in contrast to the previously tested HEK 293T. MDCK cells have to be detached from culture flask walls enzymatically, whereas HEK 293T can be detached by only rinsing. For cell detachment, the protease trypsin is usually used, which is able to digest extracellular proteins. However, there have been previous reports that trypsin treatment impairs the detection of NKp44 ligands, possibly due to its proteolytic activity (Byrd et al., 2007). Therefore, in the NKp-44-fc staining series on MDCK cells, we also included a comparison between cells detached with trypsin to the ones with a trypsin-/enzyme free dissociation buffer (Figure 26).

Overall, MDCK cells displayed a high binding to NKp44-fc, indicating a strong NKp44 ligand expression. This finding is congruent with our functional readouts. However, after enzymatic cell detachment with trypsin, NKp44-fc binding was substantially reduced. Therefore, MDCK cells in subsequent experiments were exclusively detached from cell culture flasks with enzyme-free dissociation buffer.

MDCK cells are of canine origin and in accordance with their NKp44 ligand expression, NKp44 receptor is expressed in canines (Huang et al., 2008). In order to test for potential NKp44 ligand-expressing cells of human origin that could play a role *in vivo*, further tumor cell lines were analyzed; among them the human colon-derived tumor epithelial cell lines SW620 (human colorectal adenocarcinoma cell line), HT29 (human colon adenocarcinoma cell line) and Caco2 (human colorectal carcinoma cell line) (Figures 27 and 28).

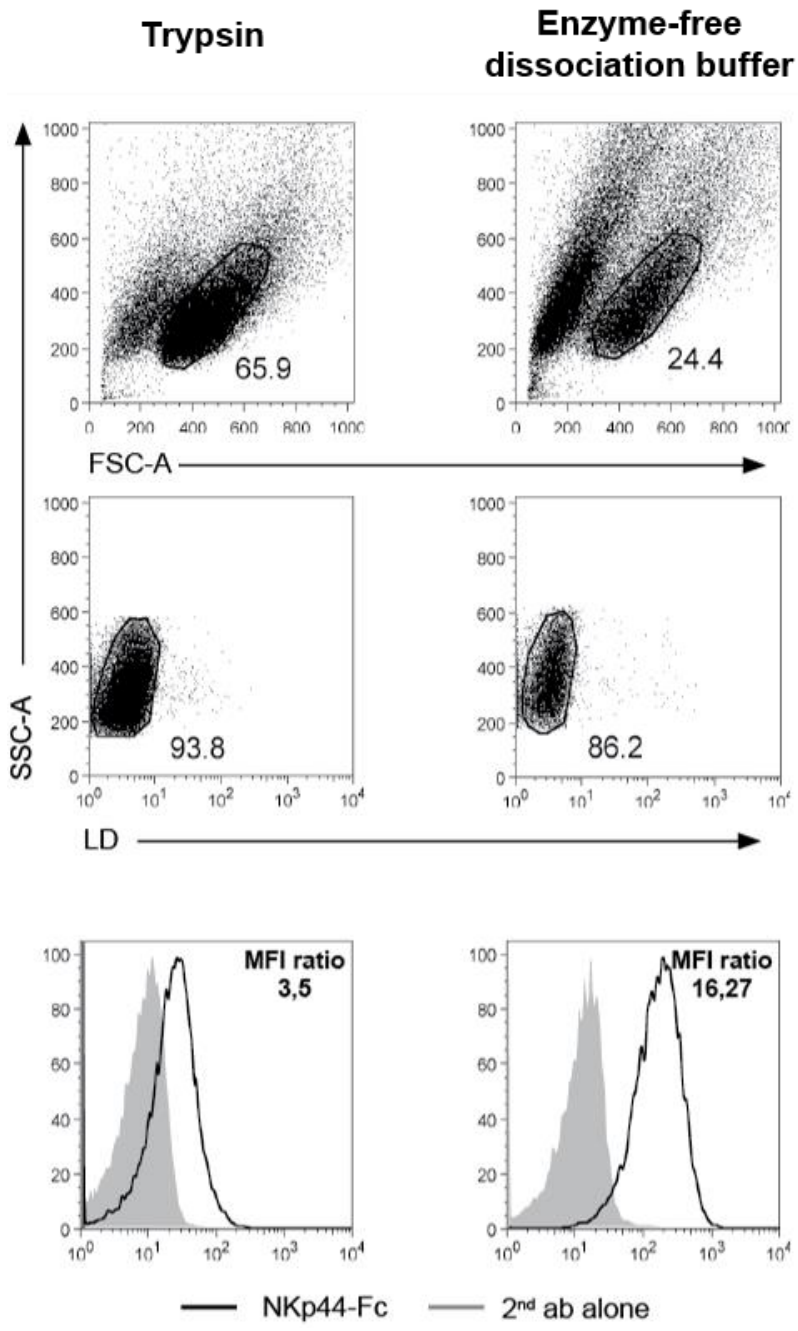

Figure 26 NKp44 ligands are expressed by MDCK cells and are sensitive to trypsin treatment

MDCK cells were stained with NKp44-fc after detachment from the culture flask wall with either trypsin (left vertical row) or enzyme-free dissociation buffer (right vertical row). FC dot plots show the gating strategy to identify viable MDCK cells in the FSC-A/SSC-A scatter and with a LIVE/DEAD (LD) staining. The histograms show the fluorescence intensity of MDCK cells after staining with NKp44-fc + 2^{nd} ab (black solid line) or 2^{nd} ab alone (grey solid histogram). MFI ratios = MFI of NKp44-fc + 2^{nd} ab / MFI of 2^{nd} ab alone.

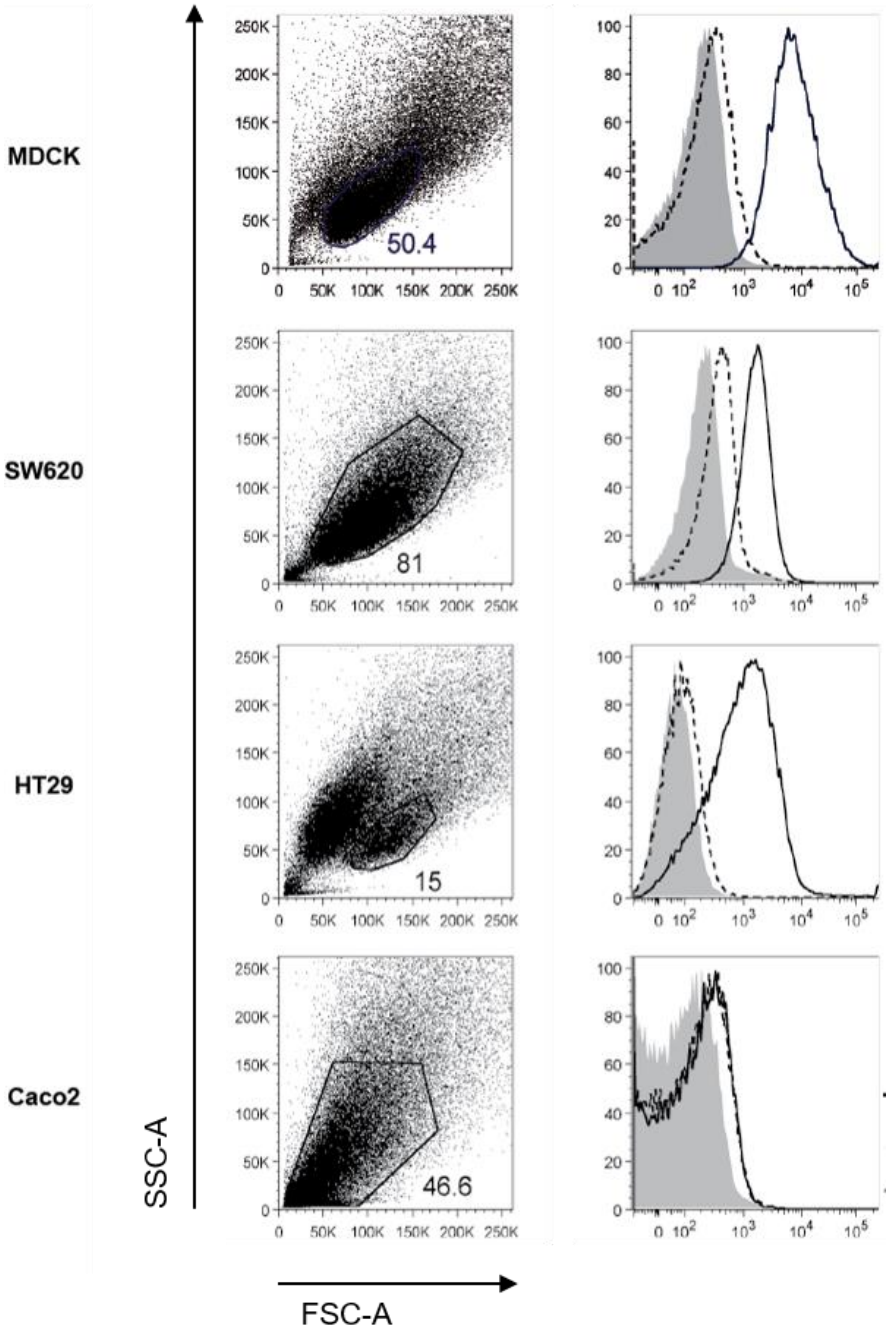

Figure 27 NKp44-fc staining on MDCK cells and human colon-derived tumor epithelial cell lines

MDCK cells, SW620 cells, HT29 cells and Caco2 cells were stained and analyzed by FC. The FC dot plots (left vertical row) show the distinct SSC/FSC scatter gate for each cell line. The histograms (right vertical row) show the fluorescence intensities after staining with either NKp44-fc + 2nd ab (black solid line), control-fc (black dotted line) or the 2nd ab alone (grey solid histogram). One representative is shown (MDCK: n = 7, SW620: n = 7, HT29: n = 3, Caco2: n = 2).

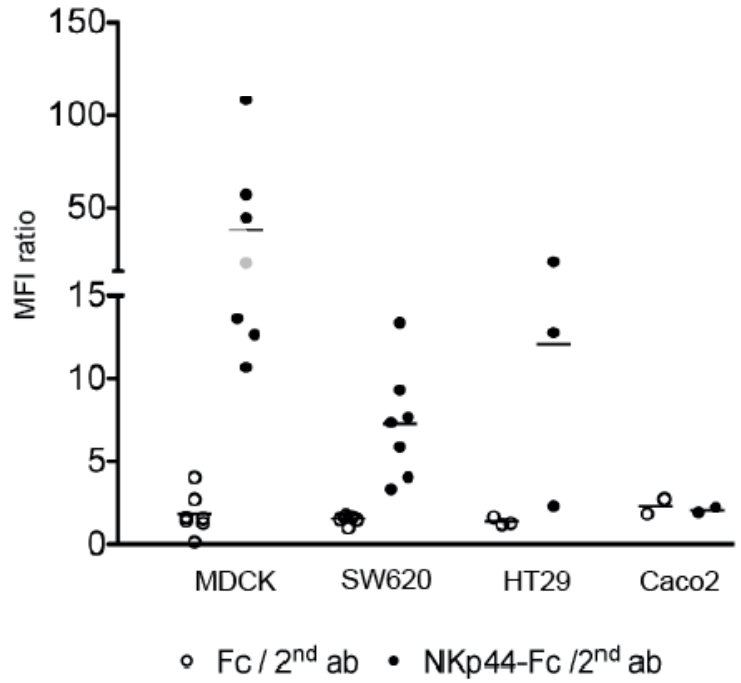

Figure 28 Summary of NK44-fc staining on MDCK, SW620, HT29 and Caco2 cells

MDCK cells, SW620 cells, HT29 cells and Caco2 cells were stained and analyzed by FC. Displayed above are the MFI ratios of NKp44-fc + 2^{nd} ab / 2^{nd} ab (NKp44-fc / 2^{nd} ab, closed circles) in comparison to the MFI ratios of control-fc + 2^{nd} ab / 2^{nd} ab (Fc / 2^{nd} ab, open circles) for the indicated cell lines.

MDCK cells, SW620 cells as well as HT29 cells consistently showed NKp44-fc binding in comparison to control-fc binding. MDCK cells exhibited the highest NKp44-fc binding of all cell lines investigated. Caco2 cells showed no difference between NKp44-fc binding and control-fc binding. There was a considerable variation in NK44-fc staining levels of one cell line in different experiments, as previously reported by other groups (Arnon et al., 2001, Byrd et al., 2007).

The expression of NKp44 ligands by MDCK and SW620 cells was confirmed by an NKp44-reporter system that was kindly provided by O. Mandelboim (Hebrew University Hadassah Medical School, Jerusalem, Israel). For the production of NKp44 reporter cells, the extracellular portion of the NKp44 receptor was fused to the CD3ζ chain. The CD3ζ chain represents one part of the T cell antigen receptor that induces IL-2 production upon ligation of the extracellular portion (Irving and Weiss, 1991). Murine BW cells (murine thymoma cells) were then stably transfected and thus expressed the transmembrane NKp44-CD3ζ fusion protein. These transfected cells are referred to in the following as BW-NKp44 cells. In the presence of NKp44 ligands, BW-NKp44 cells - but not non-transfected BW cells - produce IL-2. We confirmed NKp44 expression on the BW-NKp44 cells by flow cytometry (Figure 29).

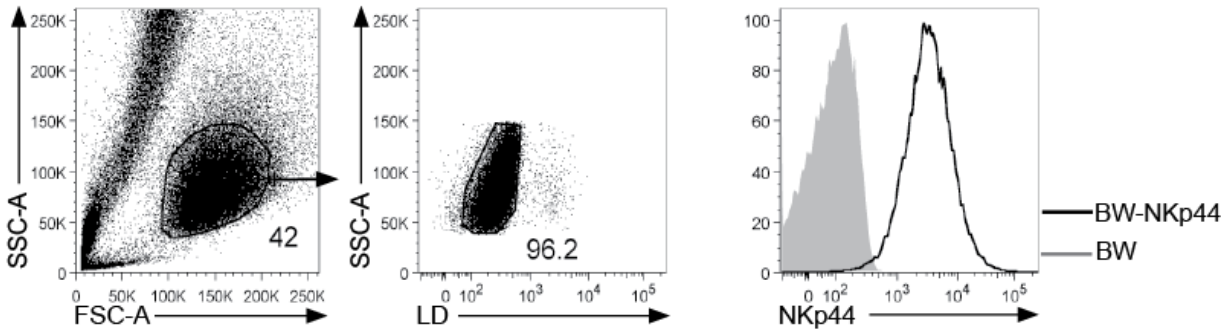

Figure 29 Expression of the extracellular NKp44 portion by BW-NKp44 but not non-transfected BW cells

BW-NKp44 and BW cells were stained on the cell surface for NKp44 and analyzed by FC. The FC dot plots indicate the gating for viable BW or BW-NKp44 cells (SSC/FSC scatter gate and exclusion of dead cells by a LIVE/DEAD staining). The histogram on the right shows the expression of NKp44 by BW-NKp44 cells (black solid line) and non-transfected BW cells (grey solid histogram).

MDCK cells and SW620 cells were irradiated and then co-cultured with BW or BW-NKp44 cells. IL-2 production was measured afterwards in the supernatants by ELISA (Figure 30). Both MDCK cell as well as SW620 cell co-culture with BW-NKp44 cells - but not with non-transfected BW cells - resulted in the production of IL-2, indicating ligation of the NKp44-CD3ζ fusion protein. MDCK cells induced a stronger IL-2 production than SW620 cells. This finding corresponded to the more pronounced NKp-44-fc binding and supposed higher expression of NKp44 ligands by MDCK cells.

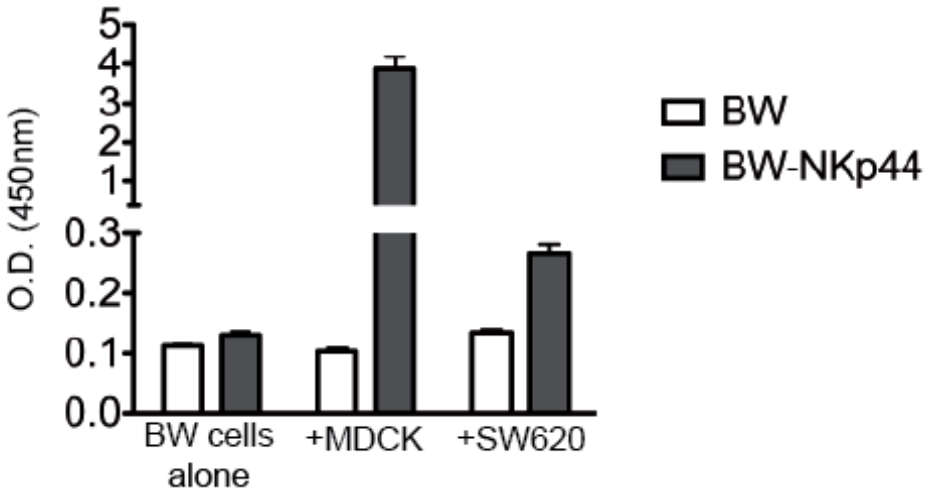

Figure 30 Co-culture of MDCK cells and SW620 cells with BW-NKp44

MDCK cells and SW620 cells were co-cultured with either BW-NKp44 cells (black bars) or non-transfected BW cells (white bars) and the resulting IL-2 production under each condition was measured by ELISA. IL-2 levels are displayed as mean absorbance (O.D. 450 nm) ± SEM of duplicates (BW: n = 3, BW-NKp44: n = 2). Experiments were performed in cooperation with Timor Glatzer.

In summary, this data shows that the NKp44-fc binds to MDCK cells, SW620 cells and HT29 at varying levels and thereby indicates that these cell lines express NKp44 ligands. NKp44 ligand expression on MDCK cells and SW620 cells is confirmed by BW-NKp44 reporter cells. MDCK cells display the highest NKp44 ligand expression of the cell lines investigated.

4.7 Engagement of NKp44 by transformed or tumor-derived epithelial cell lines induces effector functions in RORγt$^+$ ILC3

Once having confirmed the presence of NKp44 ligands on the cell surface of different transformed cell lines and tumor-derived cell lines, their capability of engaging the NKp44 receptor of RORγt$^+$ ILC3 was evaluated. For this purpose, MDCK cells and SW620 cells were co-cultured with human (tonsil derived) RORγt$^+$ ILC3 and the resulting intracellular cytokine production was analyzed by flow cytometry (Figures 31 and 32). Co-culture of MDCK cells with human RORγt$^+$ ILC3 resulted in the expression of TNF. Moreover, MDCK cells co-cultured in the presence of the cytokines IL-1 + IL-7 + IL-23 resulted in an increased expression of both TNF and IL-22, higher than under stimulation with cytokines alone. The cytokine responses after co-culture with MDCK cells with or without cytokines replicated the one observed after mAb-mediated NKp44 crosslinking. The observed response was NKp44-dependent, since it could be selectively abrogated by an anti-NKp44 blocking monoclonal antibody and not by a control monoclonal antibody (Figures 31 and 32).

Besides MDCK cells, the human colorectal adenocarcinoma-derived cell line SW620 expresses NKp44 ligands, though to an overall smaller extent (Figures 27 and 28). Co-culture of SW620 with human RORγt$^+$ ILC3 resulted in a cytokine response similar to MDCK co-culture and mAb-mediated NKp44 crosslinking (Figures 33 and 34). However, the cytokine induction was less pronounced and could only partially be inhibited by a blocking anti-NKp44 monoclonal antibody. This indicated that the observed effect was only partially NKp44-dependent.

Collectively, this data shows that NKp44 of human RORγt$^+$ ILC3 can be engaged by NKp44 ligands expressed on transformed cell lines or tumor-derived epithelial cell lines. This engagement results in a TNF production similar to the one observed under mAb-mediated NKp44 crosslinking. Furthermore, like NKp44 crosslinking, NKp44 engagement by ligand expressing cells with the cytokines IL-1 + IL-7 + IL-23 synergistically increases the expression of both TNF and IL-22.

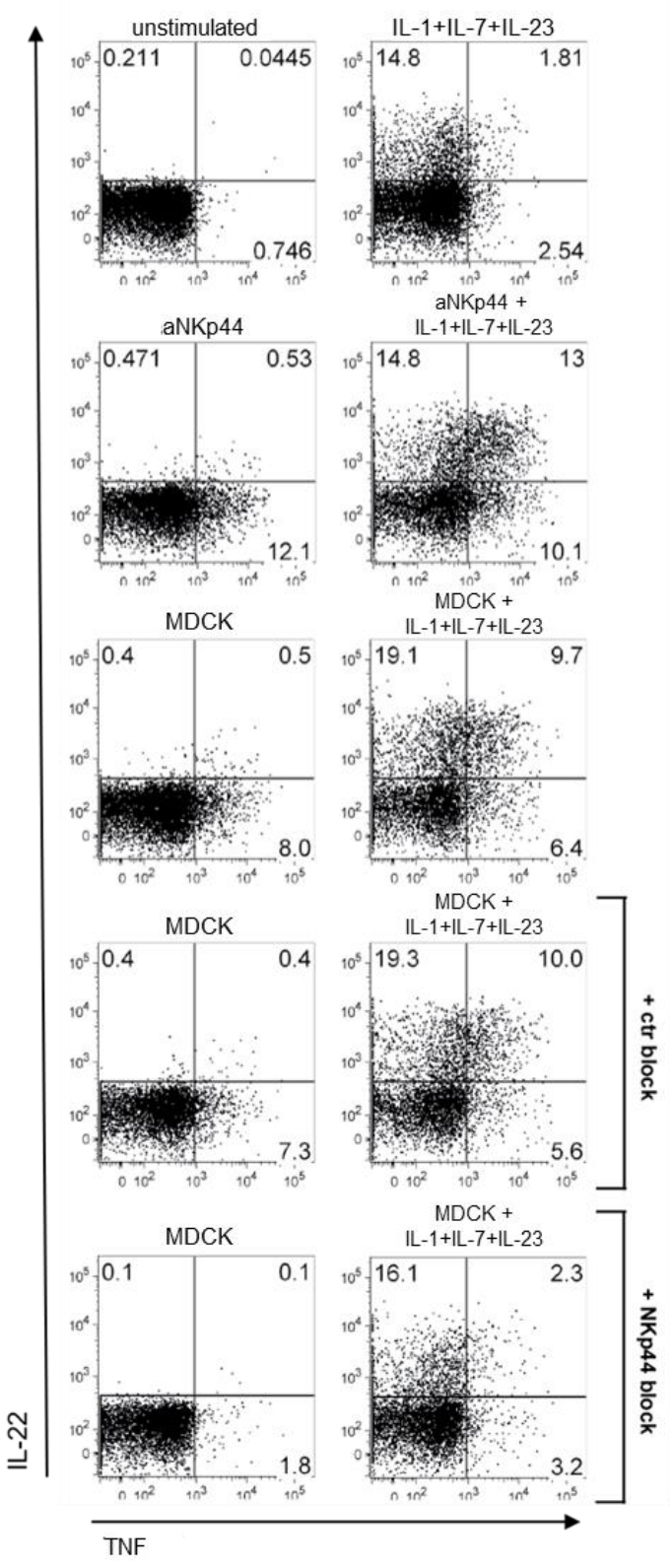

Figure 31 Engagement of NKp44 by MDCK cells results in a cytokine response in RORγt$^+$ ILC3

FACS-sorted human tonsil CD3$^-$ CD19$^-$ CD127^{high} CD56$^+$ cells (RORγt$^+$ ILC3) were co-cultured with MDCK cells in the presence or absence of the cytokines IL-1 + IL-7 + IL-23, and in the presence or absence of an NKp44 blocking monoclonal antibody (NKp44 block) or a control blocking monoclonal antibody (ctr block). As control conditions, we used mAb-mediated NKp44 crosslinking (aNKp44), IL-1 + IL-7 + IL-23 and aNKp44 + IL-1 + IL-7 + IL-23. One representative is shown (n = ≥ 5). Experiments were performed in cooperation with Monica Killig.

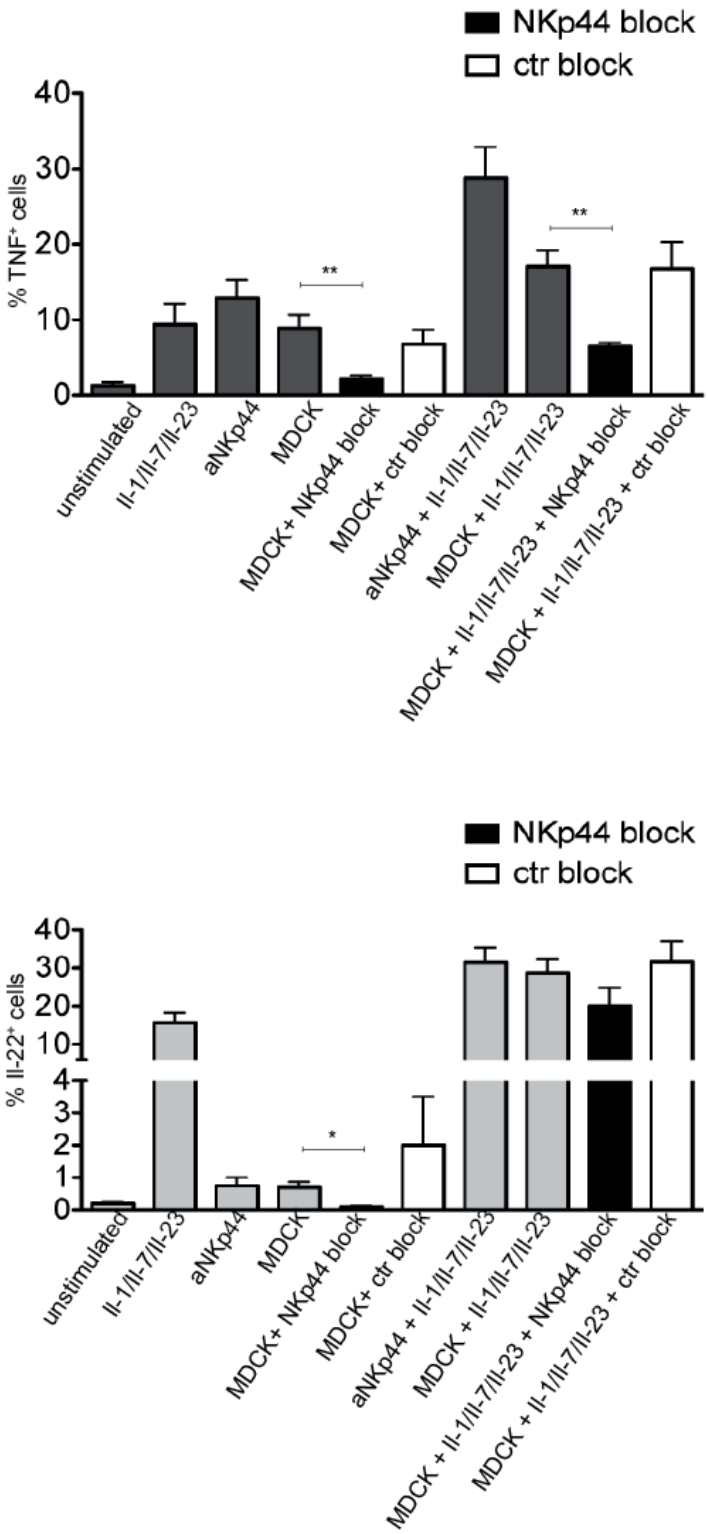

Figure 32 Summary of co-culture experiments with MDCK cells and RORγ$^+$ ILC3

MDCK cells were co-cultured with RORγt$^+$ ILC3 as described in Figure 31. Shown above are the mean percentages ± SEM of TNF+ cells (above) and IL-22$^+$ cells (below) after stimulation (n ≥ 6, except for the conditions MDCK + NKp44 block/ MDCK + ctr block / MDCK + IL-1 + IL-7 + IL-23 + NKp44 block / MDCK + IL-1 + IL-7+ IL-23 + ctr block: n = 5). Statistical analysis with the Wilcoxon signed rank two-tailed test. Experiments were performed in cooperation with Monica Killig.

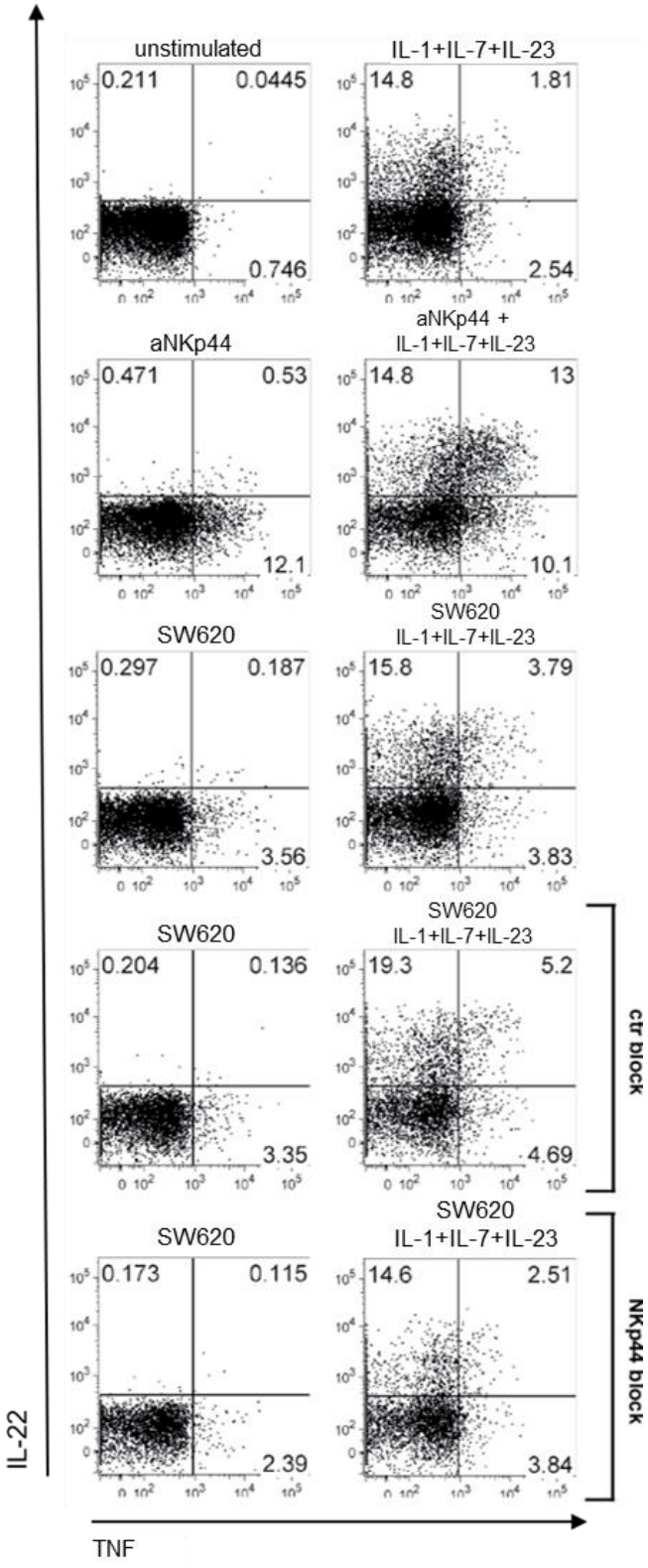

Figure 33 Co-culture with SW620 cells results in a partially NKp44-dependent cytokine response

FACS-sorted human tonsil CD3$^-$ CD19$^-$ CD127^{high} CD56$^+$ cells (RORγt$^+$ ILC3) were co-cultured with SW620 cells in the presence or absence of the cytokines IL-1 + IL-7 + IL-23, and in the presence or absence of an NKp44 blocking monoclonal antibody (NKp44 block) or a control blocking monoclonal antibody (ctr block). As control conditions, we used mAb-mediated NKp44 crosslinking (aNKp44), IL-1 + IL-7 + IL-23 and aNKp44 + IL-1 + IL-7 + IL-23. One representative is shown ($n \geq 4$, except for SW620 + ctr block / SW620 + IL-1 + IL-7 + IL-23 + ctr block: $n = 3$).

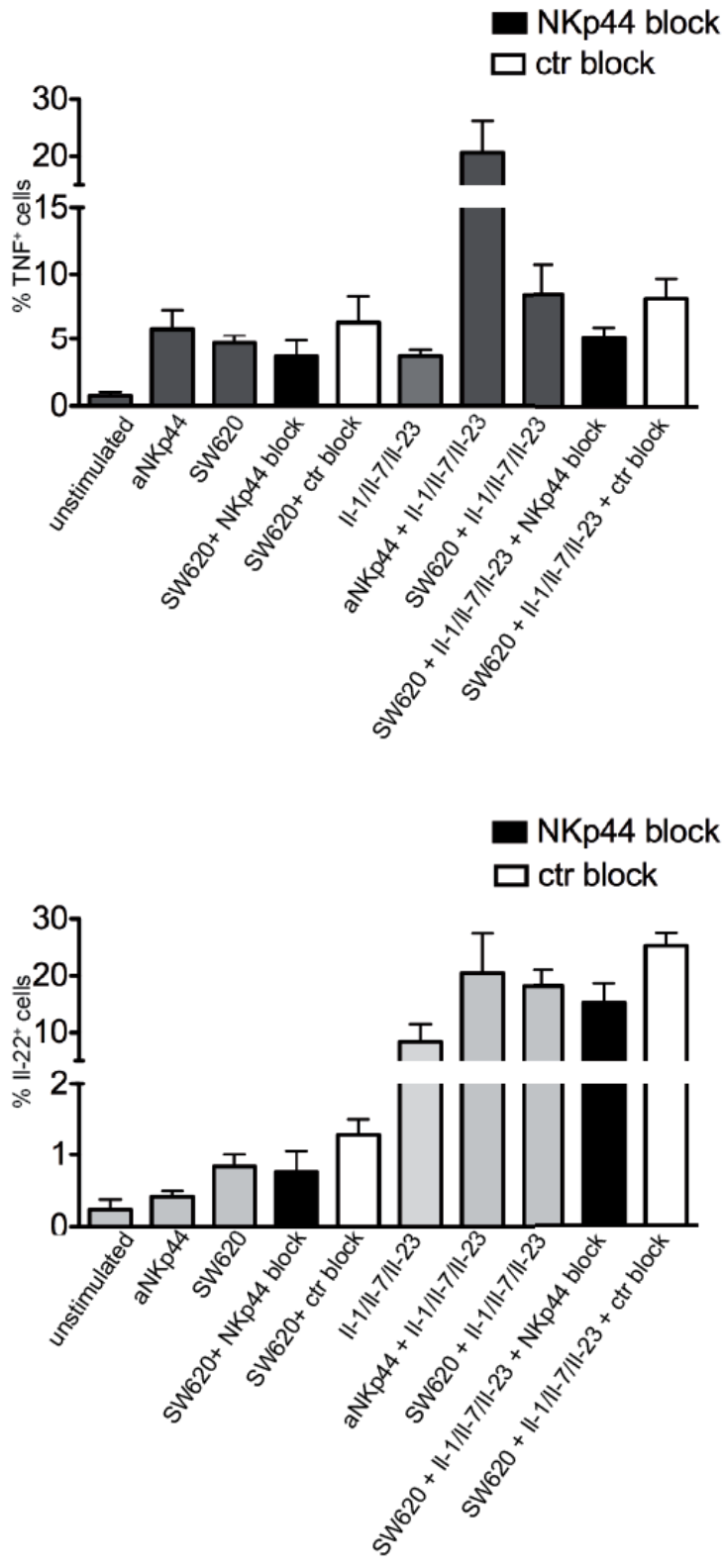

Figure 34 Summary of co-culture experiments with SW620 cells and RORγ$^+$ ILC3

SW620 cells were co-cultured with RORγt$^+$ ILC3 as described in Figure 33. Shown above are the mean percentages ± SEM of TNF+ cells (above) and IL-22+ cells (below) after stimulation ($n \geq 4$, except for the conditions SW620 + ctr block and SW620 + IL-1 + IL-7 + IL-23 + ctr block: $n = 3$). Experiments were performed in cooperation with Monica Killig.

4.8 Expression of NKp44 ligands by human intestinal epithelial cells

So far, we were able to show that the human colorectal adenocarcinoma cell line SW620 of epithelial origin expresses NKp44 ligands, which can engage the NKp44 receptor of RORγ$^+$ ILC3 and elicit a cytokine response. However, it remains speculative as to which NKp44 ligands are present *in vivo*. It is tempting to hypothesize that damaged intestinal epithelial cells (IEC) or microbiota species might express NKp44 ligands which are recognized by RORγ$^+$ ILC3 during intestinal inflammation.

To test this hypothesis, human IECs were isolated from surgical resections of non-IBD and IBD patients and NKp44-fc binding to IEC was assessed by flow cytometry. IEC were identified by the expression of the epithelial cell adhesion molecule (EpCAM) and the absence of the marker of cells of hematopoietic origin. IECs were thus defined as viable CD45$^-$ EpCAM$^+$ cells (Figure 35).

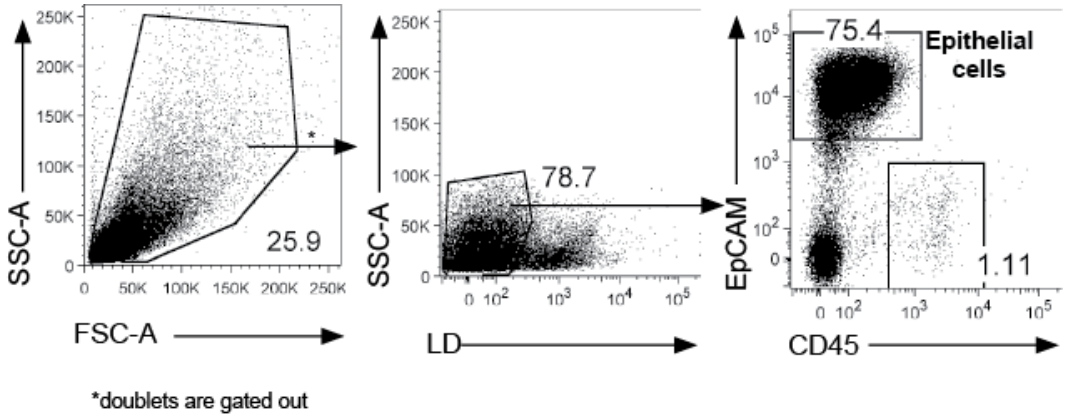

Figure 35 Identification of human intestinal epithelial cells by flow cytometry

Displayed above is the FC gating strategy to identify viable IEC. The SSC/FSC gate showed that IECs are very heterogeneous in cell size and granularity, dead cells were excluded by a LIVE/DEAD staining (LD) and IEC were positively selected by the cell surface marker EpCAM.

Next, NKp44-fc binding to IEC was analyzed (Figure 36). In some of the experiments performed, a small fraction of the IEC bound to NKp44-fc and not the control-fc. The comparison of IEC from non-inflamed and inflamed samples did not show noticeable differences. However, the detection of the NKp44 positive population was inconsistent throughout the 5 IBD-patient samples analyzed and no definitive conclusion can be drawn from these results.

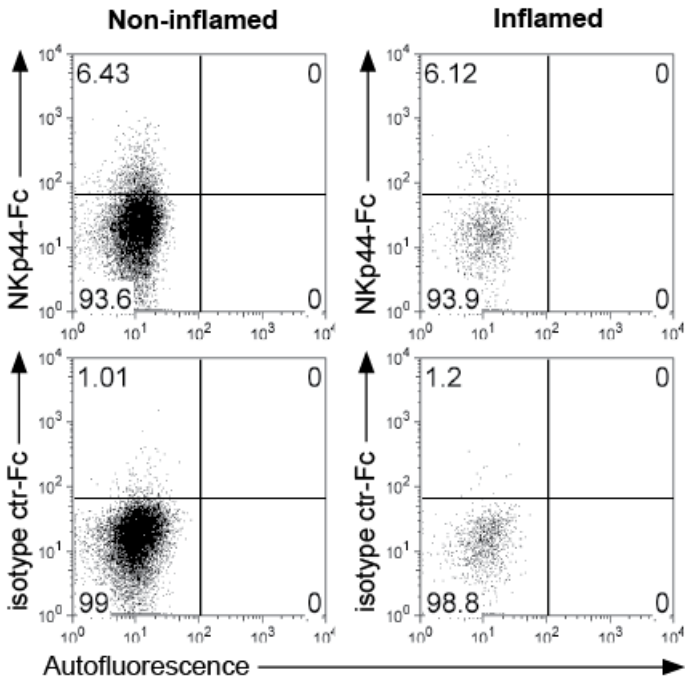

Figure 36 NKp44 ligand expression by human intestinal epithelial cells in IBD

IEC were isolated from either the non-inflamed (left vertical row) or inflamed (right vertical row) mucosa of IBD patients. Displayed above are the FC dot plots showing the binding to the NKp44-fc in comparison to a control-fc (CD99-fc). The represented experiment was performed five times, but NKp44-fc binding was inconsistent.

In summary, these preliminary experiments address the crucial question of whether human IEC might present NKp44 ligands and thereby influence the RORγ^+ ILC3 activation status. In some experiments, a small fraction of IEC expressed NKp44 ligands as assessed by NKp44-fc staining. However, this finding was inconsistent and further experiments are needed to follow up this question.

5. Discussion

The aim of this thesis project was to investigate the possible role of RORγt$^+$ ILC3 in the pathogenesis of inflammatory bowel diseases. A deeper understanding of their role and the underlying mechanisms can broaden the understanding of IBD pathogenesis and possibly pave the way for new treatment options.

The crucial role of RORγt$^+$ ILC3 in epithelial barrier integrity and maintenance of intestinal homeostasis has been increasingly recognized. However, there is also accumulating evidence that they possibly display a pro-inflammatory role in the context of intestinal inflammation. Several innate mouse models as well as human studies have supported either a tissue-protective or pro-inflammatory role (Zenewicz et al., 2008, Vonarbourg et al., 2010, Buonocore et al., 2010, Geremia et al., 2011, Cella et al., 2009, Sugimoto et al., 2008, Sawa et al., 2011, Takayama et al., 2010). Thus, the role of RORγt$^+$ ILC3 in the development of intestinal inflammation has been controversially discussed.

Previously to my thesis, our group demonstrated that the stimulation of human tonsil RORγt$^+$ ILC3 via the NKp44 receptor mainly results in the production of TNF and a pro-inflammatory gene signature. In contrast, cytokine stimulation preferentially induces the production of IL-22. Building on these results, we hypothesized that NKp44 might be engaged *in vivo* during intestinal inflammation, possibly directing RORγt$^+$ ILC3 from a tissue-protective role towards a pro-inflammatory activation status.

In order to address the aim of this thesis, there were two major stages. First, the distribution of RORγt$^+$ ILC3 and their NKp44 expression in inflamed or non-inflamed intestinal lamina propria of IBD patients were assessed. In a second stage, expression of potential NKp44 ligands on different cell lines and the functional consequences of their engagement by RORγt$^+$ ILC3 was analyzed.

5.1 Characterization of human lamina propria RORγt$^+$ ILC3 and their NKp44 expression in the context of IBD

For the first stage, tissue samples were obtained from non-affected, non-inflamed colons of patients with colorectal carcinoma or sigma diverticulitis, as well as from inflamed and non-inflamed segments of patients with IBD. Lamina propria mononuclear cells (LP MNC) were isolated and analysed by flow cytometry. We defined RORγt$^+$ ILC3 by their surface expression

of the IL-7-Receptor (CD127) and the absence of markers of other lineages. Within the lineage negative compartment, a $CD127^{high}$ population could clearly be distinguished that was heterogenous in the expression of CD56. In line with previous reports, this population is strongly enriched in RORγt$^+$ ILC3 (Cupedo et al., 2009, Crellin et al., 2010, Geremia et al., 2011). In line with this data, the majority of this population was found among the $CD45^{intermediate}$ cells (Cupedo et al., 2009), further confirming their ILC3 identity. A weakness in this gating strategy is that CD127 is not exclusively expressed by RORγt$^+$ ILC3, and that contamination with ILC2 and ILC1 cells cannot be excluded (Spits et al., 2013). An additional surface staining of CRTH2 (chemoattractant receptor-homologous molecule expressed on Th2 lymphocytes) could have distinguished ILC2 from RORγt$^+$ ILC3, while staining of CD117 (c-KIT) could have excluded ILC1 cells among the Lin^- $CD45^{int/high}$ $CD127^+$ population. Nevertheless, it has been delineated by several reports that RORγt$^+$ ILC3 constitute the major ILC population within the human colonic mucosa, and to a slightly lesser degree in the mucosa of the ileum, while ILC2 are virtually absent (Kramer et al., 2017, Forkel et al., 2019, Hoorweg et al., 2012). Thus, one can assume that most of the cells within the Lin^- $CD45^{int/high}$ $CD127^{high}$ population are indeed RORγt$^+$ ILC3. This assumption is corroborated by the high levels of *RORC* and *AHR* transcripts observed in this sorted population, two hallmarks of RORγt$^+$ ILC3. The majority of intestinal RORγt$^+$ ILC3 expressed the NKp44 receptor. This finding speaks for a compartment-specific distribution, not only for the ILC subpopulations overall but also for the NKp44$^+$ and NKp44$^-$ ILC3 subset. The observation that NKp44$^+$ RORγt$^+$ ILC3 are the predominant ILC population in the human colonic LP has also been made in additional reports (Forkel et al., 2019, Kramer et al., 2017).

The NKp44 receptor has previously been shown to be functional in tonsil-derived RORγt$^+$ ILC3 (by our group, published in Glatzer et al., 2013). Herein, we assessed whether intestinal LP-derived RORγt$^+$ ILC3 show a similar responsiveness. The receptor was activated by monoclonal antibody-mediated crosslinking. In response to this activation, a small amount of TNF production could be observed, yet in comparison to the tonsil counterparts at a very low level (<10% of TNF-producing cells). The cytokine combination IL-1 + IL-7 + IL-23 induced a clear production of IL-22, similarly to the response seen in tonsil-derived RORγt$^+$ ILC3. A combined stimulation via NKp44 crosslinking and cytokines synergistically increased IL-22 production, but not TNF production. This synergistic effect indicates that the NKp44 receptor is indeed functional in intestinal RORγt$^+$ ILC3. However, it remains unclear why intestinal RORγt$^+$ ILC3 upregulated little intracellular expression of TNF after NKp44 triggering, as compared to their tonsil counterparts. In contrast to protein expression, measurement of mRNA

revealed a clear induction of *TNF* transcripts after NKp44 triggering of intestinal RORγt$^+$ ILC3, thus further supporting the assumption that NKp44 is also functional in the intestine (Glatzer et al., 2013). This discrepancy might be due to the fact that TNF can be post-transcriptionally regulated. Interestingly, MAP-kinase-activated protein kinase 2 (MK2), which modulates the translation and stability of TNF mRNA (Kotlyarov et al., 1999), is upregulated in stimulated tonsil RORγt$^+$ ILC3 (Glatzer, unpublished data), possibly contributing to modulate TNF expression in this compartment. Whether intestinal RORγt$^+$ ILC3 might express low levels of MK2 needs to be ascertained.

After having looked at the distribution and NKp44 expression of RORγt$^+$ ILC3 in the non-inflammatory intestinal LP, possible alterations in the context of IBD were assessed. A series of tissue samples was collected from IBD patients that had undergone surgery. From each patient, macroscopically non-inflamed and inflamed mucosa samples were obtained. Together with the samples of unaffected LP of colorectal carcinoma or sigma diverticulitis patients, the distribution of RORγt$^+$ ILC3 was compared within the following three groups: the non-IBD non-affected mucosa, the IBD non-inflamed mucosa, and the IBD inflamed mucosa. No significant difference was seen between these groups when looking at the frequency of RORγt$^+$ ILC3. Strikingly, a clearly diminished NKp44 expression among RORγt$^+$ ILC3 in the inflamed LP of IBD samples was observed. In contrast, NKp44 expression in the non-inflamed IBD samples and the non-IBD, non-affected samples was comparable. When analysing NKp44 expression in the inflamed and the non-inflamed mucosa of one IBD patient, the decrease of NKp44 expression was consistent throughout all individuals regardless of the baseline, which varied to some extent inter-individually.

Several aspects have to be considered in the evaluation of this data. First, the number of samples analysed was rather low. Also, it would have been of interest to have more information about the donors, such as time since disease onset, previous and current treatment (especially immunomodulating therapies) or the grade of inflammation. Furthermore, samples for Crohn´s disease (CD) and Ulcerative Colitis (UC) were not analysed separately, as the same trend of NKp44 downregulation was observed in both pathologies. However, as pathophysiology of the two diseases only partially overlaps (Neurath, 2014), further studies with a more detailed acquisition of data and separate analysis for CD and UC samples would be of great interest.

Despite these aspects, the decrease of the NKp44$^+$ RORγt$^+$ ILC3 subset was consistent throughout all samples and specifically for the inflamed, and not the non-inflamed, segments

of IBD mucosal samples. This observation is congruent with other published studies on ILCs in human IBD (Takayama et al., 2010, Bernink et al., 2013, Forkel et al., 2019). The underlying reason for the decrease of NKp44 expression in LP RORγt$^+$ ILC3 in the context of IBD as well as its consequences have so far not been understood.

We hypothesized that the NKp44 receptor of RORγt$^+$ ILC3 might be engaged *in vivo* in the inflammatory state of IBD by exogenous or endogenous ligands, resulting in a pro-inflammatory response and downregulation of the receptor. Another possible explanation is that the cytokine environment in inflammation promotes the conversion of RORγt$^+$ ILC3 or the accumulation of other NKp44$^-$ ILC lineages. For example, one study has suggested that human NKp44$^+$ RORγt$^+$ ILC3 can, under the influence of IL-2 and IL-12, differentiate into CD127$^+$ ckit$^-$ NKp44$^-$ ILC1, which produce IFN-γ instead of IL-22. In this study, LP NKp44$^+$ ILC3 were decreased in inflamed tissue of CD at the expense of ILC1 (Bernink et al., 2013). Another report on CD patients described a decrease of IL-23 responsive, IL-22-producing CD127$^+$ CD56$^+$ ILCs, with an increase of CD127$^+$ CD56$^-$ ILC that produce IL-17 (Geremia et al., 2011). However, in another research work, an enrichment of IFN-γ-producing, CD103$^+$NKp44$^+$ intraepithelial ILC1 cells was observed (Fuchs et al., 2013). Recently, a further study on the distribution of LP and peripheral blood ILC subsets in Crohn´s disease and Ulcerative colitis was published that took the time after disease onset, disease severity and treatment into account (Forkel et al., 2019). The central finding was that, already at disease onset, the frequency of NKp44$^+$ ILC3 is decreased in the inflamed tissue of both CD and UC patients. No alterations of the frequencies were seen in non-inflamed colonic sections or in peripheral blood. At the same time, the frequency of ILC1 is increased in patients with CD, and the frequency of ILC2 is increased in patients with UC. At a later time point after disease onset, both ILC1 and ILC2 are increased in CD as well as in UC (Forkel et al., 2019). The fact that, simultaneously with the decrease of NKp44$^+$ ILC3, an increase of ILC of other phenotypes was observed by the cited reports could also be explained by ILC plasticity. In line with this, an experimental colitis model with anti-CD40 antibodies showed that IL-22-producing NKp46$^+$ ILC progressively lose RORγt expression and the NKp46$^+$ RORγt$^-$ subset contributes to IFN-γ production (Vonarbourg et al., 2010). A promising technique that could enlighten these so far only partially understood relations is single-cell RNA sequencing (scRNA-Seq). scRNA-Seq of human tonsil ILC has highlighted the identity of four main ILC lineages, namely corresponding to ILC1, ILC2, ILC3 and NK cells (Bjorklund et al., 2016). Among the ILC3 cluster, three transcriptionally and functionally diverse subpopulations could be distinguished. Besides the IL-22-producing NKp44$^+$ subset, a possibly naïve, non-cytokine producing one, as well as another that exhibited

antigen-presenting features, are described. Applying this technique on human LP ILCs in the context of IBD would certainly advance the understanding of the mechanisms that occur in the ILC compartment during disease development.

5.2 Evaluation of a physiologic engagement of the NKp44 receptor in RORγt$^+$ ILC3

As signaling via the NKp44 receptor could be a potential environmental cue to direct RORγt$^+$ ILC3 from a tissue protective to a pro-inflammatory function, the second part of this thesis investigated a possible physiologic engagement of the NKp44 receptor in RORγt$^+$ ILC3.

To this end, we addressed the question of whether the NKp44 receptor of RORγt$^+$ ILC3 can be engaged by putative exogenous or endogenous ligands, leading to activation of RORγt$^+$ ILC3. Most of our understanding about the functions of NKp44 and its ligands derives from NK cells, while no other data are available on RORγt$^+$ ILC3. Engagement of NKp44 as well as the other natural cytotoxicity receptors (NCR) activates NK cells and leads to cytotoxic activity and cytokine production (Moretta et al., 2001, Lanier, 2005). The first NKp44 ligands that were described in literature are influenza hemagglutinin and hemagglutinin neuraminidase of the Sendai virus. It has been shown that the binding of NKp44 to influenza hemagglutinin improves the ability of some NK cell clones to lyse influenza virus-infected cells (Arnon et al., 2001). Additionally, a broad variety of tumor cell lines, and thereby putative endogenous sources, are reported to express NKp44 ligands (Arnon et al., 2001, Byrd et al., 2007). Despite these findings, the molecular identity of the NKp44 ligands is still undefined. After my experimental work was completed, two reports identified a novel isoform of the mixed-lineage leukemia-5 protein (Baychelier et al., 2013) and HLA-DP (Niehrs et al., 2019) as putative NKp44 ligands. While the physiological relevance of mixed-lineage leukemia-5 protein as a NKp44 ligand remains unclear, HLA-DP represents a very attractive candidate to test in further experiments.

In a first step, we established a method to detect the presence of NKp44 ligands on cell surfaces by flow cytometry using an NKp44-fc fusion protein. In a second step, stimulation experiments with putative NKp44 ligands were performed in tonsil-derived RORγt$^+$ ILC3. In general, the conditions were set up as had previously been established by our work group on tonsil-derived RORγt$^+$ ILC3 (Glatzer et al., 2013). In addition, putative NKp44 ligands were added as a further condition either alone or together with the cytokines IL-1, IL-7 and IL-23.

The first putative NKp44 ligand we tested for engaging the NKp44 receptor in RORγt$^+$ ILC3 was influenza hemagglutinin of influenza virus (IV HA). Three different setups were tested: co-culture with H5 expressing HEK 239 T cells, direct incubation with H1N1 and finally co-culture with IV-infected MDCK cells (the two latter ones were in collaboration with the Molecular Biology Department of the Max Planck Institute for Infection Biology). Firstly, RORγt$^+$ ILC3 were co-cultured with IV hemagglutinin 5 transfected HEK 293T cells (H5-HEK 293T) (Ho et al., 2008). Both non-H5-transfected and H5-transfected HEK293T stained positive for the NKp44-fc. Neither HEK 293T nor H5-HEK 293T induced considerable production of TNF or of IL-22 when co-cultured alone. However, both HEK 293T and H5-HEK 293T, in a synergistic way together with IL-1, IL-7 and IL-23, enhanced the production of IL-22 and to a small extent that of TNF. This setup was problematic for several reasons. Among the H5-HEK293T culture, only between 30-50% were expressing H5 at the cell surface as seen by flow cytometry analysis, and this percentage could not be raised by positively sorting H5-HEK-293T and re-culturing them. Moreover, no difference was seen between HEK 293T and H5-HEK 293T in their synergistic effect on IL-22 production. Due to these obstacles, this setup was not followed up further. Instead, a direct stimulation with the influenza virus of the strain A/WSN/33 (H1N1) was tested. Direct stimulation with influenza virus has been performed before on NK cells and led to their activation (Jost et al., 2011). Here, in RORγt$^+$ ILC3, the stimulation with influenza virus alone did not induce any cytokine production. Although exposure to influenza virus enhanced IL-22 production induced by IL-1, IL-7 and IL-23, TNF was hardly detected. This effect was in contrast to the one seen after crosslinking with anti-NKp44 monoclonal antibody, as the latter acted synergistically with IL-1, Il-7 and Il-23 on both IL-22 and TNF production. Furthermore, the response could not be blocked by an anti-NKp44-blocking monoclonal antibody, suggesting that the IV-mediated effects on RORγt$^+$ ILC3 are not NKp44-dependent. Finally, it was analysed whether IV-infected cells can elicit an NKp44-mediated response. To this end, H1N1 IV-infected MDCK (Madin-Darby canine kidney) cells, which are known to be highly susceptible to IV infection (Gaush et al., 1966), were co-cultured with RORγt$^+$ ILC3. Somewhat surprisingly, co-culture with non-infected MDCK and with H1N1-infected MDCK cells elicited a similar IL-22 and TNF production, and this response was comparable to the one induced after crosslinking with anti-NKp44 monoclonal antibody. This finding suggests that RORγt$^+$ ILC3 activation in this system is not mediated by the influenza infection, but rather by molecules expressed by uninfected MDCK cells. In summary, although hemagglutinin of influenza virus has been previously identified as ligand of NKp44 for NK cells, neither H5 nor H1N1 seems to induce NKp44-depended IL-22 or TNF production by RORγt$^+$ ILC3. One

possible explanation for this discrepancy is that a critical requirement for the recognition of IV HA by the NKp44 receptor is the sialylation of its glycoproteins (Arnon et al., 2001). Furthermore, influenza neuraminidase protein can change the sialylation status and prevent the recognition of HA by NKp44 (Bar-On et al., 2014). Whether the NKp44 receptor in RORγt$^+$ ILC3 might be differently glycosylated than in NK cells would require further investigation.

With the first findings indicating that MDCK cells might indeed be able to engage the NKp44 receptor of RORγt$^+$ ILC3, we sought to ensure that non-IV-infected MDCK cells consistently express NKp44 ligands. By performing NKp44-fc staining it was demonstrated that MDCK cells display a strong binding to NKp44-fc. However, as MDCK cells are of canine origin, the relevance of this finding for the human system is disputable. Therefore, the search for NKp44 ligand-expressing cells was extended to other human cell lines. Besides MDCK cells, SW620 (human colorectal adenocarcinoma cell line) and HT29 (human colon adenocarcinoma cell line) resulted as positive for NKp44-fc staining, although to a lesser extent than MDCK cells. Conversely, the human colon adenocarcinoma cell line Caco2 did not show NKp44-fc binding. One issue in the analysis of the NKp44 ligand expression was a considerable variation in the level of NKp44-fc binding within each cell line in different experiments. This variation has been reported before by other groups (Arnon et al., 2001). The reason for this inter-experiment variation remains unclear. It has been previously shown that the cell cycle might affect NKp44 ligand expression as NKp44-fc staining is reduced in cells arrested in the G2/M phase (Byrd et al., 2007). It is therefore possible that the culture time and density of the cells in the culture flask might influence the NKp44 ligand expression level. This hypothesis would need further testing. For additional validation of NKp44 ligand expression on MDCK cells and SW620 cells as indicated by the NKp44-fc binding, an NKp44-reporter system was used, endowed with a transmembrane NKp44-CD3ζ fusion protein. Co-culture of both MDCK and SW620 elicited the activation of the reporter cell line. Moreover, MDCK cells induced a stronger response than SW620, in line with the higher NKp44-fc binding. Collectively, two independent methods for the detection of NKp44 ligands showed that MDCK and SW620 cells express NKp44 ligands on their cell surface.

After having analyzed the NKp44 ligand expression pattern on the different cell lines, RORγt$^+$ ILC3 were stimulated by MDCK cells and SW620 cells alone, or in the presence of the cytokines IL-1, IL-7 and IL-23. For each experiment, stimulation with the anti-NKp44 monoclonal antibody was performed as well in order to compare the resulting cytokine responses. It was demonstrated that stimulation with MDCK cells alone or in combination with

IL-1, IL-7 and Il-23 replicate what was previously observed in the stimulation with the anti-NKp44 monoclonal antibody. In order to further test whether this response resulted indeed from an NKp44 receptor-ligand interaction, an NKp44 blocking antibody as well as a control blocking antibody were included in the setting. The NKp44 blocking antibody reliably blocked the effect of the MDCK cells, both when co-cultured alone or in the presence of cytokines. The cytokine induction under stimulation with SW620 was similar, but less pronounced than the one detected with MDCK cells or with NKp44 crosslinking. On the one hand, this could result from the lower NKp44 ligand expression on SW620 cells. On the other hand, the cytokine induction by SW620 was only partially inhibited by the NKp44 blocking antibody, suggesting that additional signals might be responsible for RORγt$^+$ ILC3 activation in this system.

Finally, the question was raised of whether primary epithelial cells derived from human intestinal mucosa express NKp44 ligands. To this end, intestinal epithelial cells (IEC) were isolated. In preliminary experiments, a small fraction of IEC displayed binding to NKp44-fc. However, this finding was inconsistent, as it could not be observed in all samples analyzed. Thus, at this point in time, no conclusion can be drawn. Yet this question and the described approach would certainly be worthwhile to pursue further.

The finding that the NKp44 receptor in human RORγt$^+$ ILC3 can be engaged in a more physiologic way by NKp44 ligand-expressing model cell lines, and that this elicits the production of the pro-inflammatory cytokine TNF, is novel. What has not been answered by this work is whether NKp44 engagement occurs also *in vivo* and indeed contributes to a pro-inflammatory role of RORγt$^+$ ILC3 in IBD. To approach this question, it would be of interest to test whether blockage of the NKp44 receptor can possibly prevent or diminish inflammatory processes. For this purpose, co-culture of intestinal organoids with RORγt$^+$ ILC3 could be used. Furthermore, it would be important to identify NKp44 ligands *in vivo* and investigate whether these are potentially upregulated during intestinal inflammation. It is tempting to hypothesize that intestinal epithelial cells or microorganisms might express certain NKp44 ligands which impact the balance of intestinal homeostasis and inflammation. However, corresponding experiments are pending.

In a final summary, from the data obtained in this thesis, it can be concluded that NKp44 receptor expression is clearly diminished in RORγt$^+$ ILC3 derived from the inflamed mucosa of IBD patients. Whether this finding is due to either downregulation of the NKp44 receptor because of *in vivo* engagement, or to a different activation status of these cells, or to ILC

plasticity remains to be clarified. Furthermore, it was shown that the engagement of the NKp44 receptor in RORγt$^+$ ILC3 by NKp44 ligands on model cell lines leads to the production of the pro-inflammatory cytokine TNF, while cytokine stimulation preferentially induces IL-22. These findings, taken together with the previous results from my group, suggest a potential dual nature for RORγt$^+$ ILC3 depending on the environmental context. Thus, NKp44 might represent a possible target to modulate the pro-inflammatory versus protective features of RORγt$^+$ ILC3 during IBD.

6. References

ARNON, T. I., ACHDOUT, H., LEVI, O., MARKEL, G., SALEH, N., KATZ, G., GAZIT, R., GONEN-GROSS, T., HANNA, J., NAHARI, E., PORGADOR, A., HONIGMAN, A., PLACHTER, B., MEVORACH, D., WOLF, D. G. & MANDELBOIM, O. 2005. Inhibition of the NKp30 activating receptor by pp65 of human cytomegalovirus. *Nat Immunol,* 6**,** 515-23.

ARNON, T. I., LEV, M., KATZ, G., CHERNOBROV, Y., PORGADOR, A. & MANDELBOIM, O. 2001. Recognition of viral hemagglutinins by NKp44 but not by NKp30. *European Journal of Immunology,* 31**,** 2680-2689.

ARTIS, D. 2008. Epithelial-cell recognition of commensal bacteria and maintenance of immune homeostasis in the gut. *Nat Rev Immunol,* 8**,** 411-20.

ARTIS, D. & SPITS, H. 2015. The biology of innate lymphoid cells. *Nature,* 517**,** 293-301.

AUGUGLIARO, R., PAROLINI, S., CASTRICONI, R., MARCENARO, E., CANTONI, C., NANNI, M., MORETTA, L., MORETTA, A. & BOTTINO, C. 2003. Selective cross-talk among natural cytotoxicity receptors in human natural killer cells. *Eur J Immunol,* 33**,** 1235-41.

BAR-ON, Y., SEIDEL, E., TSUKERMAN, P., MANDELBOIM, M. & MANDELBOIM, O. 2014. Influenza virus uses its neuraminidase protein to evade the recognition of two activating NK cell receptors. *J Infect Dis,* 210**,** 410-8.

BAUMGART, D. C. & SANDBORN, W. J. 2007. Inflammatory bowel disease: clinical aspects and established and evolving therapies. *Lancet,* 369**,** 1641-57.

BAYCHELIER, F., SENNEPIN, A., ERMONVAL, M., DORGHAM, K., DEBRE, P. & VIEILLARD, V. 2013. Identification of a cellular ligand for the natural cytotoxicity receptor NKp44. *Blood,* 122**,** 2935-42.

BERNINK, J. H., PETERS, C. P., MUNNEKE, M., TE VELDE, A. A., MEIJER, S. L., WEIJER, K., HREGGVIDSDOTTIR, H. S., HEINSBROEK, S. E., LEGRAND, N., BUSKENS, C. J., BEMELMAN, W. A., MJOSBERG, J. M. & SPITS, H. 2013. Human type 1 innate lymphoid cells accumulate in inflamed mucosal tissues. *Nat Immunol,* 14**,** 221-9.

BIOSCIENCES, B. 2015. *BD FACSCANTO II* [Online]. Becton, Dickinson and Company. Available: http://www.bdbiosciences.com/in/instruments/facscanto/index.jsp [Accessed 1.02.2013 2013].

BJORKLUND, A. K., FORKEL, M., PICELLI, S., KONYA, V., THEORELL, J., FRIBERG, D., SANDBERG, R. & MJOSBERG, J. 2016. The heterogeneity of human CD127(+) innate lymphoid cells revealed by single-cell RNA sequencing. *Nat Immunol,* 17**,** 451-60.

BRAND, S., BEIGEL, F., OLSZAK, T., ZITZMANN, K., EICHHORST, S. T., OTTE, J. M., DIEPOLDER, H., MARQUARDT, A., JAGLA, W., POPP, A., LECLAIR, S.,

HERRMANN, K., SEIDERER, J., OCHSENKUHN, T., GOKE, B., AUERNHAMMER, C. J. & DAMBACHER, J. 2006. IL-22 is increased in active Crohn's disease and promotes proinflammatory gene expression and intestinal epithelial cell migration. *Am J Physiol Gastrointest Liver Physiol,* 290**,** G827-38.

BUONOCORE, S., AHERN, P. P., UHLIG, H. H., IVANOV, II, LITTMAN, D. R., MALOY, K. J. & POWRIE, F. 2010. Innate lymphoid cells drive interleukin-23-dependent innate intestinal pathology. *Nature,* 464**,** 1371-5.

BYRD, A., HOFFMANN, S. C., JARAHIAN, M., MOMBURG, F. & WATZL, C. 2007. Expression analysis of the ligands for the Natural Killer cell receptors NKp30 and NKp44. *PLoS One,* 2**,** e1339.

CANTONI, C., BOTTINO, C., VITALE, M., PESSINO, A., AUGUGLIARO, R., MALASPINA, A., PAROLINI, S., MORETTA, L., MORETTA, A. & BIASSONI, R. 1999. NKp44, a triggering receptor involved in tumor cell lysis by activated human natural killer cells, is a novel member of the immunoglobulin superfamily. *J Exp Med,* 189**,** 787-96.

CELLA, M., FUCHS, A., VERMI, W., FACCHETTI, F., OTERO, K., LENNERZ, J. K. M., DOHERTY, J. M., MILLS, J. C. & COLONNA, M. 2009. A human natural killer cell subset provides an innate source of IL-22 for mucosal immunity. *Nature,* 457**,** 722-725.

CRELLIN, N. K., TRIFARI, S., KAPLAN, C. D., CUPEDO, T. & SPITS, H. 2010. Human NKp44+IL-22+ cells and LTi-like cells constitute a stable RORC+ lineage distinct from conventional natural killer cells. *J Exp Med,* 207**,** 281-90.

CUPEDO, T., CRELLIN, N. K., PAPAZIAN, N., ROMBOUTS, E. J., WEIJER, K., GROGAN, J. L., FIBBE, W. E., CORNELISSEN, J. J. & SPITS, H. 2009. Human fetal lymphoid tissue-inducer cells are interleukin 17-producing precursors to RORC+ CD127(+) natural killer-like cells. *Nature Immunology,* 10**,** 66-74.

DIGNASS, A., VAN ASSCHE, G., LINDSAY, J. O., LEMANN, M., SODERHOLM, J., COLOMBEL, J. F., DANESE, S., D'HOORE, A., GASSULL, M., GOMOLLON, F., HOMMES, D. W., MICHETTI, P., O'MORAIN, C., ORESLAND, T., WINDSOR, A., STANGE, E. F., TRAVIS, S. P., EUROPEAN, C. S. & COLITIS, O. 2010. The second European evidence-based Consensus on the diagnosis and management of Crohn's disease: Current management. *J Crohns Colitis,* 4**,** 28-62.

EBERL, G. 2005. Inducible lymphoid tissues in the adult gut: recapitulation of a fetal developmental pathway? *Nat Rev Immunol,* 5**,** 413-20.

ESIN, S., BATONI, G., COUNOUPAS, C., STRINGARO, A., BRANCATISANO, F. L., COLONE, M., MAISETTA, G., FLORIO, W., ARANCIA, G. & CAMPA, M. 2008. Direct binding of human NK cell natural cytotoxicity receptor NKp44 to the surfaces of mycobacteria and other bacteria. *Infection and Immunity,* 76**,** 1719-1727.

FORKEL, M., VAN TOL, S., HOOG, C., MICHAELSSON, J., ALMER, S. & MJOSBERG, J. 2019. Distinct Alterations in the Composition of Mucosal Innate Lymphoid Cells in

Newly Diagnosed and Established Crohn's Disease and Ulcerative Colitis. *J Crohns Colitis,* 13**,** 67-78.

FUCHS, A., VERMI, W., LEE, J. S., LONARDI, S., GILFILLAN, S., NEWBERRY, R. D., CELLA, M. & COLONNA, M. 2013. Intraepithelial type 1 innate lymphoid cells are a unique subset of IL-12- and IL-15-responsive IFN-gamma-producing cells. *Immunity,* 38**,** 769-81.

GARRETT, W. S., LORD, G. M., PUNIT, S., LUGO-VILLARINO, G., MAZMANIAN, S. K., ITO, S., GLICKMAN, J. N. & GLIMCHER, L. H. 2007. Communicable ulcerative colitis induced by T-bet deficiency in the innate immune system. *Cell,* 131**,** 33-45.

GAUSH, C. R., HARD, W. L. & SMITH, T. F. 1966. Characterization of an established line of canine kidney cells (MDCK). *Proc Soc Exp Biol Med,* 122**,** 931-5.

GAZIT, R., GRUDA, R., ELBOIM, M., ARNON, T. I., KATZ, G., ACHDOUT, H., HANNA, J., QIMRON, U., LANDAU, G., GREENBAUM, E., ZAKAY-RONES, Z., PORGADOR, A. & MANDELBOIM, O. 2006. Lethal influenza infection in the absence of the natural killer cell receptor gene Ncr1. *Nat Immunol,* 7**,** 517-23.

GEREMIA, A., ARANCIBIA-CARCAMO, C. V., FLEMING, M. P., RUST, N., SINGH, B., MORTENSEN, N. J., TRAVIS, S. P. & POWRIE, F. 2011. IL-23-responsive innate lymphoid cells are increased in inflammatory bowel disease. *J Exp Med,* 208**,** 1127-33.

GLADIATOR, A., WANGLER, N., TRAUTWEIN-WEIDNER, K. & LEIBUNDGUT-LANDMANN, S. 2013. Cutting edge: IL-17-secreting innate lymphoid cells are essential for host defense against fungal infection. *J Immunol,* 190**,** 521-5.

GLATZER, T., KILLIG, M., MEISIG, J., OMMERT, I., LUETKE-EVERSLOH, M., BABIC, M., PACLIK, D., BLUTHGEN, N., SEIDL, R., SEIFARTH, C., GRONE, J., LENARZ, M., STOLZEL, K., FUGMANN, D., PORGADOR, A., HAUSER, A., KARLAS, A. & ROMAGNANI, C. 2013. RORgammat(+) innate lymphoid cells acquire a proinflammatory program upon engagement of the activating receptor NKp44. *Immunity,* 38**,** 1223-35.

HANASH, A. M., DUDAKOV, J. A., HUA, G., O'CONNOR, M. H., YOUNG, L. F., SINGER, N. V., WEST, M. L., JENQ, R. R., HOLLAND, A. M., KAPPEL, L. W., GHOSH, A., TSAI, J. J., RAO, U. K., YIM, N. L., SMITH, O. M., VELARDI, E., HAWRYLUK, E. B., MURPHY, G. F., LIU, C., FOUSER, L. A., KOLESNICK, R., BLAZAR, B. R. & VAN DEN BRINK, M. R. 2012. Interleukin-22 protects intestinal stem cells from immune-mediated tissue damage and regulates sensitivity to graft versus host disease. *Immunity,* 37**,** 339-50.

HERSHKOVITZ, O., ROSENTAL, B., ROSENBERG, L. A., NAVARRO-SANCHEZ, M. E., JIVOV, S., ZILKA, A., GERSHONI-YAHALOM, O., BRIENT-LITZLER, E., BEDOUELLE, H., HO, J. W., CAMPBELL, K. S., RAGER-ZISMAN, B., DESPRES, P. & PORGADOR, A. 2009. NKp44 receptor mediates interaction of the envelope glycoproteins from the West Nile and dengue viruses with NK cells. *J Immunol,* 183**,** 2610-21.

HO, J. W., HERSHKOVITZ, O., PEIRIS, M., ZILKA, A., BAR-ILAN, A., NAL, B., CHU, K., KUDELKO, M., KAM, Y. W., ACHDOUT, H., MANDELBOIM, M., ALTMEYER, R., MANDELBOIM, O., BRUZZONE, R. & PORGADOR, A. 2008. H5-type influenza virus hemagglutinin is functionally recognized by the natural killer-activating receptor NKp44. *J Virol,* 82**,** 2028-32.

HOORWEG, K., PETERS, C. P., CORNELISSEN, F., APARICIO-DOMINGO, P., PAPAZIAN, N., KAZEMIER, G., MJOSBERG, J. M., SPITS, H. & CUPEDO, T. 2012. Functional Differences between Human NKp44(-) and NKp44(+) RORC(+) Innate Lymphoid Cells. *Frontiers in immunology,* 3.

HUANG, Y. C., HUNG, S. W., JAN, T. R., LIAO, K. W., CHENG, C. H., WANG, Y. S. & CHU, R. M. 2008. CD5-low expression lymphocytes in canine peripheral blood show characteristics of natural killer cells. *J Leukoc Biol,* 84**,** 1501-10.

IRVING, B. A. & WEISS, A. 1991. The cytoplasmic domain of the T cell receptor zeta chain is sufficient to couple to receptor-associated signal transduction pathways. *Cell,* 64**,** 891-901.

IVANOV, II, ATARASHI, K., MANEL, N., BRODIE, E. L., SHIMA, T., KARAOZ, U., WEI, D., GOLDFARB, K. C., SANTEE, C. A., LYNCH, S. V., TANOUE, T., IMAOKA, A., ITOH, K., TAKEDA, K., UMESAKI, Y., HONDA, K. & LITTMAN, D. R. 2009. Induction of intestinal Th17 cells by segmented filamentous bacteria. *Cell,* 139**,** 485-98.

IVANOV, II, FRUTOS RDE, L., MANEL, N., YOSHINAGA, K., RIFKIN, D. B., SARTOR, R. B., FINLAY, B. B. & LITTMAN, D. R. 2008. Specific microbiota direct the differentiation of IL-17-producing T-helper cells in the mucosa of the small intestine. *Cell Host Microbe,* 4**,** 337-49.

JARAHIAN, M., WATZL, C., FOURNIER, P., ARNOLD, A., DJANDJI, D., ZAHEDI, S., CERWENKA, A., PASCHEN, A., SCHIRRMACHER, V. & MOMBURG, F. 2009. Activation of natural killer cells by newcastle disease virus hemagglutinin-neuraminidase. *J Virol,* 83**,** 8108-21.

JOST, S., QUILLAY, H., REARDON, J., PETERSON, E., SIMMONS, R. P., PARRY, B. A., BRYANT, N. N., BINDER, W. D. & ALTFELD, M. 2011. Changes in cytokine levels and NK cell activation associated with influenza. *PLoS One,* 6**,** e25060.

JOSTINS, L., RIPKE, S., WEERSMA, R. K., DUERR, R. H., MCGOVERN, D. P., HUI, K. Y., LEE, J. C., SCHUMM, L. P., SHARMA, Y., ANDERSON, C. A., ESSERS, J., MITROVIC, M., NING, K., CLEYNEN, I., THEATRE, E., SPAIN, S. L., RAYCHAUDHURI, S., GOYETTE, P., WEI, Z., ABRAHAM, C., ACHKAR, J. P., AHMAD, T., AMININEJAD, L., ANANTHAKRISHNAN, A. N., ANDERSEN, V., ANDREWS, J. M., BAIDOO, L., BALSCHUN, T., BAMPTON, P. A., BITTON, A., BOUCHER, G., BRAND, S., BUNING, C., COHAIN, A., CICHON, S., D'AMATO, M., DE JONG, D., DEVANEY, K. L., DUBINSKY, M., EDWARDS, C., ELLINGHAUS, D., FERGUSON, L. R., FRANCHIMONT, D., FRANSEN, K., GEARRY, R., GEORGES, M., GIEGER, C., GLAS, J., HARITUNIANS, T., HART, A., HAWKEY, C., HEDL, M., HU, X., KARLSEN, T. H., KUPCINSKAS, L., KUGATHASAN, S., LATIANO, A., LAUKENS, D., LAWRANCE, I. C., LEES, C.

W., LOUIS, E., MAHY, G., MANSFIELD, J., MORGAN, A. R., MOWAT, C., NEWMAN, W., PALMIERI, O., PONSIOEN, C. Y., POTOCNIK, U., PRESCOTT, N. J., REGUEIRO, M., ROTTER, J. I., RUSSELL, R. K., SANDERSON, J. D., SANS, M., SATSANGI, J., SCHREIBER, S., SIMMS, L. A., SVENTORAITYTE, J., TARGAN, S. R., TAYLOR, K. D., TREMELLING, M., VERSPAGET, H. W., DE VOS, M., WIJMENGA, C., WILSON, D. C., WINKELMANN, J., XAVIER, R. J., ZEISSIG, S., ZHANG, B., ZHANG, C. K., ZHAO, H., INTERNATIONAL, I. B. D. G. C., SILVERBERG, M. S., ANNESE, V., HAKONARSON, H., BRANT, S. R., RADFORD-SMITH, G., MATHEW, C. G., RIOUX, J. D., et al. 2012. Host-microbe interactions have shaped the genetic architecture of inflammatory bowel disease. *Nature,* 491**,** 119-24.

KASER, A., ZEISSIG, S. & BLUMBERG, R. S. 2010. Inflammatory bowel disease. *Annu Rev Immunol,* 28**,** 573-621.

KENNETH M. MURPHY, P. T., MARK WALPORT 2014. *Janeway's Immunologie*, Springer Spektrum.

KILLIG, M., GLATZER, T. & ROMAGNANI, C. 2014. Recognition strategies of group 3 innate lymphoid cells. *Front Immunol,* 5**,** 142.

KLATT, E. C. 2015. The Internet Pathology Laboratory for Medical Education. Savannah, Georgia, USA: Mercer University School of Medicine.

KLOSE, C. S. & ARTIS, D. 2016. Innate lymphoid cells as regulators of immunity, inflammation and tissue homeostasis. *Nat Immunol,* 17**,** 765-74.

KLOSE, C. S., FLACH, M., MOHLE, L., ROGELL, L., HOYLER, T., EBERT, K., FABIUNKE, C., PFEIFER, D., SEXL, V., FONSECA-PEREIRA, D., DOMINGUES, R. G., VEIGA-FERNANDES, H., ARNOLD, S. J., BUSSLINGER, M., DUNAY, I. R., TANRIVER, Y. & DIEFENBACH, A. 2014. Differentiation of type 1 ILCs from a common progenitor to all helper-like innate lymphoid cell lineages. *Cell,* 157**,** 340-56.

KLOSE, C. S., KISS, E. A., SCHWIERZECK, V., EBERT, K., HOYLER, T., D'HARGUES, Y., GOPPERT, N., CROXFORD, A. L., WAISMAN, A., TANRIVER, Y. & DIEFENBACH, A. 2013. A T-bet gradient controls the fate and function of CCR6-RORgammat+ innate lymphoid cells. *Nature,* 494**,** 261-5.

KOSTIC, A. D., XAVIER, R. J. & GEVERS, D. 2014. The microbiome in inflammatory bowel disease: current status and the future ahead. *Gastroenterology,* 146**,** 1489-99.

KOTLYAROV, A., NEININGER, A., SCHUBERT, C., ECKERT, R., BIRCHMEIER, C., VOLK, H. D. & GAESTEL, M. 1999. MAPKAP kinase 2 is essential for LPS-induced TNF-alpha biosynthesis. *Nat Cell Biol,* 1**,** 94-7.

KRAMER, B., GOESER, F., LUTZ, P., GLASSNER, A., BOESECKE, C., SCHWARZE-ZANDER, C., KACZMAREK, D., NISCHALKE, H. D., BRANCHI, V., MANEKELLER, S., HUNEBURG, R., VAN BREMEN, T., WEISMULLER, T., STRASSBURG, C. P., ROCKSTROH, J. K., SPENGLER, U. & NATTERMANN, J. 2017. Compartment-specific distribution of human intestinal innate lymphoid cells is altered in HIV patients under effective therapy. *PLoS Pathog,* 13**,** e1006373.

KRUGLOV, A. A., GRIVENNIKOV, S. I., KUPRASH, D. V., WINSAUER, C., PREPENS, S., SELEZNIK, G. M., EBERL, G., LITTMAN, D. R., HEIKENWALDER, M., TUMANOV, A. V. & NEDOSPASOV, S. A. 2013. Nonredundant function of soluble LTalpha3 produced by innate lymphoid cells in intestinal homeostasis. *Science,* 342**,** 1243-6.

KRUSE, P. H., MATTA, J., UGOLINI, S. & VIVIER, E. 2014. Natural cytotoxicity receptors and their ligands. *Immunol Cell Biol,* 92**,** 221-9.

LANIER, L. L. 2005. NK cell recognition. *Annu Rev Immunol,* 23**,** 225-74.

LONGMAN, R. S., DIEHL, G. E., VICTORIO, D. A., HUH, J. R., GALAN, C., MIRALDI, E. R., SWAMINATH, A., BONNEAU, R., SCHERL, E. J. & LITTMAN, D. R. 2014. CX(3)CR1(+) mononuclear phagocytes support colitis-associated innate lymphoid cell production of IL-22. *J Exp Med,* 211**,** 1571-83.

LUCI, C., REYNDERS, A., IVANOV, II, COGNET, C., CHICHE, L., CHASSON, L., HARDWIGSEN, J., ANGUIANO, E., BANCHEREAU, J., CHAUSSABEL, D., DALOD, M., LITTMAN, D. R., VIVIER, E. & TOMASELLO, E. 2009. Influence of the transcription factor RORgammat on the development of NKp46+ cell populations in gut and skin. *Nat Immunol,* 10**,** 75-82.

MAGRI, G., MIYAJIMA, M., BASCONES, S., MORTHA, A., PUGA, I., CASSIS, L., BARRA, C. M., COMERMA, L., CHUDNOVSKIY, A., GENTILE, M., LLIGE, D., COLS, M., SERRANO, S., AROSTEGUI, J. I., JUAN, M., YAGUE, J., MERAD, M., FAGARASAN, S. & CERUTTI, A. 2014. Innate lymphoid cells integrate stromal and immunological signals to enhance antibody production by splenic marginal zone B cells. *Nat Immunol,* 15**,** 354-64.

MALOY, K. J. & POWRIE, F. 2011. Intestinal homeostasis and its breakdown in inflammatory bowel disease. *Nature,* 474**,** 298-306.

MANDELBOIM, O., LIEBERMAN, N., LEV, M., PAUL, L., ARNON, T. I., BUSHKIN, Y., DAVIS, D. M., STROMINGER, J. L., YEWDELL, J. W. & PORGADOR, A. 2001. Recognition of haemagglutinins on virus-infected cells by NKp46 activates lysis by human NK cells. *Nature,* 409**,** 1055-1060.

MEBIUS, R. E. 2003. Organogenesis of lymphoid tissues. *Nat Rev Immunol,* 3**,** 292-303.

MJOSBERG, J. M., TRIFARI, S., CRELLIN, N. K., PETERS, C. P., VAN DRUNEN, C. M., PIET, B., FOKKENS, W. J., CUPEDO, T. & SPITS, H. 2011. Human IL-25- and IL-33-responsive type 2 innate lymphoid cells are defined by expression of CRTH2 and CD161. *Nat Immunol,* 12**,** 1055-62.

MONTALDO, E., TEIXEIRA-ALVES, L. G., GLATZER, T., DUREK, P., STERVBO, U., HAMANN, W., BABIC, M., PACLIK, D., STOLZEL, K., GRONE, J., LOZZA, L., JUELKE, K., MATZMOHR, N., LOIACONO, F., PETRONELLI, F., HUNTINGTON, N. D., MORETTA, L., MINGARI, M. C. & ROMAGNANI, C. 2014. Human RORgammat(+)CD34(+) cells are lineage-specified progenitors of group 3 RORgammat(+) innate lymphoid cells. *Immunity,* 41**,** 988-1000.

MONTICELLI, L. A., SONNENBERG, G. F., ABT, M. C., ALENGHAT, T., ZIEGLER, C. G., DOERING, T. A., ANGELOSANTO, J. M., LAIDLAW, B. J., YANG, C. Y., SATHALIYAWALA, T., KUBOTA, M., TURNER, D., DIAMOND, J. M., GOLDRATH, A. W., FARBER, D. L., COLLMAN, R. G., WHERRY, E. J. & ARTIS, D. 2011. Innate lymphoid cells promote lung-tissue homeostasis after infection with influenza virus. *Nat Immunol,* 12**,** 1045-54.

MORETTA, A., BOTTINO, C., VITALE, M., PENDE, D., CANTONI, C., MINGARI, M. C., BIASSONI, R. & MORETTA, L. 2001. Activating receptors and coreceptors involved in human natural killer cell-mediated cytolysis. *Annu Rev Immunol,* 19**,** 197-223.

MORO, K., YAMADA, T., TANABE, M., TAKEUCHI, T., IKAWA, T., KAWAMOTO, H., FURUSAWA, J., OHTANI, M., FUJII, H. & KOYASU, S. 2010. Innate production of T(H)2 cytokines by adipose tissue-associated c-Kit(+)Sca-1(+) lymphoid cells. *Nature,* 463**,** 540-4.

MOWAT, A. M. 2003. Anatomical basis of tolerance and immunity to intestinal antigens. *Nat Rev Immunol,* 3**,** 331-41.

NEILL, D. R., WONG, S. H., BELLOSI, A., FLYNN, R. J., DALY, M., LANGFORD, T. K., BUCKS, C., KANE, C. M., FALLON, P. G., PANNELL, R., JOLIN, H. E. & MCKENZIE, A. N. 2010. Nuocytes represent a new innate effector leukocyte that mediates type-2 immunity. *Nature,* 464**,** 1367-70.

NEURATH, M. F. 2014. Cytokines in inflammatory bowel disease. *Nat Rev Immunol,* 14**,** 329-42.

NIEHRS, A., GARCIA-BELTRAN, W. F., NORMAN, P. J., WATSON, G. M., HOLZEMER, A., CHAPEL, A., RICHERT, L., POMMERENING-ROSER, A., KORNER, C., OZAWA, M., MARTRUS, G., ROSSJOHN, J., LEE, J. H., BERRY, R., CARRINGTON, M. & ALTFELD, M. 2019. A subset of HLA-DP molecules serve as ligands for the natural cytotoxicity receptor NKp44. *Nat Immunol,* 20**,** 1129-1137.

PENDE, D., PAROLINI, S., PESSINO, A., SIVORI, S., AUGUGLIARO, R., MORELLI, L., MARCENARO, E., ACCAME, L., MALASPINA, A., BIASSONI, R., BOTTINO, C., MORETTA, L. & MORETTA, A. 1999. Identification and molecular characterization of NKp30, a novel triggering receptor involved in natural cytotoxicity mediated by human natural killer cells. *J Exp Med,* 190**,** 1505-16.

PHAM, T. A., CLARE, S., GOULDING, D., ARASTEH, J. M., STARES, M. D., BROWNE, H. P., KEANE, J. A., PAGE, A. J., KUMASAKA, N., KANE, L., MOTTRAM, L., HARCOURT, K., HALE, C., ARENDS, M. J., GAFFNEY, D. J., SANGER MOUSE GENETICS, P., DOUGAN, G. & LAWLEY, T. D. 2014. Epithelial IL-22RA1-mediated fucosylation promotes intestinal colonization resistance to an opportunistic pathogen. *Cell Host Microbe,* 16**,** 504-16.

PICKARD, J. M., MAURICE, C. F., KINNEBREW, M. A., ABT, M. C., SCHENTEN, D., GOLOVKINA, T. V., BOGATYREV, S. R., ISMAGILOV, R. F., PAMER, E. G., TURNBAUGH, P. J. & CHERVONSKY, A. V. 2014. Rapid fucosylation of intestinal epithelium sustains host-commensal symbiosis in sickness. *Nature,* 514**,** 638-41.

PICKERT, G., NEUFERT, C., LEPPKES, M., ZHENG, Y., WITTKOPF, N., WARNTJEN, M., LEHR, H. A., HIRTH, S., WEIGMANN, B., WIRTZ, S., OUYANG, W., NEURATH, M. F. & BECKER, C. 2009. STAT3 links IL-22 signaling in intestinal epithelial cells to mucosal wound healing. *J Exp Med,* 206**,** 1465-72.

POWELL, N., WALKER, A. W., STOLARCZYK, E., CANAVAN, J. B., GOKMEN, M. R., MARKS, E., JACKSON, I., HASHIM, A., CURTIS, M. A., JENNER, R. G., HOWARD, J. K., PARKHILL, J., MACDONALD, T. T. & LORD, G. M. 2012. The transcription factor T-bet regulates intestinal inflammation mediated by interleukin-7 receptor+ innate lymphoid cells. *Immunity,* 37**,** 674-84.

PRICE, A. E., LIANG, H. E., SULLIVAN, B. M., REINHARDT, R. L., EISLEY, C. J., ERLE, D. J. & LOCKSLEY, R. M. 2010. Systemically dispersed innate IL-13-expressing cells in type 2 immunity. *Proc Natl Acad Sci U S A,* 107**,** 11489-94.

QIU, J., GUO, X., CHEN, Z. M., HE, L., SONNENBERG, G. F., ARTIS, D., FU, Y. X. & ZHOU, L. 2013. Group 3 innate lymphoid cells inhibit T-cell-mediated intestinal inflammation through aryl hydrocarbon receptor signaling and regulation of microflora. *Immunity,* 39**,** 386-99.

QIU, J., HELLER, J. J., GUO, X., CHEN, Z. M., FISH, K., FU, Y. X. & ZHOU, L. 2012. The aryl hydrocarbon receptor regulates gut immunity through modulation of innate lymphoid cells. *Immunity,* 36**,** 92-104.

RADBRUCH, A. 2000. *Flow Cytometry and Cell Sorting,* Berlin Heidelberg, Springer Berlin Heidelberg.

REYNDERS, A., YESSAAD, N., VU MANH, T. P., DALOD, M., FENIS, A., AUBRY, C., NIKITAS, G., ESCALIERE, B., RENAULD, J. C., DUSSURGET, O., COSSART, P., LECUIT, M., VIVIER, E. & TOMASELLO, E. 2011. Identity, regulation and in vivo function of gut NKp46+RORgammat+ and NKp46+RORgammat- lymphoid cells. *EMBO J,* 30**,** 2934-47.

SANOS, S. L., BUI, V. L., MORTHA, A., OBERLE, K., HENERS, C., JOHNER, C. & DIEFENBACH, A. 2009. RORgammat and commensal microflora are required for the differentiation of mucosal interleukin 22-producing NKp46+ cells. *Nat Immunol,* 10**,** 83-91.

SATOH-TAKAYAMA, N., DUMOUTIER, L., LESJEAN-POTTIER, S., RIBEIRO, V. S., MANDELBOIM, O., RENAULD, J. C., VOSSHENRICH, C. A. & DI SANTO, J. P. 2009. The natural cytotoxicity receptor NKp46 is dispensable for IL-22-mediated innate intestinal immune defense against Citrobacter rodentium. *J Immunol,* 183**,** 6579-87.

SAWA, S., CHERRIER, M., LOCHNER, M., SATOH-TAKAYAMA, N., FEHLING, H. J., LANGA, F., DI SANTO, J. P. & EBERL, G. 2010. Lineage relationship analysis of RORgammat+ innate lymphoid cells. *Science,* 330**,** 665-9.

SAWA, S., LOCHNER, M., SATOH-TAKAYAMA, N., DULAUROY, S., BERARD, M., KLEINSCHEK, M., CUA, D., DI SANTO, J. P. & EBERL, G. 2011. RORgammat+

innate lymphoid cells regulate intestinal homeostasis by integrating negative signals from the symbiotic microbiota. *Nat Immunol,* 12**,** 320-6.

SCHREINER, P., NEURATH, M. F., NG, S. C., EL-OMAR, E. M., SHARARA, A. I., KOBAYASHI, T., HISAMATSU, T., HIBI, T. & ROGLER, G. 2019. Mechanism-Based Treatment Strategies for IBD: Cytokines, Cell Adhesion Molecules, JAK Inhibitors, Gut Flora, and More. *Inflamm Intest Dis,* 4**,** 79-96.

SIVORI, S., VITALE, M., MORELLI, L., SANSEVERINO, L., AUGUGLIARO, R., BOTTINO, C., MORETTA, L. & MORETTA, A. 1997. p46, a novel natural killer cell-specific surface molecule that mediates cell activation. *J Exp Med,* 186**,** 1129-36.

SONNENBERG, G. F., FOUSER, L. A. & ARTIS, D. 2011a. Border patrol: regulation of immunity, inflammation and tissue homeostasis at barrier surfaces by IL-22. *Nat Immunol,* 12**,** 383-90.

SONNENBERG, G. F., MONTICELLI, L. A., ALENGHAT, T., FUNG, T. C., HUTNICK, N. A., KUNISAWA, J., SHIBATA, N., GRUNBERG, S., SINHA, R., ZAHM, A. M., TARDIF, M. R., SATHALIYAWALA, T., KUBOTA, M., FARBER, D. L., COLLMAN, R. G., SHAKED, A., FOUSER, L. A., WEINER, D. B., TESSIER, P. A., FRIEDMAN, J. R., KIYONO, H., BUSHMAN, F. D., CHANG, K. M. & ARTIS, D. 2012. Innate lymphoid cells promote anatomical containment of lymphoid-resident commensal bacteria. *Science,* 336**,** 1321-5.

SONNENBERG, G. F., MONTICELLI, L. A., ELLOSO, M. M., FOUSER, L. A. & ARTIS, D. 2011b. CD4(+) lymphoid tissue-inducer cells promote innate immunity in the gut. *Immunity,* 34**,** 122-34.

SPITS, H., ARTIS, D., COLONNA, M., DIEFENBACH, A., DI SANTO, J. P., EBERL, G., KOYASU, S., LOCKSLEY, R. M., MCKENZIE, A. N., MEBIUS, R. E., POWRIE, F. & VIVIER, E. 2013. Innate lymphoid cells--a proposal for uniform nomenclature. *Nat Rev Immunol,* 13**,** 145-9.

SPITS, H. & CUPEDO, T. 2012. Innate Lymphoid Cells: Emerging Insights in Development, Lineage Relationships, and Function. *In:* PAUL, W. E. (ed.) *Annual Review of Immunology, Vol 30.* Palo Alto: Annual Reviews.

SUGIMOTO, K., OGAWA, A., MIZOGUCHI, E., SHIMOMURA, Y., ANDOH, A., BHAN, A. K., BLUMBERG, R. S., XAVIER, R. J. & MIZOGUCHI, A. 2008. IL-22 ameliorates intestinal inflammation in a mouse model of ulcerative colitis. *J Clin Invest,* 118**,** 534-44.

TAKATORI, H., KANNO, Y., WATFORD, W. T., TATO, C. M., WEISS, G., IVANOV, II, LITTMAN, D. R. & O'SHEA, J. J. 2009. Lymphoid tissue inducer-like cells are an innate source of IL-17 and IL-22. *J Exp Med,* 206**,** 35-41.

TAKAYAMA, T., KAMADA, N., CHINEN, H., OKAMOTO, S., KITAZUME, M. T., CHANG, J., MATUZAKI, Y., SUZUKI, S., SUGITA, A., KOGANEI, K., HISAMATSU, T., KANAI, T. & HIBI, T. 2010. Imbalance of NKp44(+)NKp46(-) and NKp44(-)NKp46(+) natural killer cells in the intestinal mucosa of patients with Crohn's disease. *Gastroenterology,* 139**,** 882-92, 892 e1-3.

TEUNISSEN, M. B., MUNNEKE, J. M., BERNINK, J. H., SPULS, P. I., RES, P. C., TE VELDE, A., CHEUK, S., BROUWER, M. W., MENTING, S. P., EIDSMO, L., SPITS, H., HAZENBERG, M. D. & MJOSBERG, J. 2014. Composition of innate lymphoid cell subsets in the human skin: enrichment of NCR(+) ILC3 in lesional skin and blood of psoriasis patients. *J Invest Dermatol,* 134**,** 2351-60.

TORRES, J., BONOVAS, S., DOHERTY, G., KUCHARZIK, T., GISBERT, J. P., RAINE, T., ADAMINA, M., ARMUZZI, A., BACHMANN, O., BAGER, P., BIANCONE, L., BOKEMEYER, B., BOSSUYT, P., BURISCH, J., COLLINS, P., EL-HUSSUNA, A., ELLUL, P., FREI-LANTER, C., FURFARO, F., GINGERT, C., GIONCHETTI, P., GOMOLLON, F., GONZALEZ-LORENZO, M., GORDON, H., HLAVATY, T., JUILLERAT, P., KATSANOS, K., KOPYLOV, U., KRUSTINS, E., LYTRAS, T., MAASER, C., MAGRO, F., MARSHALL, J. K., MYRELID, P., PELLINO, G., ROSA, I., SABINO, J., SAVARINO, E., SPINELLI, A., STASSEN, L., UZZAN, M., VAVRICKA, S., VERSTOCKT, B., WARUSAVITARNE, J., ZMORA, O. & FIORINO, G. 2020. ECCO Guidelines on Therapeutics in Crohn's Disease: Medical Treatment. *J Crohns Colitis,* 14**,** 4-22.

TUMANOV, A. V., KOROLEVA, E. P., GUO, X., WANG, Y., KRUGLOV, A., NEDOSPASOV, S. & FU, Y. X. 2011. Lymphotoxin controls the IL-22 protection pathway in gut innate lymphoid cells during mucosal pathogen challenge. *Cell Host Microbe,* 10**,** 44-53.

UHLIG, H. H., MCKENZIE, B. S., HUE, S., THOMPSON, C., JOYCE-SHAIKH, B., STEPANKOVA, R., ROBINSON, N., BUONOCORE, S., TLASKALOVA-HOGENOVA, H., CUA, D. J. & POWRIE, F. 2006. Differential activity of IL-12 and IL-23 in mucosal and systemic innate immune pathology. *Immunity,* 25**,** 309-18.

VITALE, M., BOTTINO, C., SIVORI, S., SANSEVERINO, L., CASTRICONI, R., MARCENARO, E., AUGUGLIARO, R., MORETTA, L. & MORETTA, A. 1998. NKp44, a novel triggering surface molecule specifically expressed by activated natural killer cells, is involved in non-major histocompatibility complex-restricted tumor cell lysis. *J Exp Med,* 187**,** 2065-72.

VIVIER, E., ARTIS, D., COLONNA, M., DIEFENBACH, A., DI SANTO, J. P., EBERL, G., KOYASU, S., LOCKSLEY, R. M., MCKENZIE, A. N. J., MEBIUS, R. E., POWRIE, F. & SPITS, H. 2018. Innate Lymphoid Cells: 10 Years On. *Cell,* 174**,** 1054-1066.

VIVIER, E., NUNES, J. A. & VELY, F. 2004. Natural killer cell signaling pathways. *Science,* 306**,** 1517-9.

VIVIER, E., TOMASELLO, E., BARATIN, M., WALZER, T. & UGOLINI, S. 2008. Functions of natural killer cells. *Nat Immunol,* 9**,** 503-10.

VONARBOURG, C., MORTHA, A., BUI, V. L., HERNANDEZ, P. P., KISS, E. A., HOYLER, T., FLACH, M., BENGSCH, B., THIMME, R., HOLSCHER, C., HONIG, M., PANNICKE, U., SCHWARZ, K., WARE, C. F., FINKE, D. & DIEFENBACH, A. 2010. Regulated expression of nuclear receptor RORgammat confers distinct functional fates to NK cell receptor-expressing RORgammat(+) innate lymphocytes. *Immunity,* 33**,** 736-51.

WALLACE, K. L., ZHENG, L. B., KANAZAWA, Y. & SHIH, D. Q. 2014. Immunopathology of inflammatory bowel disease. *World J Gastroenterol,* 20**,** 6-21.

ZENEWICZ, L. A., YANCOPOULOS, G. D., VALENZUELA, D. M., MURPHY, A. J., STEVENS, S. & FLAVELL, R. A. 2008. Innate and Adaptive Interleukin-22 Protects Mice from Inflammatory Bowel Disease. *Immunity,* 29**,** 947-957.

ZHENG, Y., VALDEZ, P. A., DANILENKO, D. M., HU, Y., SA, S. M., GONG, Q., ABBAS, A. R., MODRUSAN, Z., GHILARDI, N., DE SAUVAGE, F. J. & OUYANG, W. 2008. Interleukin-22 mediates early host defense against attaching and effacing bacterial pathogens. *Nat Med,* 14**,** 282-9.

7. Appendix

7.1 Eidesstattliche Versicherung

Ich, Isabelle Ommert, versichere an Eides statt durch meine eigenhändige Unterschrift, dass ich die vorgelegte Dissertation mit dem Thema:

„Role and potential therapeutic use of interleukin-22^{+} Innate Lymphoid Cells in colitis“

selbstständig und ohne nicht offengelegte Hilfe Dritter verfasst und keine anderen als die angegebenen Quellen und Hilfsmittel genutzt habe.

Alle Stellen, die wörtlich oder dem Sinne nach auf Publikationen oder Vorträgen anderer Autoren/innen beruhen, sind als solche in korrekter Zitierung kenntlich gemacht. Die Abschnitte zu Methodik (insbesondere praktische Arbeiten, Laborbestimmungen, statistische Aufarbeitung) und Resultaten (insbesondere Abbildungen, Graphiken und Tabellen) werden von mir verantwortet.

Ich versichere ferner, dass ich die in Zusammenarbeit mit anderen Personen generierten Daten, Datenauswertungen und Schlussfolgerungen korrekt gekennzeichnet und meinen eigenen Beitrag sowie die Beiträge anderer Personen korrekt kenntlich gemacht habe (siehe Anteilserklärung). Texte oder Textteile, die gemeinsam mit anderen erstellt oder verwendet wurden, habe ich korrekt kenntlich gemacht.

Meine Anteile an etwaigen Publikationen zu dieser Dissertation entsprechen denen, die in der untenstehenden gemeinsamen Erklärung mit dem/der Erstbetreuer/in, angegeben sind. Für sämtliche im Rahmen der Dissertation entstandenen Publikationen wurden die Richtlinien des ICMJE (International Committee of Medical Journal Editors; www.icmje.og) zur Autorenschaft eingehalten. Ich erkläre ferner, dass ich mich zur Einhaltung der Satzung der Charité – Universitätsmedizin Berlin zur Sicherung Guter Wissenschaftlicher Praxis verpflichte.

Weiterhin versichere ich, dass ich diese Dissertation weder in gleicher noch in ähnlicher Form bereits an einer anderen Fakultät eingereicht habe.

Die Bedeutung dieser eidesstattlichen Versicherung und die strafrechtlichen Folgen einer unwahren eidesstattlichen Versicherung (§§156, 161 des Strafgesetzbuches) sind mir bekannt und bewusst.“

Datum Unterschrift

7.2 Anteilserklärung an etwaigen erfolgten Publikationen

Ich, Isabelle Ommert, hatte folgenden Anteil an der folgenden Publikation:

Glatzer, T., Killig, M., Meisig, J., Ommert, I., Luetke-Eversloh, M., Babic, M., Paclik, D., Bluthgen, N., Seidl, R., Seifarth, C., Grone, J., Lenarz, M., Stolzel, K., Fugmann, D., Porgador, A., Hauser, A., Karlas, A., Romagnani, C., „RORgammat(+) innate lymphoid cells acquire a proinflammatory program upon engagement of the activating receptor NKp44“, Immunity, 38**,** 1223-35, 2013.

1. Für den Abschnitt “Engagement of NKp44 Ligands on Tumor Epithelial Cell Lines Leads to Cytokine Expression in RORγt$^+$ ILCs” habe ich mit der NKp44-fc Färbung verschiedener Tumor Epithelzelllinien beigetragen (Figure 5 A, B). Zudem habe ich in Zusammenarbeit mit Timor Glatzer die BW-NKp44 reporter cell line Experimente durchgeführt (Figure C). In Zusammenarbeit mit Monika Killig und Timor Glatzer habe ich die Stimulationsexperimente der RORgt$^+$ ILCs mit Influenza Virus (Figure S4A and B), sowie mit MDCK und SW620 Zellen durchgeführt (Figure 5 D – G).

2. Zu dem Abschnitt “Characterization and NKp44 Responsiveness of Colon-Derived RORγt$^+$ ILCs” habe ich mit der Charakterisierung der NKp44 Expression von mononukleären Zellen der Lamina propria von chirurgischen Darmresektaten beigetragen. Dabei habe ich die Unterschiede in der NKp44 Expression zwischen entzündeten und nicht entzündeten Schleimhautabschnitten mittels der Grafik 7 D dargestellt. In Zusammenarbeit mit Timor Glatzer habe ich die Stimulationsexperimenten der Lamina propria RORγt$^+$ ILCs mit Zytokinen sowie der Stimulation über den NKp44 Rezeptor durchgeführt.

_____

Unterschrift, Datum und Stempel der erstbetreuenden Hochschullehrerin

_____

Unterschrift der Doktorandin

7.3 Curriculum Vitae

My curriculum vitea will not be published in the electronic version of my dissertation for data protection reseasons.

7.4 Publication

GLATZER, T., KILLIG, M., MEISIG, J., OMMERT, I., LUETKE-EVERSLOH, M., BABIC, M., PACLIK, D., BLUTHGEN, N., SEIDL, R., SEIFARTH, C., GRONE, J., LENARZ, M., STOLZEL, K., FUGMANN, D., PORGADOR, A., HAUSER, A., KARLAS, A. & ROMAGNANI, C. 2013. RORgammat(+) innate lymphoid cells acquire a proinflammatory program upon engagement of the activating receptor NKp44. *Immunity,* 38**,** 1223-35.

7.5 Acknowledgements

I thank in the first place Prof. Dr. Chiara Romagnani for the excellent mentoring of my thesis, her constructive and creative conceptual work. I appreciate a lot the motivation and will on her side, that enabled me to finish the thesis even after several years. I want to acknowledge and thank here again, as declared in the result part, Monica Killig and Timor Glatzer for their support and cooperation in several of the experiments. At the time I joined the working group *Innate Immunity*, both of them have already been well established in the project, the scientific background and many of the methods. It was a great pleasure to learn from them and, in the course of the thesis, contribute to their project "RORγt^{+} Innate Lymphoid Cells Acquire a Proinflammatory Program upon Engagement of the Activating Receptor NKp44". I also thank the other members of Chiara Romagnani`s working group *Innate Immunity.* A special thank is due to Toralf Kaiser and Jenny Kirsch of the flow cytometry & cell sorting department of the DRFZ, that maintained and adjusted the FACS and cell sorting devices and were available for support any time. I would like to name Lars Bieber, who accompanied me through the research year with all ups and downs. I thank the friends, that discussed with me this thesis and gave valuable advice – Jordan Löliger, Carla Rigling and Philipp Krabusch. And finally, I appreciate my sister Eva Ommert and Marius Elkuch who are always there for me.